November 2015

The Investigation of Rhodiola Crenulata Root Extract Effects on Obesity Associated Inflammation and the Antineoplastic Mechanism in Breast Cancer Cells

Lotfi M. Bassa
University of Massachusetts - Amherst

THE INVESTIGATION OF *RHODIOLA CRENULATA* ROOT EXTRACT EFFECTS ON OBESITY ASSOCIATED INFLAMMATION AND THE ANTINEOPLASTIC MECHANISM IN BREAST CANCER CELLS

A Dissertation Presented

By

LOTFI MATEO BASSA

Submitted to the Graduate School of the
University of Massachusetts Amherst in partial fulfillment
of the requirements for the degree of

DOCTOR OF PHILOSOPHY

September 2015

Animal Biotechnology and Biomedical Science Program

THE INVESTIGATION OF *RHODIOLA CRENULATA* ROOT EXTRACT EFFECTS ON OBESITY ASSOCIATED INFLAMMATION AND ANTI-NEOPLASTIC MECHANISMS IN BREAST CANCER CELLS

A Dissertation Presented

By

LOTFI MATEO BASSA

Approved as to style and content by:

_____

Sallie Smith Schneider, Chair

_____

Kathleen Arcaro, Member

_____

Lisa Minter, Member

_____

Young-Cheul Kim, Member

_____

Lisa Minter, Animal Biotechnology and

Biomedical Science Graduate Program Director

DEDICATION

To the greatest woman I have ever witnessed, my mother Nadjia Yacoub. And to my inspirer Dr. Barton Kamen. Thank you for everything!

ACKNOWLEDGMENTS

"Stand for the teacher and honor his rank, for a teacher is almost as a prophet. Do you know of someone nobler than, he who nurtures minds and hearts. " -Ahmed Shawqi

As I end my graduate student career I would like to first and foremost thank God the most gracious and merciful. Thank you for keeping me healthy, focused, and allowing me to reach this point in life.

My journey in life would not have led me to this path if I did not have the people who inspired, guided, supported and mentored me all along. Without your unconditional love and support, I would not be here today.

To the women who raised, cared and sacrificed everything for me, my mother Nadjia Yacoub; thank you for raising me the way you did and emphasizing the importance of education. Thank you for your patience with me throughout the good and rough times, especially when I told you I was quitting school in 11^{th} grade. If it weren't for you, I would have not gotten to this point today. Words could not express my gratitude for having you in my life.

To my near and dear sister, Hana Bassa, boy oh boy! What would my life be without you? Thank you for staying by my side and supporting me all along. Without your push I would've never made it this far.

To my undergraduate and life mentors, the two who opened my eyes to scientific research: Dr. Ann Marie DiLorenzo and Dr. Caryl Ann Becerra. Thank you for leading me to this path. Caryl, without your mentoring, guidance and advice, I would have never thought that graduate school would be an option for me. Thank you for giving me the first set of pipettes and project in science, your motivation got me here. Dr. D, thank you for giving me the opportunity to work in your lab, take part of your classes, and giving me my first teaching experience. You

lead me to the beginning of the tunnel, and without your support, this journey might have never happened.

To my UMass NEAGEP/PREP directors Dr. Sandra Petersen, Mrs. Vanessa Hill, Dr. Marlina Duncan, thank you for giving me a chance and bringing me to UMass. SPUR was my first opportunity to do research, and every time I reread my personal statement for the program, I don't understand why you accepted me into the SPUR program. I guess it was my destiny. Vanessa and Marlina, thank you for your patience with me through my rough beginnings with PREP, and for allowing me this great opportunity that got me here today. Most importantly thank you for being great older sisters throughout this journey.

To my UMASS NEAGEP/PREP family, thank you for the good conversation, the fun times and experiences. Also thank you to my peer mentors and friends of course, Dr. Kyle Morrison, Dr. Jeniffer Concepción and Dr. Monique Johnson, thank you for the stimulating conversation and encouragements. A special thank you to Patricia Lehouiller, for being super woman and making sure our finances are in check. I appreciate all that you have done for me during my time here.

A special thank you to my UMASS NEAGEP/PREP brother and sisters, Dr. Cornelius Tabaazuing, Radhameris Gomez, Candace Harris, Dr. Chanelle Adams and Carolina Morell-Perez. Thank you for being by my side through the good and bad. Without your support and fun nights, as Cornelius says, " Live for the nights you won't remember with the people you'll never forget". I am happy and thankful for having you in my life. You all made this journey enjoyable.

A special thank you to my graduate school partner in good and crime, my sister from another mister: Christina Chisholm. It all started in the science library for our first study session when everyone bailed out on us, and we pushed through the material. It was tough and slow at first, but we got to know each other well. We kept going and supported each other all along this

journey. Then I realized that I found my younger sister. Thank you for always being there, for your support and for never judging me. You are a true friend indeed!

To my favorite Lebanese person whom I met the first day of graduate school, Abla Tannous. Thank you for your great friendship, support and guidance throughout the graduate school journey, and most importantly thank you keeping Arabic on my tongue.

I also would like to acknowledge my friends outside of UMass, or more correctly my cheering squad, either back in New York/ New Jersey area, in my homeland Algeria and my childhood friends who are spread around the world. I would like to especially thank Sami and Jessica Mohamed for always supporting me since my real estate career era. To my dear friends from New Jersey Badih Alkhalil and Sohail Sherifsulaiman: thank you for always reminding me why I embarked on this journey and for being there. Also I want to thank Ahmad Yaman Kebba, Abdul Jalil Aljafary, Anas Abu Mayaala, Mohanad Diab and the rest of "el wara'een el ajaneb" crew. Thank you for your support and keeping a piece of the past always present regardless of the eight-hour time zone difference. I would like to specially thank my best friend Hatoona "Mohamed Hussein Yasin" and his family, for their kindness acceptance and making me one of their family. Hatoo, your words, kindness and support were always appreciated especially during the Sydney days. You will always be my brother.

The scientific work presented in this document would've never been possible without the help of my wonderful lab mates, Dr. Kaitlyn Wong, Dr. Carmen Mora, Maxine Dudek, Jen Ser Delonsky, and especially Elizabeth Henchey and Dr. Kelly Gauger. Without their scientific and non-scientific support and advice, things would've been rough. I want to also thank all the past and previous members of the Pioneer Valley Life Science Institute (PVLSI) and animal care facility for their teaching, support, great laughs and conversation.

To my mentees and students throughout this journey, thank you for inspiring me to become who I am today, and allowing me to enlighten your minds in any sort of way. I do apologize for making any of you cry, but my goal was not to hurt your spirit, but to push you to be great scientists and brilliant thinkers. It is called tough love

Last but not least, I would like to thank all my committee members, Drs. Kathleen Arcaro, Lisa Minter and Young-Cheul Kim, your support and suggestions helped shape me as a researcher and continuously pushed me to always think. Most importantly I want to thank my great advisor, Dr. Sallie Schneider. Thank you for taking a chance on me, and training me. You saw the good and the bad in me and guided me through this journey. You have blessed my soul and brightened my mind, and regardless of how difficult I can be sometimes, you shaped me to the scientist and mentor that I am today. I will always be grateful to you and the experiences you have given to me during the past 5 and half years.

ABSTRACT

THE INVESTIGATION OF *RHODIOLA CRENULATA* ROOT EXTRACT EFFECTS ON OBESITY ASSOCIATED INFLAMMATION AND THE ANTINEOPLASTIC MECHANISM IN BREAST CANCER CELLS

SEPTEMBER 2015

LOTFI MATEO BASSA, A.S. ESSEX COUNTY COLLEGE B.S., MONCLAIR STATE UNIVERSITY

PH.D., UNIVERSITY OF MASSACHUSETTS AMHERST

Directed by: Professor Sallie Smith Schneider

Obesity and breast cancer are two disease models that directly affect the United States population, as more than 35% of the adult population is obese [8], and more than 200,000 new cases of breast cancer are diagnosed in the United States per year. [34]. Several diseases are associated with obesity including, cardiovascular disease, insulin resistance, increased inflammation and increased cancer risk [9,10]. Therefore it essential to understand the risks associated with obesity as well as to investigate possible preventive and/or therapeutic treatment strategies.

Rhodiola crenulata is a Tibetan plant that has been used in Eastern traditional medicine to relieve depression, anxiety, fatigue and to aid in high altitude biological adjustment [1]. Studies have also suggested that treatment with *Rhodiola sp.* and their components can improve glucose homeostasis in rodent models of insulin resistance[2-4] and inhibit tumor growth in various rodent models for cancer [5-7]. However, these studies have been plagued by the lack of strong mechanistic data.

The overall goal of this dissertation is to determine the mechanism by which *R. crenulata* affects glucose homeostasis in female mice subjected to Diet Induced Obesity (DIO) and to evaluate the effect of *R. crenulata* on 2 important cancer signaling pathways (canonical

Wnt signaling and Estrogen receptor signaling) in breast cancer cells *in vitro*. In the work presented in this dissertation, we tested two main hypotheses; 1) 12 weeks of treatment with *R. crenulata* extract will decrease adiposity, improves glucose metabolism and obesity associated inflammation in female mice subjected to a high fat diet and 2) *R. crenulata* treatment will decrease Wnt/β–catenin signaling and Estrogen Receptor (ER) signaling in cancer cell lines *in vitro.* We used a wide variety of *in vitro* and *in vivo* techniques to test our hypotheses. Our results suggest that that *R. crenulata* can be beneficial for controlling insulin resistance and liver inflammation in a model for diet induced obesity. We also demonstrate two critical pathways in breast cancer cells that are controlled by *R. crenulata*. We show that treatment with a hydroalcoholic extract inhibits the canonical Wnt signaling pathway, which could explain some of the anti-neoplastic observations previously described by the Schneider lab. We also confirm that this *R. crenulata* extract contains estrogenic compounds; however despite this estrogenic activity, *R.crenulata* controlled proliferation and decreased tumorsphere growth and survival when cultures were treated for a longer period of time. Optimistically, the results from these studies will encourage further research on *R. crenulata* and possible usage as a preventive agent.

References:

[1] Khanum F, Bawa AS, Singh B. Rhodiola rosea: A Versatile Adaptogen. Comprehensive Reviews in Food Science and Food Safety 2005;4:55–62. doi:10.1111/j.1541-4337.2005.tb00073.x.

[2] Wang J, Rong X, Li W, Yang Y, Yamahara J, Li Y. Rhodiola crenulata root ameliorates derangements of glucose and lipid metabolism in a rat model of the metabolic syndrome and type 2 diabetes. J Ethnopharmacol 2012;142:782–8. doi:10.1016/j.jep.2012.05.063.

[3] Li F, Tang H, Xiao F, Gong J, Peng Y, Meng X. Protective Effect of Salidroside from Rhodiolae Radix on Diabetes-Induced Oxidative Stress in Mice. Molecules 2011;16:9912–24. doi:10.3390/molecules16129912.

[4] Kim SH, Hyun SH, Choung SY. Antioxidative effects of Cinnamomi cassiaeand Rhodiola roseaextracts in liver of diabetic mice. BioFactors 2006;26:209–19. doi:10.1002/biof.5520260306.

[5] Senthilkumar R, Parimelazhagan T, Chaurasia OP, Srivastava RB. Free radical scavenging property and antiproliferative activity of Rhodiola imbricata Edgew extracts in HT-29 human colon cancer cells. Asian Pacific Journal of Tropical Medicine 2012;6:11–9. doi:10.1016/S1995-7645(12)60194-1.

[6] Liu Z, Li X, Simoneau AR, Jafari M, Zi X. Rhodiola rosea extracts and salidroside decrease the growth of bladder cancer cell lines via inhibition of the mTOR pathway and induction of autophagy. Mol Carcinog 2011;51:257–67. doi:10.1002/mc.20780.

[7] Gauger KJ, Rodriguez-Cortes A. Rhodiola Crenulata inhibits the tumorigenic properties of invasive mammary epithelial cells with stem cell characteristics. Journal of Medicinal Food 2010. doi:10.5897/JMPR09.395.

[8] Flegal KM, Carroll MD, Ogden CL, Curtin LR. Prevalence and Trends in Obesity Among US Adults, 1999-2008. Jama 2010;303:235–41. doi:10.1001/jama.2009.2014.

[9] Polednak AP. Estimating the number of U.S. incident cancers attributable to obesity and the impact on temporal trends in incidence rates for obesity-related cancers. Cancer Detect Prev 2008;32:190–9. doi:10.1016/j.cdp.2008.08.004.

[10] Hotamisligil GS. Inflammation and metabolic disorders. Nature 2006. doi:10.1038/nature05485.

TABLE OF CONTENTS

Page

LIST OF TABLES

Table Page

LIST OF FIGURES

CHAPTER 1
INTRODUCTION

1.1 Obesity

In 2012, over 35% of the adult population in the United States of America had a body mass index (BMI) higher than 30, which is considered obese [1] [2]. By 2030, it is predicted that over 53% of the population will be obese [3]. Obesity is a severe epidemic that leads to the predisposition of several metabolic diseases such as cardiovascular diseases, insulin resistance and type 2 diabetes as well as increased inflammation [4,5]. Additionally, obesity is linked to cancer development as it has been shown that 5.8% of cancer incidences in the US in 2007 were impacted by obesity [4]. Therefore, it is essential to reduce and control obesity associated complications and explore novel treatment agents for preventive and/or for therapeutic strategies. There are several factors that were implicated in the development of obesity-related diseases, including adipocyte produced adipokines, fatty acids, mitochondrial dysfunction, endoplasmic reticulum stress, and hypoxia [6].

1.2 Glucose homeostasis and obesity.

Physiologically, obesity occurs by an increase in adipocyte size followed by an increase in preadipocyte differentiation due to excess caloric intake. Dietary fatty acids and excess carbohydrates are primarily stored in white adipose tissue (WAT) as triglycerides. Due to the presence of excess glucose, its normal homeostasis is deranged. WAT, along with skeletal muscle and the liver are the three major organs that regulate glucose homeostasis in the body. Under normal conditions, when glucose levels are increased in the blood, islet cells in the pancreas respond by secreting insulin into the blood, enhancing glucose uptake by the body's tissues and suppressing lipolysis. The final outcome is a decrease in blood glucose

concentration. Excess glucose is converted to triglycerides, stored in WAT or converted to glucagon and stored in the liver. Under nutrient fasting conditions, the pancreas responds by releasing glycogen from α-cells, which converts glycogen to glucose and restores blood homeostasis. A schematic of normal glucose homeostasis is shown in Figure1.1.

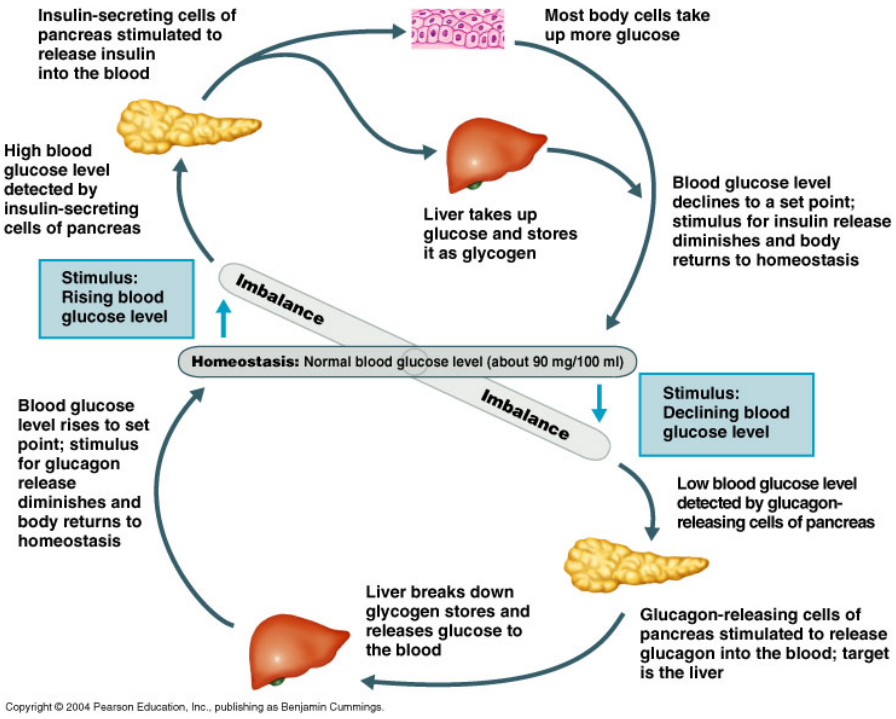

Figure 1.1: Schematic of glucose homeostasis in mammals

Derangements in glucose homeostasis can occur several ways. Tissues can decrease their glucose uptake by reducing the expression of glucose transporters or become irresponsive to insulin stimulation. In the pancreas, β-cells could become less efficient in producing insulin as well as α-cells could increase glucagon production resulting in a sustained hyperglycemic state. Hence several impairments result in the glucose derangements.

At the cellular level, obesity-induces insulin resistance by hindering the insulin-signaling pathway in insulin-responsive cells (i.e. adipocytes, hepatocytes, myocytes and β-cells). WAT

secrete hormones that can affect insulin sensitivity and glucose uptake. Resistin, a WAT produced hormone, has been shown to suppress insulin stimulated glucose uptake in adipocytes and skeletal muscle cells [7]. In addition, several studies have implicated cytokines and adipokines, secreted as a result of obesity, in the regulation of glucose homeostasis.

1.3 Obesity associated inflammation

Obesity induced inflammation is a special type of inflammation resulting from over nutrition and activation of stress pathways that drive abnormal metabolic homeostasis (e.g., high levels of lipid and glucose). The inflammation associated with obesity is classified as a low-grade inflammation and results in an increase in pro-inflammatory cytokine expression in the blood and in the inflamed tissue (adipose, liver and muscle tissues). It is also considered a chronic inflammation since it occurs over a long period of time. It is classically marked by an increase in macrophage and neutrophil infiltration and production of pro-inflammatory cytokines such as IL-6 and TNFα. Cytokines are key players in the process of inflammation, as they can act directly on cells (such as TNFα [8] [9]) as well as regulate the recruitment, development and activation of other tissue-resident immune cells. Therefore obesity-activated immune cells contribute and produce mediators that perturb insulin sensitivity in cells. The main factors shown to play a role in this interaction are the cytokines and tissue resident macrophages and neutrophils. A schematic of the progress of obesity-induced inflammation in the adipose tissue is shown in Figure1.2

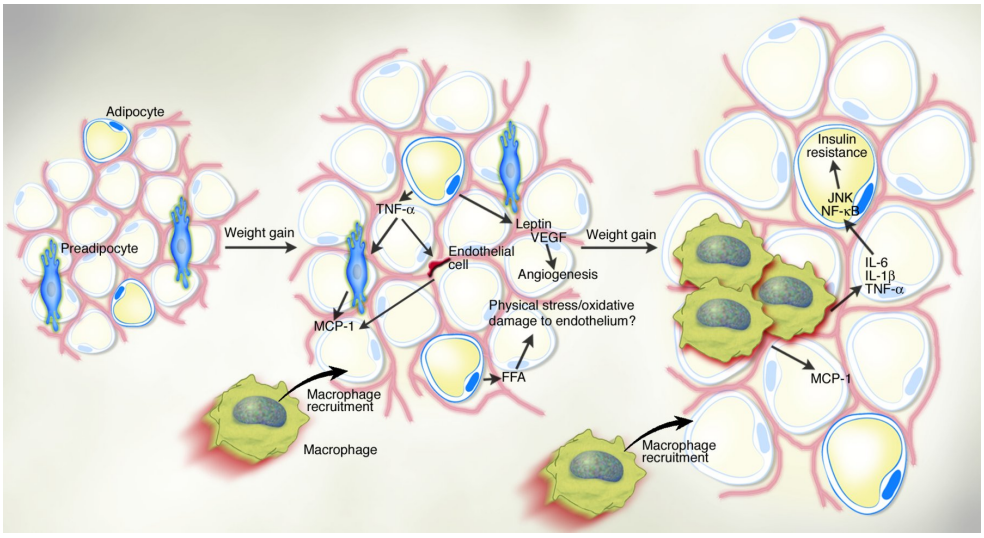

Figure 1.2 Schematic of the progress of obesity-induced inflammation in the adipose tissue. Figure J Clan Invest. 2003;112(12): 1785-1788. doi:10.1172/JCI20514.

1.3.1 Cytokines

TNFα was the first identified pro-inflammatory cytokine to be implicated in the regulation of obesity-induced insulin resistance [8,9]. These studies showed that TNFα treated adipocytes had a dysregulation in their insulin signaling due to changes in the transcription of insulin signaling receptor, IRS-1, and glucose transporter gene 4, Glut 4 [8,9]. Other studies have shown that TNFα can induce the inhibitory phosphorylation of IRS resulting in a decreased insulin response [10]. Several animal studies confirmed that increased TNFα levels induced insulin resistance, and that its functional inhibition improved obesity-induced inflammation and insulin sensitivity [11] [12] [13] [14]. IL-6 is another pro-inflammatory cytokine that is involved in this type of inflammation. It is now considered a risk factor for the development of T2D in humans [15]. A study shows that acute IL-6 infusion into mice induced spontaneous insulin resistance independent of obesity [16], therefore suggesting its ability to modulate insulin sensitivity in adipose tissue. Increased IL-6 and IL-1β levels were shown to increase hepatic expression of pro-inflammatory cytokines resulting in an increase of immune cell recruitment

[17], hence creating a secondary recruitment wave. Additionally, persistent IL-6 expression levels induced by obesity have been shown to increase the risk of hepatic cancer development [18]. Anti-inflammatory cytokines, such as IL-10 were also noted in obesity-induced inflammation. IL-10 is thought to primarily dampen the immune response in affected tissues, since it is a potent inhibitor of the pro-inflammatory cytokines and chemokines [19]. This was obvious when a study that subjected mice overexpressing IL-10 to HFD, showed an improvement in insulin sensitivity and protection from obesity induced insulin resistance compared to wild type animals. They reinforced their findings by injecting exogenous IL-10 into their wild type animals causing a decrease in Adipose Tissue Macrophages (ATM) and pro-inflammatory cytokines; further implicating reduction in macrophage and cytokine responses in the amelioration in insulin sensitivity [16].

As mentioned earlier, cytokines also increase immune cell recruitment and activation in the inflamed tissue. Two major components of the innate immune cells are implicated in this process, macrophages and neutrophils.

1.3.2 Macrophages

The main role of macrophages is to protect the body from infections by removing infected cells via phagocytosis as well as recruiting other cells using cytokines [20]. When pro-inflammatory cytokine expression is increased secondary to obesity, resident tissue macrophages such as ATMs and Kuffer cells (in livers), are polarized in a pro-inflammatory fashion, termed M1 polarization, which recruit more immune cells [21]. In the adipose tissue, M1 polarized macrophages cluster around dead adipocytes, forming crown-like structures (CLSs), to extract dead adipocytes from the rest of the tissue [22]. On the other hand macrophages could also be activated and polarized by anti-inflammatory cytokines, such as IL-4

and IL-10, and are thought to play different roles, namely in dampening the pro-inflammatory signals, tissue remodeling and wound healing [21] [23]. The general consensus in the field suggests that ATMs resident macrophages have M2 polarization and that obesity-induced inflammation changes its polarization into M1 state.

Macrophages were first implicated in the development of obesity-induced inflammation when ATM numbers were noted to be significantly higher upon feeding animals a high fat diet [24,25], also correlating with an increase in insulin resistance. Several successive studies in animal models and humans confirmed that an increase in ATM numbers is a hallmark of obesity-induced inflammation and weight loss leads to decreases in infiltrated ATMs [26] [22] [27].

1.3.3 Neutrophils

Neutrophils are an important component of innate immunity responding to obesity complications [28]. They utilize intracellular vesicles (granules) that bear enzymes such as neutrophil elastase [29] and myeloperoxidase [30], and release it in the inflammation site to break down extracellular matrix protein [31] and aid in combating invading microbes. However, neutrophils also produce large amounts of cytokines and chemokines, including TNF-α, IL-1β, IL-8 and MIP-1α, allowing recruitment of more immune cells, particularly macrophages [28].

Neutrophils have been implicated in the development of obesity-induced inflammation [30] [32]. They invade liver and adipose tissue early in the obesity process [29], and similarly to their response to microbes, neutrophils secrete macrophage-recruiting cytokines, creating a secondary recruitment of immune cells. Neutrophil released enzymes also play a role in obesity-induced insulin resistance, specifically neutrophil elastase. In one study that used high fat diet feeding to induce inflammation it was demonstrated that neutrophil elastase degrades IRS-1 hence increasing insulin resistance [29]. It was further shown that pharmacological and genetic

inhibition of neutrophil elastase improves obesity-induced insulin resistance and inflammation in the adipose and liver tissue [29]. Another study suggested that the imbalance between neutrophil elastase and its inhibitor α1-antitrypsin, which is produced by the liver, is responsible for causing insulin sensitivity and inflammation [33].

1.4 Breast cancer

Breast cancer is the most common type of cancer among women. It has been estimated that each year more than 200,000 new cases are diagnosed in the United States [34]. In 2013, approximately 40,000 deaths occurred due to this disease [35]. Breast cancer incidence has been steadily increasing and mortality rates decreasing over the past 10 years largely due to the improvement in public awareness and early detection methods such as mammography screening [36]. Several risk factors have been found to contribute to breast cancer development including alcohol consumption [37], family history [38], early menarche and late menopause [39], circulating hormone levels [40], inflammation [41], diet [42] and body mass index (BMI) [42,43],

1.4.1 Breast cancer development

Breast cancer is a collection of diseases characterized by an abnormal proliferation of the epithelium in the breast. Breast tumors typically start in the epithelium of the mammary gland, consisting of lobules and ducts, when an epithelial cell acquires a genetic mutation allowing it to survive at a higher rate than other cells in the tissue. Up to this point, the tissue is benign and is termed hyperplasia. As more mutations are acquired over time, cell proliferation increases and nuclear morphology changes. With increased mutations, local tumors form in the tissue (in situ), invade and eventually metastasize to other organs. An example of ductal carcinoma progression is depicted in figure 1.3

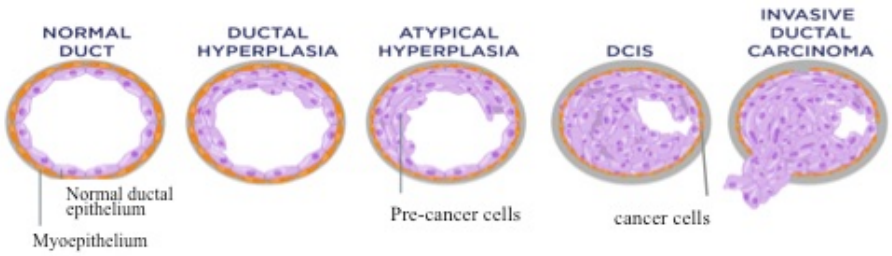

Figure 1.3 Schematic of ductal carcinoma progression. Adapted from http://aegiscreative.com/wp-content/uploads/2014/01/Figure-1.png

1.4.2 Breast cancer types and treatment

Tumors are pathologically categorized by the expression or absence of certain protein markers, including estrogen receptors (ER+/ ER-), progesterone receptors (PR+/PR-), and human epidermal growth factor receptor 2 (HER2+/HER2-) [44,45]. These markers assist in tailoring breast cancer treatments and in prognosis predictions. Among the subgroups of breast cancer is Triple Negative Breast Cancer (TNBC)(ER-, PR- Her2-), which is considered one of the most aggressive forms of breast cancer since it lacks expression of these three receptors, making it challenging to target therapeutically [44] [46].

Upon characterization of the malignant tumor, a combination of treatments is given to affected individuals. Current treatment options consist of surgery, which can be a complete removal of the breast (mastectomy) or breast-conserving surgery (also known as partial mastectomy, quadrantectomy, and lumpectomy). For the latter options the tumor and margins consisting of normal tissue around the tumor are removed. Radiation therapy is typically used post-surgery, aimed to kill left over cancer cells at the tumor location and it has been shown to reduce reoccurrence rates by 50% [47,48]. Systemic therapies are also another treatment option that can be combined with the other therapies and several treatment strategies have been developed over time. Initially, chemotherapeutics were used based on tumor size and cellular characteristic. However, more advanced targeted approaches have emerged: Hormonal

therapy, such as Tamoxifen, targets the estrogen receptor, which is upregulated in ER+ subtypes. Humanized antibodies, such as Herceptin, can target the HER2 receptor in HER2+ subtypes. Some drawbacks have been observed with these therapies like nausea and vomitting occur in patients, additionally, cancer cells can develop resistance to targeted therapies. Hence, novel therapeutic approaches to either reduce the side effects or improve patient prognosis would be beneficial.

1.5 The WNT signaling pathway

Several signaling pathways have been implicated in driving proliferation of normal mammary epithelial and cancer cells, maintaining their stem cell characteristics and survival by activating embryonic and developmental signaling pathways. The Wnt signaling pathway is an excellent example. Activation of Wnt signaling occurs when Wnt ligands bind to Frizzled (FZD) receptors in conjunction with one of the LDL receptor-related proteins (LRP5 or LRP6). Receptor activation leads to increased nuclear β-catenin levels and its translocation to the nucleus, where it forms a complex with the TCF/LEF1 family of HMG box transcription factors and stimulates the expression of specific target genes. Wnt signaling can be antagonized by secreted frizzled-related proteins (SFRPs) that mimic WNT co-receptor FZD. The Wnt/β-catenin signaling pathway is a critical pathway that has been implicated in several functions in relation with obesity and its complications. It has been shown to regulate adipogenesis in a paracrine and autocrine manner and to control adipocyte differentiation [49] [6] [50] [51], as have the the Wnt regulators, SFRPs [52] [53]. Other studies have also shown how Wnts and SFRPs influence inflammation [53] [54-56]. Current research is aimed at trying to inhibit these pathways to affect a cure. Interestingly, a number of phytochemicals have been shown to alter such pathways.

1.6 Nutraceuticals

The number of individuals who have adopted complementary and alternative medicine is gradually increasing as an approach to benefit personal health and complement conventional medicine. Various plants used in traditional medicine have been demonstrated to have anti-oxidative, anti-cancer and immune-modulatory effects [57] [58] [59] [60]. Several active components have been identified and characterized from these plants, and have been termed nutraceuticals. Alternative means to manage and prevent diseases has been a motive to explore nutraceuticals and understand how cellular changes are mediated, which lead to an overall improvement in the presented symptoms. Nutraceuticals are typically non-toxic, which gives it an advantage over synthetic drugs, however improper use could lead to serious clinical complications [61]. Therefore, investigations of the mechanism of action, side effects and targets of these plants are needed in order to better dietary supplement recommendations, more effective disease prevention and treatment strategies.

1.7 *Rhodiola crenulata*

Rhodiola sp. is a perennial herbaceous plant growing primarily in dry sandy ground at high altitudes in the arctic areas of Europe and Asia, and more than 70 species have been reported to exist [62]. *Rhodiola sp.* roots have been traditionally used to increase physical endurance, reduce fatigue, prevent high altitude sickness, and to relieve depression [63]. It has been reported that *Rhodiola sp.* has adaptogenic, anti-hypoxic, and anti-carcinogenic properties [64-66], in addition to learning and memory enhancements [63].

1.7.1 *Rhodiola sp*. studies with obesity and its complications

Interestingly, *Rhodiola sp.* have been used traditionally to treat diabetes [67]. Several studies have reported that *Rhodiola sp.*,more specifically *Rhodiola rosea* and *R. crenulata,* can

lower blood glucose levels. In a clinical study with 27 type 2 diabetic patients, *R. crenulata* tea treatment for 12–24 months significantly lowered blood glucose concentration, and improved liver and kidney functions. *R. crenulata* and *R. rosea* have also been shown to have amylase and glucosidase inhibitory activity, suggesting that these plants might have the ability to reduce complex sugars in the small intestine [68]. Extracts or isolated components from *R. rosea* have been implicated in glucose metabolism enhancement in various cell types and tissues. For instance,*Rhodiola rosea* increases essential energy metabolites, including adenosine triphosphate (ATP) and creatine phosphate, in the muscle and brain mitochondria of mice made to swim to their limit [69]. Salidroside, a major component of *Rhodiola sp.*, has been shown to stimulate glucose uptake in skeletal muscle cells and 3T3L1 cells by activating AMP-activated protein kinase [70,71]. Additionally, *R. crenulata* has been shown to inhibit adipogenesis *in vitro*[72] and has been shown to reduce blood triglyceride levels *in vivo* [73]. Lastly, a diabetic rat model treated with *R. crenulata* has been shown to decrease fasting insulin levels, serum triglycerides and free fatty acids [73]. To date, it is unclear by which mechanism whole *Rhodiola sp.* root extract ameliorates glucose metabolic disorders and insulin sensitivity.

1.7.2 *Rhodiola* anti-neoplastic studies

Over the past decade several studies have documented that *Rhodiola sp*, also has properties that could be used towards the prevention or treatment of cancer. *Rhodiola rosea* was shown to decrease DNA damage in bone morrow cells from mice in response to the mutagen N-nitroso-N-methylurea [74]. It has been shown to increase cell death in several cancer cell lines (i.e. HL-60 cells)[75]. Also, *R. rosea* and salidroside, have been shown to induce autophagy in bladder cancer cell lines [66]. In humans, *R.rosea* has been shown to improve superficial bladder carcinoma urothelial tissue integration, an indicator of good prognosis, and

increase as well as improve T-cell immunity [76]. In our lab, we have previously demonstrated *R. crenulata*'s ability to decrease tumor growth in mice harboring a syngeneic triple negative mesenchymal- like breast tumor[77], decrease cancer stem cell characteristics *in vitro* (tumorsphere formation and invasion) and increase sensitivity to anoikis (cell death in response to loss of attachment)[78].

Many plant supplements/phytochemicals have been shown to have estrogenic activity, however it is currently unknown whether *Rhodiola sp.* exhibits estrogenic effects. A unique abstract suggested that *R. rosea* was able to bind to the estrogen receptor [79], but no effects on transcriptional activation were described. This is an important question because if *R. rosea* is estrogenic, then women who have had ER+ breast cancer should be advised not to supplement with it to alleviate depression. Therefore, we were interested in determining whether *R. crenulata* exhibits estrogenic activity *in vivo* or *in vitro*.

1.8 Statement of thesis

The overall goal of the dissertation work outlined here was to provide new insights on how *R. crenulata* enhances glucose homeostasis under DIO conditions, and uncover possible mechanisms of *R. crenulata*'s anti-neoplastic characteristics. *R. crenulata* roots have been used in Eastern medicine for more than 100 years to alleviate high altitude sickness and fatigue without causing negative side effects. With that promising prospective, we thought it would be beneficial to understand how *R.crenulata* influences the observed improvements in these two disease states. In this dissertation I focused on two conditions: obesity and its complications and breast cancer.

In chapter 2, we describe and characterize how diet-induced obesity (DIO) affected mice lacking the expression of *Sfrp 1*. Considering the involvement of SFRP1 in adipogenesis and

inflammation, it still remained unknown how DIO obesity affected adipogenesis and inflammation in *Sfrp 1* knock out mouse model. We report that loss of *Sfrp1* exacerbates weight gain, glucose homeostasis and inflammation in mice in response to diet induced obesity (DIO). *Sfrp1*$^{-/-}$ mice fed a high fat diet (HFD) exhibited an increase in body mass accompanied by increases in body fat percentage, visceral WAT mass, and adipocyte size. Moreover, *Sfrp1* deficiency increases the mRNA levels of key *de novo* lipid synthesis genes (*Fasn*, *Acaca*, *Acly*, *Elovl*, *Scd1*) and the transcription factors that regulate their expression (*Lxr-, Srebp1, Chreb,* and *Nr1h3*) in WAT. Also, fasting glucose levels were elevated, glucose clearance was impaired, hepatic gluconeogenesis regulators were aberrantly upregulated (*G6pc* and *Pck1*), and glucose transporters were repressed (*Slc2a2* and *Slc2a4*) in *Sfrp1*$^{-/-}$ mice fed a HFD. Additionally, we observed increased steatosis in the livers of *Sfrp1*$^{-/-}$ mice. When there is an expansion of adipose tissue there is a sustained inflammatory response accompanied by adipokine dysregulation, which leads to chronic subclinical inflammation. Thus, we assessed the inflammatory state of different tissues and revealed that *Sfrp1*$^{-/-}$ mice fed a HFD exhibited increased macrophage infiltration and expression of pro-inflammatory markers including *Il-6.* Our findings demonstrate that the expression of *Sfrp1* is a critical factor required for maintaining appropriate cellular signaling in response to the onset of obesity.

In chapter 3, we describe the protective effect of *R. crenulata* hydroalcaholic treatment on mice being fed a HFD for 12 weeks. Our results show that *R. crenulata* enhanced insulin sensitivity in an obese mouse model and decreased liver inflammation. These observations suggest a possible mechanism to explain how *R. crenulata* affects insulin sensitivity, and suggests that *R. crenulata* is a candidate for the attenuation of liver inflammation. Additionally, we describe how glucose homeostasis is affected by *R. crenulata* treatment in the extreme obesity model developed in chapter 2.

In chapter 4, we reveal the inhibition of WNT/ β-catenin signaling by *R. crenulata* in the triple negative breast cancer cell line, MDA-MB-231. As mentioned earlier, the lab had previously shown that *R. crenulata* inhibits migration and increases sensitivity to cell death in TNBC cell lines [78], and we sought to identify the mechanism by which it imparts these effects. We demonstrate that *R. crenulata* inhibits the canonical WNT signaling pathway in MDA-MB-231 cells by showing reduced β-catenin transcriptional activity and function. We further show that *R. crenulata* inhibits β-catenin activity even when β-catenin accumulation is induced ligand independently, and that it prevents β-catenin nuclear localization. Our data convincingly show that *R. crenulata* inhibits a critical pathway, WNT/ β-catenin signaling, in a triple negative breast cancer cell line and suggests a likely mechanism by which *R. crenulata* inhibits invasion and increases sensitivity to death.

In chapter 5, we describe *R. crenulata* estrogenic activity on ER+ breast cancer cell line (MCF7) over time *in vitro*, and how it affects normal mammary epithelial ER target gene expression *in vivo.* We show an initial activation of ER transcriptional activity by dual reporter assay, qPCR and proliferation of MCF7 cells in response to 24 hours of *R. crenulata* treatment. However, upon longer treatment basal and *R. crenulata* induced transcriptional activity was suppressed. Additionally, there was a decrease in cell doubling times and a decrease in tumorsphere formation. In association with these changes, ERα transcript levels were decreased and active β−catenin levels were reduced in the cells treated for 2 weeks. Finally, we show no change in estrogen targets in normal mammary cells *in vivo.* These data suggest that the *R. crenulata* extract contains components with estrogenic activity. However, *R. crenulata* treatment could still be as protective in ER+ breast cancer cells, as longer treatment reduced the transcriptional activity of β−catenin and ER responses leading to reduced proliferation and

tumorsphere formation. Furthermore, administration of 20 mg/kg/day *R. crenulata* to mice did not have an observable effect on mammary epithelial ERα target gene expression *in vivo*.

1.9 References

[1] An R. Prevalence and Trends of Adult Obesity in the US, 1999-2012. ISRN Obes 2014;2014:185132.

[2] Ogden CL, Carroll MD, Kit BK, Flegal KM. Prevalence of obesity among adults: United States, 2011-2012. NCHS Data Brief 2013:1–8.

[3] Flegal KM, Carroll MD, Ogden CL, Curtin LR. Prevalence and Trends in Obesity Among US Adults, 1999-2008. Jama 2010;303:235–41.

[4] Polednak AP. Estimating the number of U.S. incident cancers attributable to obesity and the impact on temporal trends in incidence rates for obesity-related cancers. Cancer Detect Prev 2008;32:190–9.

[5] Hotamisligil GS. Inflammation and metabolic disorders. Nature 2006.

[6] Sun K, Kusminski CM, Scherer PE. Adipose tissue remodeling and obesity. J Clin Invest 2011;121:2094–101.

[7] Moon B, Kwan J, Duddy N. Resistin inhibits glucose uptake in L6 cells independently of changes in insulin signaling and GLUT4 translocation. American Journal of … 2003.

[8] Stephens JM, Pekala PH. Transcriptional repression of the C/EBP-alpha and GLUT4 genes in 3T3-L1 adipocytes by tumor necrosis factor-alpha. Regulations is coordinate and independent of protein synthesis. J Biol Chem 1992;267:13580–4.

[9] Stephens JM, Lee J, Pilch PF. Tumor necrosis factor-alpha-induced insulin resistance in 3T3-L1 adipocytes is accompanied by a loss of insulin receptor substrate-1 and GLUT4 expression without a loss of insulin receptor-mediated signal transduction. J Biol Chem 1997;272:971–6.

[10] Rui L, Aguirre V, Kim JK, Shulman GI, Lee A, Corbould A, et al. Insulin/IGF-1 and TNF-alpha stimulate phosphorylation of IRS-1 at inhibitory Ser307 via distinct pathways. J Clin Invest 2001;107:181–9.

[11] Hotamisligil GS, Shargill NS, Spiegelman BM. Adipose expression of tumor necrosis factor-alpha: direct role in obesity-linked insulin resistance. Science 1993;259:87–91.

[12] Cheung AT. An in Vivo Model for Elucidation of the Mechanism of Tumor Necrosis Factor- (TNF-)-Induced Insulin Resistance: Evidence for Differential Regulation of Insulin Signaling by TNF. Endocrinology 1998;139:4928–35.

[13] De Taeye BM, Novitskaya T, McGuinness OP, Gleaves L, Medda M, Covington JW, et al. Macrophage TNF- contributes to insulin resistance and hepatic steatosis in diet-induced obesity. AJP: Endocrinology and Metabolism 2007;293:E713–25.

[14] Uysal KT, Wiesbrock SM, Marino MW, Hotamisligil GS. Protection from obesity-induced insulin resistance in mice lacking TNF-α function. Nature 1997;389:610–4.

[15] Pradhan AD, Manson JE, Rifai N, Buring JE, Ridker PM. C-reactive protein, interleukin 6, and risk of developing type 2 diabetes mellitus. Jama 2001;286:327–34.

[16] Hong E-G, Ko HJ, Cho Y-R, Kim H-J, Ma Z, Yu TY, et al. Interleukin-10 prevents diet-induced insulin resistance by attenuating macrophage and cytokine response in skeletal muscle. Diabetes 2009;58:2525–35.

[17] Cai D, Yuan M, Frantz DF, Melendez PA, Hansen L, Lee J, et al. Local and systemic insulin resistance resulting from hepatic activation of IKK-β and NF-κB. Nature Medicine 2005;11:183–90.

[18] Park EJ, Lee JH, Yu G-Y, He G, Ali SR, Holzer RG, et al. Dietary and Genetic Obesity Promote Liver Inflammation and Tumorigenesis by Enhancing IL-6 and TNF Expression. Cell 2010;140:197–208.

[19] Akdis CA, Blaser K. Mechanisms of interleukin-10-mediated immune suppression. Immunology 2001;103:131–6.

[20] Gordon S, Taylor PR. Monocyte and macrophage heterogeneity. Nat Rev Immunol 2005;5:953–64.

[21] Gordon S. Alternative activation of macrophages. Nat Rev Immunol 2003;3:23–35.

[22] Cinti S. Adipocyte death defines macrophage localization and function in adipose tissue of obese mice and humans. The Journal of Lipid Research 2005;46:2347–55.

[23] Suganami T, Ogawa Y. Adipose tissue macrophages: their role in adipose tissue remodeling. Journal of Leukocyte Biology 2010;88:33–9.

[24] Xu H, Barnes GT, Yang Q, Tan G, Yang D, Chou CJ, et al. Chronic inflammation in fat plays a crucial role in the development of obesity-related insulin resistance. J Clin Invest 2003;112:1821–30.

[25] Weisberg SP, McCann D, Desai M, Rosenbaum M, Leibel RL, Ferrante AW Jr. Obesity is associated with macrophage accumulation in adipose tissue. J Clin Invest 2003;112:1796–808.

[26] Osborn O, Olefsky JM. The cellular and signaling networks linking the immune system and metabolism in disease. Nature Medicine 2012;18:363–74.

[27] Lee J. Adipose tissue macrophages in the development of obesity-induced inflammation, insulin resistance and type 2 Diabetes. Arch Pharm Res 2013;36:208–22.

[28] Pham CTN. Neutrophil serine proteases: specific regulators of inflammation. Nat Rev Immunol 2006;6:541–50.

[29] Talukdar S, Oh DY, Bandyopadhyay G, Li D, Xu J, McNelis J, et al. Neutrophils mediate insulin resistance in mice fed a high-fat diet through secreted elastase. Nature Medicine 2012;18:1407–12.

[30] Nijhuis J, Rensen SS, Slaats Y, van Dielen FMH, Buurman WA, Greve JWM. Neutrophil Activation in Morbid Obesity, Chronic Activation of Acute Inflammation. Obesity 2009;17:2014–8.

[31] Waki H, Yamauchi T, Kamon J, Kita S, Ito Y, Hada Y, et al. Generation of Globular Fragment of Adiponectin by Leukocyte Elastase Secreted by Monocytic Cell Line THP-1. Endocrinology 2005;146:790–6.

[32] Elgazar-Carmon V, Rudich A, Hadad N, Levy R. Neutrophils transiently infiltrate intra-abdominal fat early in the course of high-fat feeding. The Journal of Lipid Research 2008;49:1894–903.

[33] Mansuy-Aubert V, Zhou QL, Xie X, Gong Z, Huang J-Y, Khan AR, et al. Imbalance between Neutrophil Elastase and its Inhibitor α1-Antitrypsin in Obesity Alters Insulin Sensitivity, Inflammation, and Energy Expenditure. Cell Metabolism 2013;17:534–48.

[34] DeSantis CE, Lin CC, Mariotto AB, Siegel RL, Stein KD, Kramer JL, et al. Cancer treatment and survivorship statistics, 2014. CA: a Cancer Journal for Clinicians 2014;64:252–71.

[35] Siegel R, Naishadham D, Jemal A. Cancer statistics, 2013. CA: a Cancer Journal for Clinicians 2013;63:11–30.

[36] Breen N, Gentleman JF, Schiller JS. Update on mammography trends. Cancer 2010;117:2209–18.

[37] Ellison RC, Zhang Y, McLennan CE, Rothman KJ. Exploring the relation of alcohol consumption to risk of breast cancer. Am J Epidemiol 2001;154:740–7.

[38] Pharoah PD, Day NE, Duffy S, Easton DF, Ponder BA. Family history and the risk of breast cancer: a systematic review and meta-analysis. Int J Cancer 1997;71:800–9.

[39] Brinton LA, Schairer C, Hoover RN, Fraumeni JF. Menstrual factors and risk of breast cancer. Cancer Invest 1988;6:245–54.

[40] Nelson HD, Humphrey LL, Nygren P, Teutsch SM, Allan JD. Postmenopausal Hormone Replacement Therapy. Jama 2002;288:872–10.

[41] Grivennikov SI, Greten FR, Karin M. Immunity, inflammation, and cancer. Cell 2010.

[42] Singletary SE. Rating the risk factors for breast cancer. Ann Surg 2003;237:474–82.

[43] Tretli S. Height and weight in relation to breast cancer morbidity and mortality. A prospective study of 570,000 women in Norway. International Journal of Cancer 1989;44:23–30.

[44] FRCPath PJSR-F, MD PLP. Breast Cancer 2Gene expression profiling in breast cancer: classification, prognostication, and prediction. The Lancet 2011;378:1812–23.

[45] Alizart M, Saunus J, Cummings M, Lakhani SR. Molecular classification of breast carcinoma. Diagnostic Histopathology 2012;18:97–103.

[46] Goldhirsch A, Wood WC, Coates AS, Gelber RD, Thurlimann B, Senn HJ, et al. Strategies for subtypes--dealing with the diversity of breast cancer: highlights of the St. Gallen International Expert Consensus on the Primary Therapy of Early Breast Cancer 2011. Ann. Oncol., vol. 22, 2011, pp. 1736–47.

[47] EBCTCG EBCTCG. Effect of radiotherapy after breast-conserving surgery on 10-year recurrence and 15-year breast cancer death: meta-analysis of individual patient data for 10â€ˆ801 women in 17 randomised trials. The Lancet 2011;378:1707–16.

[48] Buchholz TA. Radiotherapy and survival in breast cancer. The Lancet 2011;378:1680–2.

[49] Bennett CN. Regulation of Wnt Signaling during Adipogenesis. Journal of Biological Chemistry 2002;277:30998–1004.

[50] Ross SE, Hemati N, Longo KA, Bennett CN, Lucas PC, Erickson RL, et al. Inhibition of Adipogenesis by Wnt Signaling. Science 2000;289:950–3.

[51] Bennett CN, Hodge CL, MacDougald OA, Schwartz J. Role of Wnt10b and C/EBPα in spontaneous adipogenesis of 243 cells. Biochemical and Biophysical Research Communications 2003;302:12–6.

[52] Lagathu C, Christodoulides C, Tan CY, Virtue S, Laudes M, Campbell M, et al. Secreted frizzled-related protein 1 regulates adipose tissue expansion and is dysregulated in severe obesity. International Journal of Obesity 2010;34:1695–705.

[53] Mori H, Prestwich TC, Reid MA, Longo KA, Gerin I, Cawthorn WP, et al. Secreted frizzled-related protein 5 suppresses adipocyte mitochondrial metabolism through WNT inhibition. J Clin Invest 2012;122:2405–16.

[54] Pereira C, Schaer DJ, Bachli EB, Kurrer MO, Schoedon G. Wnt5A/CaMKII Signaling Contributes to the Inflammatory Response of Macrophages and Is a Target for the Antiinflammatory Action of Activated Protein C and Interleukin-10. Arteriosclerosis, Thrombosis, and Vascular Biology 2008;28:504–10.

[55] Pereira CP, Bachli EB, Schoedon G. The Wnt pathway: A macrophage effector molecule that triggers inflammation. Current Atherosclerosis Reports 2009;11:236–42.

[56] Barandon L, Casassus F, Leroux L, Moreau C, Allieres C, Lamaziere JMD, et al. Secreted Frizzled-Related Protein-1 Improves Postinfarction Scar Formation Through a

Modulation of Inflammatory Response. Arteriosclerosis, Thrombosis, and Vascular Biology 2011;31:e80–7.

[57] Kim SH, Hyun SH, Choung SY. Antioxidative effects of Cinnamomi cassiaeand Rhodiola roseaextracts in liver of diabetic mice. BioFactors 2006;26:209–19.

[58] Senthilkumar R, Parimelazhagan T, Chaurasia OP, Srivastava RB. Free radical scavenging property and antiproliferative activity of Rhodiola imbricata Edgew extracts in HT-29 human colon cancer cells. Asian Pacific Journal of Tropical Medicine 2012;6:11–9.

[59] Battistelli M, De Sanctis R, De Bellis R, Cucchiarini L, Dachà M, Gobbi P. Rhodiola rosea as antioxidant in red blood cells: ultrastructural and hemolytic behaviour. Eur J Histochem 2005;49:243–54.

[60] Li HX, Sze SCW, Tong Y, Ng TB. Production of Th1- and Th2-dependent cytokines induced by the Chinese medicine herb, Rhodiola algida, on human peripheral blood monocytes. J Ethnopharmacol 2009;123:257–66.

[61] Khanum F, Bawa AS, Singh B. Rhodiola rosea: A Versatile Adaptogen. Comprehensive Reviews in Food Science and Food Safety 2005;4:55–62.

[62] Brown RP, Gerbarg PL, Ramazanov Z. Rhodiola rosea**: A Phytomedicinal Overview**. A Phytomedicinal … 2002:40–52.

[63] Panossian A, Wikman G, Sarris J. Rosenroot (Rhodiola rosea): Traditional use, chemical composition, pharmacology and clinical efficacy. Phytomedicine 2010.

[64] Khanum F, Bawa AS, Singh B. Rhodiola rosea: a versatile adaptogen. … In Food Science and Food Safety 2005.

[65] Zheng K, Guo A, Bi C, Zhu K, Chan G, Fu Q, et al. The Extract of Rhodiolae Crenulatae Radix et Rhizoma Induces the Accumulation of HIF-1 αvia Blocking the Degradation Pathway in Cultured Kidney Fibroblasts. Planta Med 2010;77:894–9.

[66] Liu Z, Li X, Simoneau AR, Jafari M, Zi X. Rhodiola rosea extracts and salidroside decrease the growth of bladder cancer cell lines via inhibition of the mTOR pathway and induction of autophagy. Mol Carcinog 2011;51:257–67.

[67] progress of research study on pharmacological action of rhodiola rosea. Acute Chinese Medicine and Pharmacology 2003;31:57–9.

[68] Kwon Y-I, Jang H-D, Shetty K. Evaluation of Rhodiola crenulata and Rhodiola rosea for management of type II diabetes and hypertension. Asia Pac J Clin Nutr 2006;15:425–32.

[69] Abidov M, Crendal F, Grachev S, Seifulla R, Ziegenfuss T. Effect of Extracts from Rhodiola Rosea and Rhodiola Crenulata (Crassulaceae) Roots on ATP Content in Mitochondria of Skeletal Muscles. Bulletin of Experimental Biology and Medicine 2003;136:585–7.

[70] Li H-B, Ge Y-K, Zheng X-X, Zhang L. Salidroside stimulated glucose uptake in skeletal muscle cells by activating AMP-activated protein kinase. European Journal of Pharmacology 2008;588:165–9.

[71] Shu-Hai W. [Effects of salidroside on carbohydrate metabolism and differentiation of 3T3-L1 adipocytes]. Zhong Xi Yi Jie He Xue Bao 2004;2:193–5.

[72] Lee OH, Kwon YI, Apostolidis E, Shetty K. Rhodiola-induced inhibition of adipogenesis involves antioxidant enzyme response associated with pentose phosphate pathway. Phytotherapy … 2011.

[73] Wang J, Rong X, Li W, Yang Y, Yamahara J, Li Y. Rhodiola crenulata root ameliorates derangements of glucose and lipid metabolism in a rat model of the metabolic syndrome and type 2 diabetes. J Ethnopharmacol 2012;142:782–8.

[74] RA S, Aleksandrova IV, VK M, LN U, GG P. [Effect of Rhodiola rosea on the yield of mutation alterations and DNA repair in bone marrow cells]. Patologicheskaia Fiziologiia I Eksperimentalnaia Terapiia 1996.

[75] Majewska A, Grażyna H, Mirosława F, Natalia U, Agnieszka P, Alicja Z, et al. Antiproliferative and antimitotic effect, S phase accumulation and induction of apoptosis and necrosis after treatment of extract from Rhodiola rosea rhizomes on HL-60 cells. J Ethnopharmacol 2006;103:43–52.

[76] OA B, Matveev BP. The effect of a Rhodiola rosea extract on the incidence of recurrences of asuperficial bladder cancer (experimental clinical research). Urol Nefrol Mosk 1995:46–7.

[77] Tu Y, Roberts L, Shetty K, Schneider SS. Rhodiola crenulata induces death and inhibits growth of breast cancer cell lines. J Med Food 2008;11:413–23.

[78] Gauger KJ, Rodriguez-Cortes A. Rhodiola Crenulata inhibits the tumorigenic properties of invasive mammary epithelial cells with stem cell characteristics. Journal of Medicinal Food 2010.

[79] Eagon PK, Elm MS, Gerbarg PL, Houghton F Jr, Brown RP, Check JJ, et al. Evaluation of the medicinal botanical Rhodiola rosea for estrogenicity. Cancer Research 2004;64:663.

CHAPTER 2
MICE DEFICIENT IN SFRP1 EXHIBIT INCREASED ADIPOSITY, DYSREGULATED GLUCOSE METABOLISM, AND ENHANCED MACROPHAGE INFILTRATION

The work presented in this chapter was done in collaboration with Kelly Gauger (Gregory), Elizabeth M. Henchey, Josephine Wyman, Brooke Bentley, Melissa Brown, Akihiko Shimono. Parts of this chapter are taken from the original research article: Gauger KJ, Bassa LM, Henchey EM, Wyman J, Bentley B, et al. (2013) Mice Deficient in *Sfrp1* Exhibit Increased Adiposity, Dysregulated Glucose Metabolism, and Enhanced Macrophage Infiltration. PLoS ONE 8(12): e78320. doi:10.1371/journal.pone.0078320

2.1 Introduction

Obesity is a severe epidemic that causes predisposition to several metabolic diseases such as cardiovascular diseases and type-2 diabetes. It is caused by an increase in adipocyte size and eventually an increase in preadipocyte differentiation due to excess diet intake [1,2]. In 2010, the United States of America CDC reported that 35.7% of adult Americans are obese and 17% of children are obese as well [3]. This epidemic resulted in the push for more research aimed at exploring adipocyte differentiation and metabolism in order to further the understanding of molecular mechanisms, which regulate adipocyte biology in order to develop potential therapeutic targets.

Dietary fatty acids are primarily stored in white adipose tissue (WAT) as triglycerides and excess carbohydrates are converted to fats via de novo lipogenesis [4]. Most cells perform de novo lipogenesis, but adipocytes and hepatocytes are especially well adapted to the process. The genes involved in de novo lipogenesis are controlled by two master transcription regulator proteins which are regulated by either glucose (Carbohydrate Response Element Binding Protein -ChREBP) or insulin (Sterol Response Element Binding Protein 1- SREBP1). Increased de novo lipogenesis during adipogenesis is associated with improved insulin sensitivity [5], but the converse occurs in the liver where de novo lipogenesis correlates with insulin resistance, an

increase in serum triglycerides and adipocyte accumulation causing steatosis and nonalcoholic fatty liver disease [6].

Immune cells and other tissues produce cytokines, whereas WAT produce adipokines, such as adiponectin, Interleukin-6 (IL-6) and tumor necrosis factor (TNFα) [7] as well as hormones including leptin, estrogen and resistin. All of these factors play a variety of roles through different signaling pathways, including the Wnt/β-catenin signaling pathway, in multiple tissues. The physiological roles affected ranging from promoting or inhibiting adipogenesis, regulating the immunoresponse and insulin sensitization. Activation Wnt signaling occurs when Wnt ligands bind to Frizzled (FZD) receptors in conjunction with one of the LDL receptor-related proteins (LRP5 or LRP6). Receptor activation leads to increased nuclear β-catenin levels where it complexes with the TCF/LEF1 family of HMG box transcription factors and stimulates the expression of specific target genes. Wnt/β-catenin signaling has been shown to regulate adipogenesis in a paracrine and autocrine manner and to control adipocyte differentiation [8,9,10]. While Wnt6, Wnt10a and Wnt10b have been shown to inhibit preadipocyte differentiation [8,9,10], Wnt5b and Wnt4 promote adipogenesis [11,12].

Wnt activity is blocked by two different general strategies: dickkopfs (DKKs) and secreted frizzled-related proteins (SFRPs), which serve as, decoy LRP and FZD receptors respectively [13,14]. There are five members of the SFRP family of proteins in both human and mouse genomes (SFRP1and 5) with SFRP1, SFRP2 and SFRP5 forming a subfamily based on sequence similarity [15]. These proteins contain a cysteine-rich domain that is homologous to the Wnt-binding domain of FZD receptor proteins [16]. However, SFRPs do not contain a transmembrane domain and therefore reside in the extracellular compartment where they antagonize Wnt signaling by binding to Wnt ligands and prevent ligand-receptor interactions and signal transduction [17].

SFRP family members are involved in the regulation of adipogenesis. In vitro, treatment with recombinant SFRP1 or SFRP2 protein in 3T3-L1 preadipocytes inhibits the antiadipogenic Wnt/β-catenin signal and induces preadipocyte differentiation [18]. In mice, Sfrp1 expression increases during adipogenesis and in response to HFD. In humans, elevated SFRP1 levels are observed in mildly obese individuals and are reduced in response to extreme body weight in morbidly obese humans [18]. The role of Sfrp5 in obesity has been debated, as some groups have seen Sfrp5 expression increase with obesity and a protective effect against diet induced obesity (DIO) when Sfrp5 was eliminated [18,19,20], while others have observed that deletion of Sfrp5 exacerbates obesity and insulin resistance [21].

Increased obesity has been shown to increase pro-inflammatory cytokine production and macrophage infiltration and studies have shown the involvement of SFRP1 and Wnt5a in the inflammatory response. Specifically, Wnt5a is secreted by activated antigen presenting cells in rheumatoid arthiritis joints and promotes the production cytokines including Interleukin (IL)-1, IL-6 and IL-8 through the Fzd5- CamKII noncononical Wnt signaling pathway [22,23]. SFRP1 has been shown to inhibit this process [24,25] and has also been shown to block leukocyte activation and cytokine production in vitro [26] as well as decrease neutrophil infiltration in ischemic tissue in vivo [27]. Thus, SFRP1 plays an important role in modulating the inflammatory response.

Considering the involvement of SFRP1 in adipogenesis and inflammation, we sought to determine the effects of diet-induced obesity (DIO) in the Sfrp1-/- mouse model. Our data reveal that Sfrp1-/- mice exhibit increased adipocity in WAT, hepatic steotosis, glucose homeostasis irregularities and increased inflammatory responses. These novel findings suggest that SFRP1 is a key regulatory factor that modulates cellular responses to obesity.

2.2 Materials and Methods

2.2.1 Animals

This study was carried out in strict accordance with the recommendations in the Guide for the Care and Use of Laboratory Animals of the National Institutes of Health. The protocol was approved by the Baystate Medical Center Institutional Animal Care and Use Committee (Permit Number: 283237). Female129/C57Blk6 control mice (n=20) and 129/C57Blk6 *Sfrp1*$^{-/-}$ mice (n=20) were individually housed in plastic cages with food and water provided continuously, and maintained on a 12:12 light cycle. Mice (n=10/genotype) were placed on either a normal diet [(ND) Harlan Teklad global 18% protein rodent diet (#2018) containing 2.8% fat, 18.6% protein] or placed on a high fat diet [(HFD) Bio-Serv (#F1850) containing 36.0 % fat, 36.2% carbohydrate, and 20.5% protein] starting at 10 weeks of age for 12 weeks. Body weight was recorded every three days and body composition was monitored with an Echo MRI-100 (Echo Model Systems, Houston TX) prior to initiating the study, 6 weeks after putting the mice on the diet, and at the end of the study. Upon completion of metabolic measurements, mice were euthanized by CO_2 followed by cervical dislocation and bled by cardiac puncture. Mammary glands (3rd, 4th, and 5th inguinal glands), white adipose tissue [(WAT) gonadal, renal, mesenteric, and scapular fat pads], brown adipose tissue (BAT), liver, pancreas, spleen, ovary, kidney, bone, intestines and muscle were harvested, weighed and fixed in buffered formalin. In addition, mammary glands, WAT, BAT, and livers were flash frozen.

2.2.2 Adipocyte size

The mean adipocyte size of the gonadal fat pad was determined by computer-assisted image analysis of adipose tissue sections stained with hematoxylin and eosin. Briefly, fluorescent images were captured at 100X (Nikon ECLIPSE TE2000-U) and measured with

CellProfiler software (The Broad Institute). Cells were identified and false positives were removed by setting appropriate threshold. Images were then converted to a binary black and white image, membranes were shrunk to a skeleton (1 pixel wide), and then images were inverted. Adipocytes were identified by software pixels were recorded and converted to microns. False positive areas (area below 100 μm^2) were discarded.

2.2.3 Glucose tolerance test

Glucose tolerance tests (GTTs) were carried out 2, 6, and 12 weeks after animals were placed on the ND or HFD. Briefly, mice were fasted for 16 hours, weighed, and their fasting glucose levels were measured from 1-2 μl of blood obtained from the tail vein using a glucometer (OneTouch Ultra; Lifescan, Milpitas, CA). Mice were injected with glucose (2 g of D-glucose per kg of body weight) in the interperitoneal cavity and blood glucose levels were assessed 15, 30, 60, 90, and 120 minutes after injection.

2.2.4 Analysis of serum insulin

At the time of GTT analysis, blood was also collected from the tail vein into microfuge tubes before glucose injection and 15 minutes following injection. Serum was collected after centrifugation at 1,500 x g for 15 min at 4°C. Insulin levels were assessed by ultrasensitive ELISA with mouse insulin standard according to the manufacturer's instructions (Crystal Chem Inc, Downers Grove IL).

2.2.5 RNA Isolation and Real-Time PCR analysis

Total RNA was extracted from gonadal fat pad and liver of mice in each treatment group (n=6) as described previously [28]. Relative levels of the mRNA expression of target genes were determined by quantitative real-time PCR using the Mx3005P real-time PCR system (Stratagene,

La Jolla, CA) and all values were normalized to the amplification of β-Actin and calculated using the $2^{-(\Delta\Delta Ct)}$ method. The PCR primer sequences are described in Table 1 and Table S1. The assays were performed using the 1-Step Brilliant SYBRIII Green RT-PCR Master Mix Kit (Stratagene) containing 200 nM forward primer, 200 nM reverse primer, and 100 ng total RNA. The conditions for cDNA synthesis and target mRNA amplification were performed as follows: 1 cycle of 50°C for 30 min; 1 cycle of 95°C for 10 min; and 35 cycles each of 95°C for 30 s, 55°C for 1 min, and 72°C for 30 s.

2.2.6 Immunohistochemistry

Immunohistochemistry (IHC) was performed on a DakoCytomation autostainer using the Envision HRP Detection system (Dako, Carpinteria, CA). Each tissue block was sectioned at 4 μm on a graded slide, deparaffinized in xylene, rehydrated in graded ethanols, and rinsed in Tris-phosphate-buffered saline (TBS). Heat induced antigen retrieval was performed in a microwave at 98ºC in 0.01 M citrate buffer. After cooling for 20 minutes, sections were rinsed in TBS and subjected to primary antibodies 1:100 [Glut4 (Novus Biologicals, Littleton, CO) and F4/80 (AbD, Serotec, Hercules, CA)] for 45 minutes. Immunoreactivity was visualized by incubation with chromogen diaminobenzidine (DAB) for 5 minutes. Tissue sections were counterstained with hematoxylin, dehydrated through graded ethanols and xylene, and cover-slipped. Images were captured with an Olympus BX41 light microscope using SPOT Software 5.1 (SPOT™Imaging Solutions, Detroit, MI).

2.2.7 Analysis of hepatic steatosis

Formalin fixed livers were paraffin-embedded and sections were cut on a Leica microtome at a thickness of 4 μm on Superfrost-plus slides, and stained with hematoxylin and

eosin (H&E) per standard protocol. Frozen sections were used for the detection of lipid. Freshly dissected liver was cryoprotected in 30% sucrose overnight and then flash frozen in Tissue-Tek OCT compound (Sakura). Cryosections 10 μm thick were processed for Oil Red O staining in a 0.3% solution of Oil Red O (Sigma, St. Louis, MO) in 60% isopropanol for 15 min. After washes in 60% isopropanol, sections were counterstained with Mayer's hematoxylin. Images were captured with an Olympus BX41 light microscope using SPOT Software 5.1 (SPOT™Imaging Solutions).

2.2.8 Statistical Analysis

Results were analyzed using a two-way ANOVA with *Sfrp1* loss and HFD treatment as the main effects unless otherwise stated. *Post hoc* tests, where appropriate, were performed by Bonferroni's *t* test. Bonferroni's *t* test uses the mean square error from the ANOVA table as a point estimate of the pooled variance (Graphpad Prism, San Diego, CA). Group means were compared using Student's t-tests (Graphpad Prism) and results with $P<0.05$ were considered significant. Multilevel mixed-effects linear regression was used to compare genotype and diet groups on mean change in insulin secretion from 0-15 minutes, accounting for any within-subject correlation of repeated measurements of mice at 2, 6 and 12 weeks. Grubb's test was used on all data to identify statistical outliers (http://www.graphpad.com/quickcalcs). Statistical outliers were identified in some data sets, but the overall results were not altered by omission. A few samples were lost during processes; therefore, there are some unequal sample sizes.

2.2.9 Islet Isolation

Age matched male 129/C57Blk6 control mice (n=3) and 129/C57Blk6 Sfrp1-/- mice (n=3) were sacrificed and Collagenase P enzyme solution (1.2-1.4 mg/mL; Roche Diagnostics

Corporation, Indianapolis, IN) was injected to fully distend the donor pancreas. After digestion, islets were gradient purified and then handpicked. Cells were cultured with RPMI-1640 solution with 10% heat-inactivated fetal bovine serum and 1% penicillin-streptomycin (RPMI-1640, FBS and P-S all from Mediatech, Inc. Manassas, VA) in a 5% CO2 incubator overnight.

2.2.10 Glucose Stimulated Insulin Secretion Assay

Islets were equilibrated in low glucose solution (2.8 mM) for one hour. Ten size-matched islets (in triplicate samples) were placed in 12 μm Millicell Cell Culture PCF inserts (Millipore Corporation, Burlington, MA) in 24 well plates. Fresh, low glucose solution was added for 2 hours followed by moving the insert with the islets into high glucose solution (16.7 mM) for 2 hours. Insulin secretion was determined by ELISA (Mercodia, Winston Salem, NC) according to the manufacturer's instruction.

2.2.11 Islet Quantification and IHC

Formalin fixed pancreas was paraffin-embedded and subjected to H&E staining (n=6/treatment group). Sections were viewed were captured with an Olympus BX41 light microscope and the total number of islets per tissue section were counted. IHC was performed as described in the main body of the research article. Tissue was incubated with primary antibodies 1:100 [C-peptide (Cell Signaling, Danverse, MA) and Glucagon (Cell Signaling) for 45 minutes. Images were captured with an Olympus BX41 light microscope using SPOTSOFTWARE.

2.2.12 Insulin tolerance test

Mice were fasted for 4 hours, weighed, and their fasting blood glucose levels were measured from the tail vein using a glucometer (OneTouch Ultra; Lifescan, Milpitas, CA). Mice were injected with human regular insulin (Eli Lilly, Indianapolis, IN) at a concentration of 0.8 unit

of insulin per kg of body weight in the interpretational cavity and blood glucose levels were assessed 15, 30, 60, 90, and 120 minutes after injection.

2.3 Results

2.3.1 Loss of Sfrp1 exacerbates weight gain and adiposity in mice fed a HFD

Since it has previously been shown that Sfrp1 levels are reduced in the adipose tissue of severely obese mice and humans [18], we chose to evaluate the effects of diet-induced obesity (DIO) in Sfrp1-/- mice. Control and Sfrp1-/- mice were fed either a high fat diet (HFD) or a normal diet (ND) for 10 weeks after reaching 12 weeks of age. Both control and Sfrp1-/- mice fed a HFD gained weight as expected (Fig. 2.1A, left panel), with a more rapid increase in Sfrp1-/- mice when compared to control mice. A two-way ANOVA revealed a significant effect on final body weight in response to Sfrp1 deficiency ($F_{1, 36}=7.95$; $P<0.01$) and the HFD ($F_{1, 36}=17.04$; $P<0.001$), but there was no interaction between these two main effects ($F_{1, 36}=2.07$; $P<0.05$) (Fig. 2.1A, left panel). Body fat analysis demonstrated that body fat percentage is affected by Sfrp1 loss ($F_{1, 36}=45.25$; $P<0.0001$) at the time the study was initiated, but there is understandably no diet effect ($F_{1, 36}=0.12$; $P>0.05$) or interaction between the two main effects ($F_{1, 36}=3.67$; $P>0.05$) (Fig. 2.1B, 0 Weeks). On the other hand, at the later time points, body fat percentage was affected by both Sfrp1 loss (6 weeks: $F_{1, 35}=16.05$; $P<0.001$; 12 weeks: $F_{1, 35}=8.03$; $P<0.01$) and the HFD (6 weeks: $F_{1, 35}=63.83$; $P<0.0001$; 12 weeks: $F_{1, 35}=59.31$; $P<0.0001$), but there was no interaction between the two main effects (6 weeks: $F_{1, 35}=3.37$; $P>0.05$; 12 weeks: $F_{1, 35}=0.51$; $P>0.05$) (Fig 2.1B 6 &12 weeks). Evaluation of fat depot weight at the end of the study demonstrated that in response to a HFD, there was a significant increase in the white adipose tissue (WAT) from Sfrp1-/- mice, both the visceral gonadal fat pad and in the subcutaneous scapular fat pad (Fig. 2.1C). Loss of Sfrp1 did not affect the weight of 3rd, 4th,

and 5th inguinal mammary glands and also did not change the weight of brown adipose tissue (BAT) (Fig. 2.1C). Additionally, organ weight was recorded in animals on both diets and there were no significant changes in response to Sfrp1 deficiency (Fig. 2.S1). Measurement of the adipocytes comprising the gonadal fat pad demonstrated that there is a significant increase in adipocyte size from Sfrp1-/- mice compared to control mice fed a Fig. 2.1D). Taken together these data illustrate that loss of Sfrp1 exacerbates weight gain and adiposity in response to HFD.

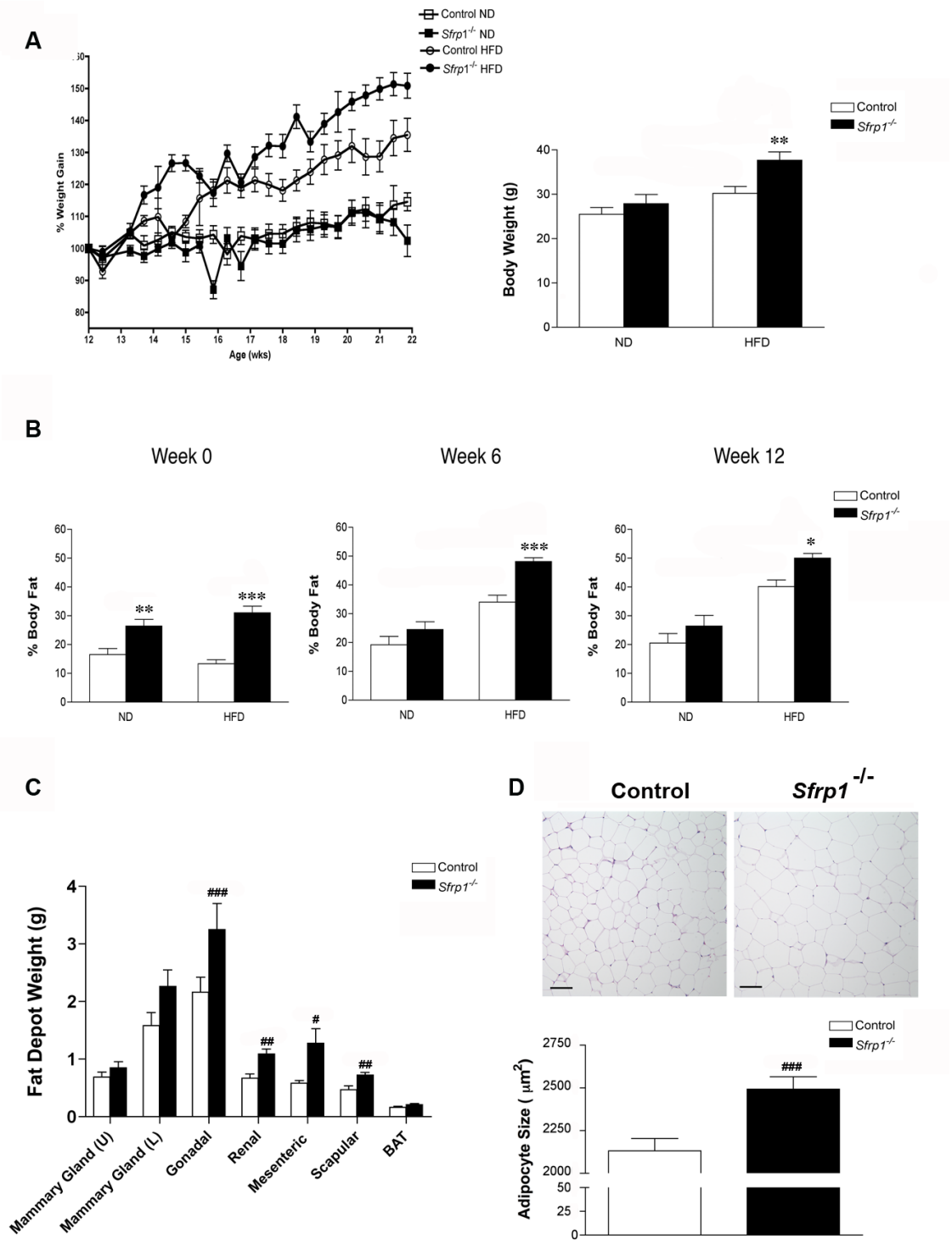

Figure 2.1. Effects of high-fat diet-induced obesity on weight gain and adiposity. (A) *Left panel*, the body weight of control and *Sfrp1*$^{-/-}$ mice put on a ND and HFD was monitored every 3 days after being put on the diet and changes are displayed graphically as percent initial body weight. *Right panel*, Final body weight after 12 weeks on the diet. (B) Body composition was analyzed by NMR-MRI at the start of the diet (0 weeks), mid-study (6

weeks), and at the end of the study (12 weeks) and fat mass was normalized to body weight and expressed as percent body fat. (C) Average weight of upper mammary glands (3rd & 4th inguinal), lower mammary gland (5th inguinal), gonadal fat pad, renal fat pad, mesenteric fat pad, scapular fat pad, and brown adipose tissue harvested from mice fed a HFD for 12 weeks. (D) *Upper panel*, Representative images of H&E staining of gonadal fad pads dissected from mice fed a HFD for 12 weeks. *Lower panel*, Quantification of gonadal adipocyte size. (*p<0.05,**p<0.01, ***p<0.001 significantly different from control mice fed a ND using Bonferroni's *t* test after a two-way ANOVA; #p<0.05, ##p<0.01, ###p<0.001 significantly different from control mice fed a HFD using student's *t* test.)

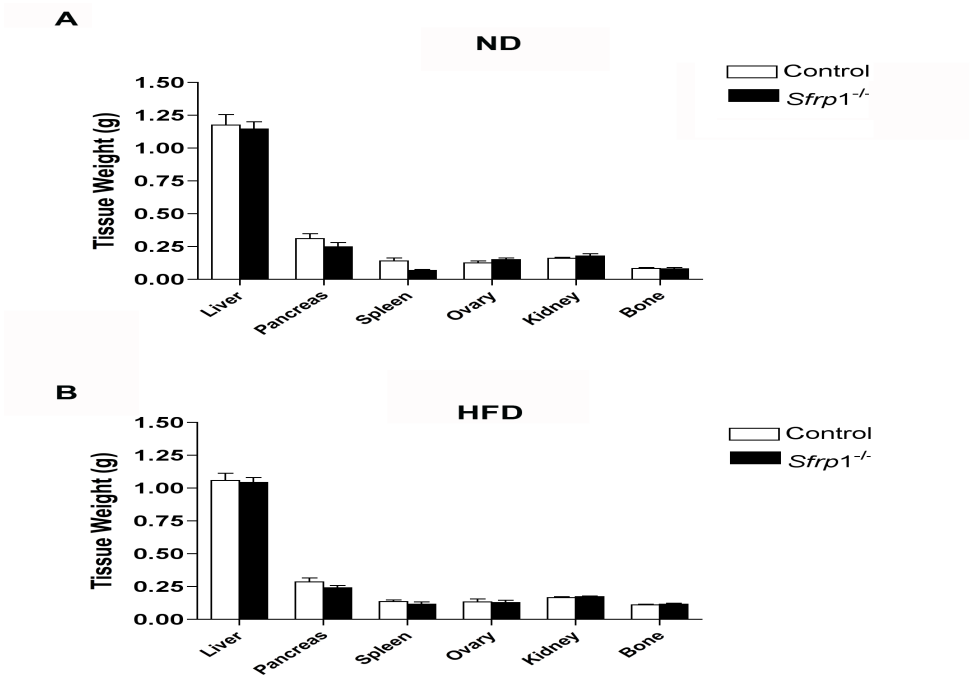

Figure 2.S1. Tissue Weights (A) Final organ weights from control and Sfrp1-/- fed a ND for 12 weeks. (B) Final organ weights from control and Sfrp1-/- fed a HFD for 12 weeks.

2.3.2 Glucose clearance and insulin secretion is deregulated in Sfrp1-/- mice in response to DIO

To explore glucose homeostasis and insulin release, a glucose tolerance test (GTT) was performed at 3 different time points within the study (Fig 2.2A). At all three time points (2, 6, and 12 weeks), Sfrp1-/- mice on a HFD showed significantly delayed glucose clearance in response to a 1 time glucose bolus compared to all other groups (Fig. 2.2A). Fasting glucose was measured at the beginning of each GTT time point and a two-way ANOVA revealed that at all

three time points, there was a significant effect on blood glucose levels in response to both Sfrp1 loss (2 weeks: F1, 35=36.16; P<0.0001; 6 weeks F1, 35=21.67; P<0.0001; 12 weeks: F1, 35=18.5; P<0.0001) and at 2 weeks and 12 weeks, there was an effect in response to the HFD (2 weeks: F1, 35=13.67; P<0.0001; 6 weeks F1, 35=2.47; P>0.05; 12 weeks: F1, 35=6.73; P<0.05). However, there were no interactions between the main effects (2 weeks: F1, 35=0.75; 6 weeks: F1, 35=1.38, P<0.05; 12 weeks: F1, 35=0.689; P<0.05) (Fig. 2.2B).

We next measured insulin secretion via ELISA throughout the study (Fig. 2.2C). Analysis of the data revealed that the mean change in insulin secretion was significantly higher in mice fed a ND compared to mice fed a HFD after adjusting for genotype. Likewise, mean change was significantly higher in control mice compared to Sfrp1-/- mice after adjusting for diet. Interestingly, there was also a significant interaction between the main effects on insulin change. The effect of Sfrp1 loss on lowering the change in insulin was present only in mice fed a HFD. In mice fed a ND, there was no difference in insulin change between control and Sfrp1-/- mice (Table 2.2). This hyperinsulinemic response in Sfrp1-/- mice was mimicked ex vivo in pancreatic islets. Specifically, a two-way ANOVA revealed that there was a significant effect on insulin secretion in response to both Sfrp1 deficiency (F1, 8=12.13; P<0.01) as well as glucose stimulation (F1, 8=32.43; P<0.001), and there was also an interaction between these main effects (F1, 8=9.99; P<0.05). (Fig. 2.S2A). Interestingly, the HFD did not affect the quantity of glucagon expressing alpha cells in pancreatic islets (Fig. 2.S2B). The total number of islets/slide was affected by Sfrp1 loss (F1, 19=4.44; P<0.05), but not the HFD (F1, 19=4.44; P<0.05), and there was a significant interaction between the two main effects (Fig. 2.S2C). Hyperglycemia in the presence of high insulin might also suggest either enhanced insulin tolerance or a secretion of inactive insulin. An insulin tolerance test (ITT) suggested that Sfrp1-/- mice may not be systemically insulin resistant and when they finally do exhibit resistance by this test, it is at a

rate similar to the control animals on a high fat diet (Fig. 2.S2E). Finally, immunohistochemical detection of C-peptide in pancreatic islets confirmed that the insulin secreted by Sfrp1-/- mice on a HFD is indeed cleaved and active (Fig. 2.S2D).

2.3.3 DIO misregulates the expression of regulatory gluconeogenesis enzymes and glucose transporters in Sfrp1-/- mice

Glucose is internally produced in the liver by way of gluconeogenesis. Wnt signaling regulates gluconeogenesis by controlling the expression of glucose-6-phosphatase (G6pc), and the rate-limiting enzyme, PEP carboxykinase (Pck1) [29]. Therefore, we measured the mRNA levels of G6pc and Pck1 in the livers of our animals (Fig. 2.2D). We observed an aberrant response in Sfrp1-/- mice fed a HFD in that despite the elevated glucose levels in these animals, they exhibited a significant increase in the expression of both G6pc and Pck1 compared with Sfrp1-/- mice fed a ND. Canonical Wnt signaling has been shown to upregulate the expression of these enzymes [30] and real-time PCR analysis of several Wnt ligand transcripts revealed that the Wnt3a ligand is significantly elevated in response to a HFD in Sfrp1-/- mice (Fig. 2.S3B).

Glucose clearance is due to several glucose transporters in the muscle, liver and fat tissues, which carry the circulating glucose from the blood stream into cells for energetic storage and so we examined the expression of glucose transporter 2 (Slc2a2 aka Glut2) in the liver. As expected, control mice fed a HFD expressed elevated levels of Slca2 when compared with control mice fed a ND. However, the expression of Slca2 was significantly reduced in Sfrp1-/- mice fed a HFD compared to ND fed mice. Similarly, in the gonadal fat pad, the transcript and protein levels of glucose transporter 4 (Slc2a4 aka Glut4) were significantly lower in Sfrp1-/- mice fed a HFD (FIg. 2.2E). Glucose transporter 4 is also responsible for insulin stimulated glucose transport into the muscle and immunohistochemical analysis revealed that HFD fed Sfrp1-/- mice express reduced Slc2a4 levels in muscle tissue (Fig. 2.4F). These results suggest

that Sfrp1 deficiency results in a multifactorial effect, which includes misregulated gluconeogenesis, with a slightly compromised ability to clear glucose, resulting in impaired glucose homeostasis and hyperinsulinemia.

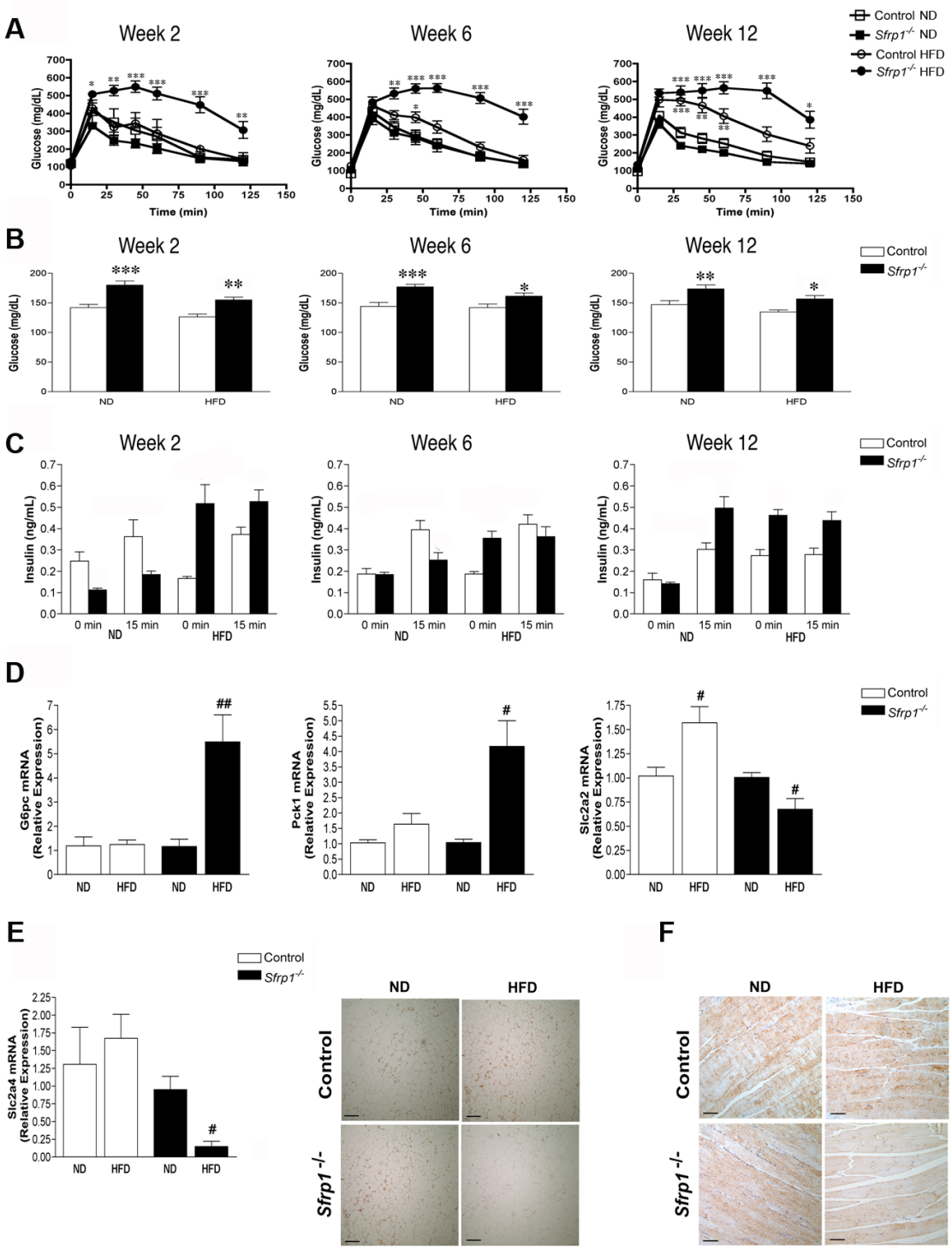

Figure 2.2. Aberrant glucose homeostasis and insulin secretion observed in *Sfrp1*$^{-/-}$ mice. (A) Glucose tolerance test (GTT) was performed at three separate time points during the study (2 weeks, 6 weeks, and 12 weeks). After a 16-18 h fast, mice were injected with 2 g/kg BW glucose and blood glucose levels were monitored for 2 h. (B) Blood glucose levels were measured prior to GTT initiation. (C) Plasma insulin levels were measured

before (0 min) and after (15 min) glucose injection. (D) For real-time PCR analysis of *G6pc*, *Pck*1, and *Slca2* gene expression, total RNA was isolated from liver of mice in each treatment group (n=6). The results shown represent experiments performed in duplicate and normalized to the amplification of β-actin mRNA. Bars represent mean ± SEM of the relative expression with respect to ND fed mice. (E) *Left panel,* For real-time PCR analysis of *Slca4* gene expression, total RNA was isolated from the gonadal fad pad from mice in each treatment group (n=6). Real-time PCR analysis was carried out as described above. *Right panel*, gonadal fat pad sections were subjected to immunohistochemical analysis and stained for *Slc2a4* (brown chromogen) and representative images were captured at 100X are displayed for mice in each treatment group (scale bar 200 μm). (F) Muscle sections were stained for *Slc2a4* and 200X images were captured as described above (scale bar 100 μm). (*p<0.05,**p<0.01, ***p<0.001 significantly different from control mice fed a ND using Bonferroni's *t* test after a two-way ANOVA; $^{\#}$p<0.05, $^{\#\#}$p<0.01, $^{\#\#\#}$p<0.001 significantly different from respective ND fed mice using student's *t* test).

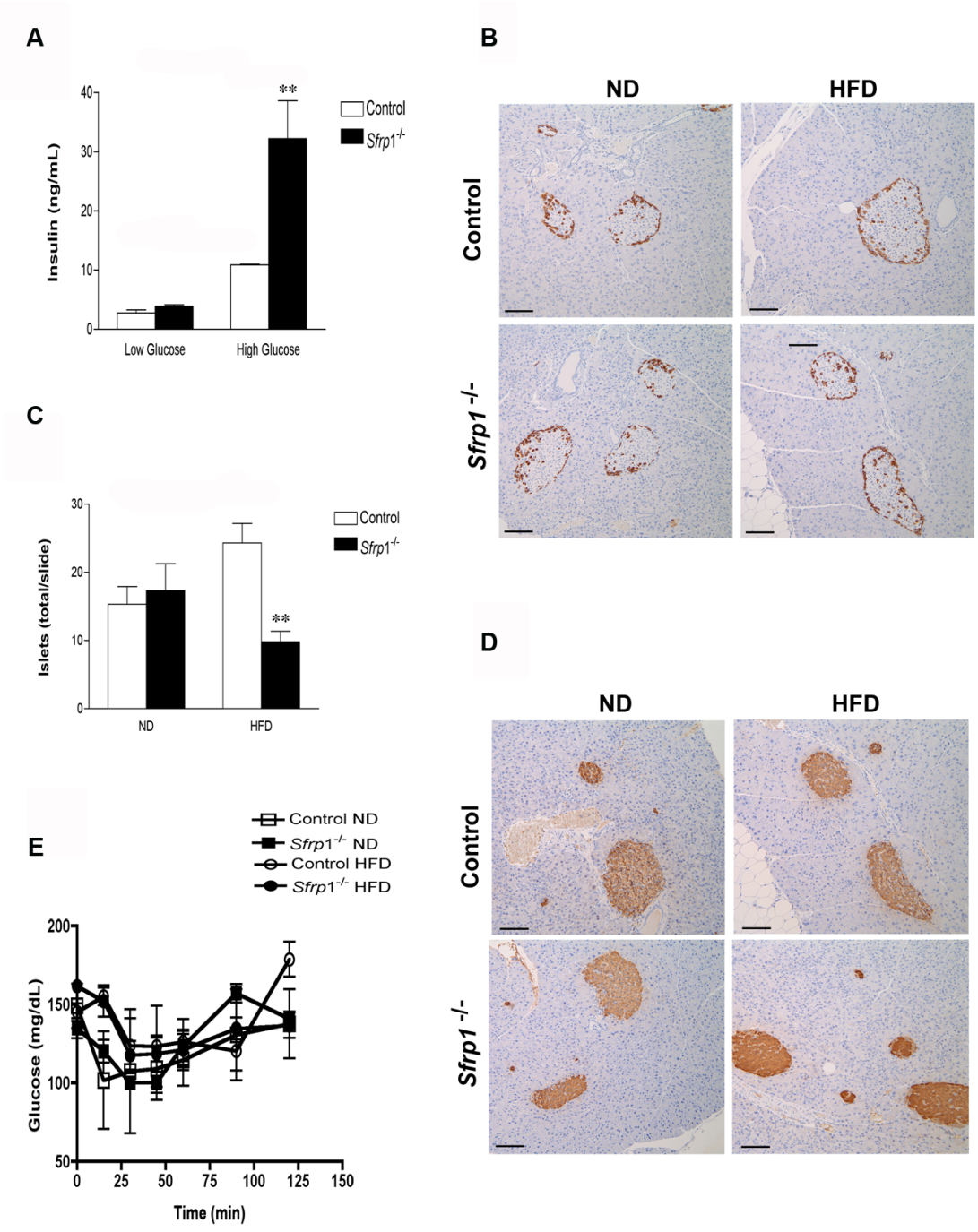

Figure 2.S2. Assessment of pancreatic function and morphology in response to DIO and Sfrp1 deficiency. (A) Functional analysis of islets derived from control and Sfrp1$_{-/-}$ mice was determined by glucose stimulated insulin secretion (GSIS). An Insulin ELISA was used to measure the concentration of insulin in the media of cultured islets stimulated with either low glucose (2.8 mM) or high glucose (16.7 mM) for 2 hours. (B) Pancreas sections

were subjected to immunohistochemical analysis and stained for Glucagon (brown chromogen) and representative images were captured at 200X are displayed for mice in each treatment group (scale bar 100 µm). (C) H&E stained pancreas slides were viewed at 40X and the total number of islets per tissue section was counted. (D)Pancreas sections were subjected to immunohistochemical analysis and stained for C-peptide (brown chromogen) and representative images were captured at 200X, are displayed for mice in each treatment group (scale bar 100 µm). (E) Insulin tolerance test (ITT) was performed at the end of the study. After a 4 h fast, mice were injected with 0.8 U/kg BW insulin and blood glucose levels were monitored for 2 hours. (**p<0.01, significantly different from control mice fed a ND using Bonferroni's t test after a two way ANOVA.)

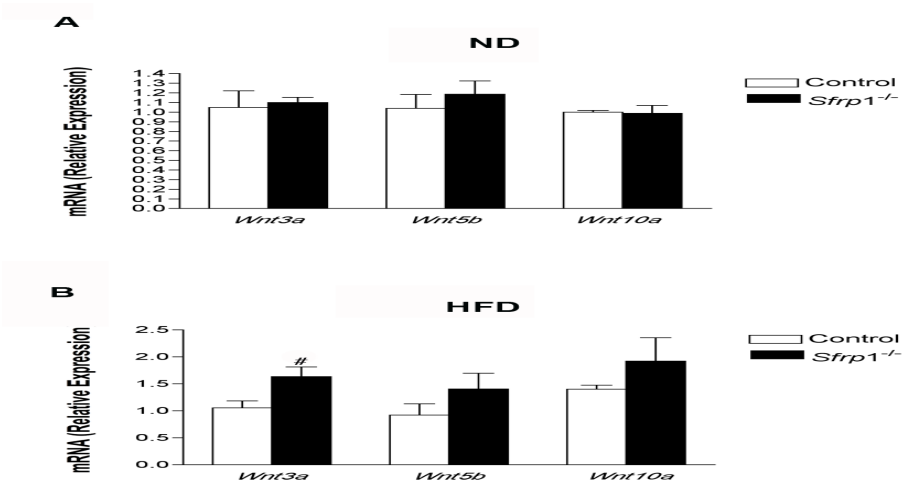

Figure 2.S3. Effect of Sfrp1 deficiency on Wnt ligand expression in the liver.

Total RNA from the liver was used for real-time PCR analysis of Wnt3a, Wnt5b, and Wnt10a gene expression in mice from each treatment group (n=6). The results shown represent experiments performed in duplicate and normalized to the amplification of β-actin mRNA. (A) Data depict relative mRNA expression in ND fed control and Sfrp1$^{-/-}$ mice. Bars represent mean ± SEM of the relative expression with respect to ND fed control mice. (B) Data depict relative mRNA expression in HFD fed control and Sfrp1$^{-/-}$ mice. Bars represent mean ± SEM of the relative expression with respect to ND fed control mice. (#p<0.05, ##p<0.01, significantly different from respective ND fed mice using student's t test.)

2.3.4 Sfrp1-/- fed HFD mice exhibit hepatic steatosis.

Considering that we observed significant Sfrp1 dependent changes in the gluconeogenic transcripts in the liver, and non-alcoholic fatty liver disease is tightly associated with obesity and hyperglycemia [31], we chose to examine the effects of a HFD in the livers of these mice.

Although we did not observe any significant differences in gross liver weight (Fig. 2.S1), we did observe increased liver steatosis in Sfrp1-/- mice fed a HFD. This is clearly illustrated by oil red O staining of frozen liver sections, which have noticeably more lipid accumulation compared to control HFD fed mice (Fig. 2.3A). These findings support the notion that the observed hepatic steatosis is a direct result of the HFD on other tissues rather then an effect of Sfrp1 loss on the misregulation of lipogenesis in the liver.

2.3.5 Sfrp1 depletion increases the expression of hepatic pro-inflammatory cytokines

The accumulation of fat in the liver is also accompanied by steatohepatitis, progressive inflammation of the liver. Thus, we looked at the effect of DIO on inflammation in our animal models. No histological signs of inflammatory infiltrate were observed in any of the livers regardless of treatment group (data not shown). A two-way ANOVA revealed that there were no effects on Tnf-α or Il-1β mRNA expression in response to Sfrp1 loss (Tnf-α: $F_{1, 20}=0.8272$; $P>0.05$; Il-1β: $F_{1, 20}=0.51$; $P>0.05$) or the HFD (Tnf-α: $F_{1, 20}=0.8841$ $P>0.05$; Il-1β: $F_{1, 20}=0.12$; $P>0.05$). There was also no interaction between theses two main effects (Tnf-α: $F_{1, 20}=0.09$ $P>0.05$; Il-1β: $F_{1, 20}=1.83$; $P>0.05$). However, a two-way ANOVA showed that Il-6 mRNA expression levels were significantly affected by Sfrp1 loss ($F_{1, 20}=25.01$; $P<0.0001$), though there was no effect in response to the HFD ($F_{1, 20}=3.44$; $P>0.05$) and there was no interaction between the main effects ($F_{1, 20}=0.25$; $P>0.05$). We next measured the mRNA levels of the pro-inflammatory adipokine Visfatin (Nampt), as it potently induces the production of Il-6 [32]. A two-way ANOVA revealed a significant effect on Nampt expression in response to Sfrp1 loss ($F_{1, 20}=31.78$; $P<0.0001$) and the HFD ($F_{1, 20}=31.86$; $P<0.0001$), as well as a significant interaction between these two main effects ($F_{1, 20}=8.34$; $P<0.01$) (Fig. 2.3D).

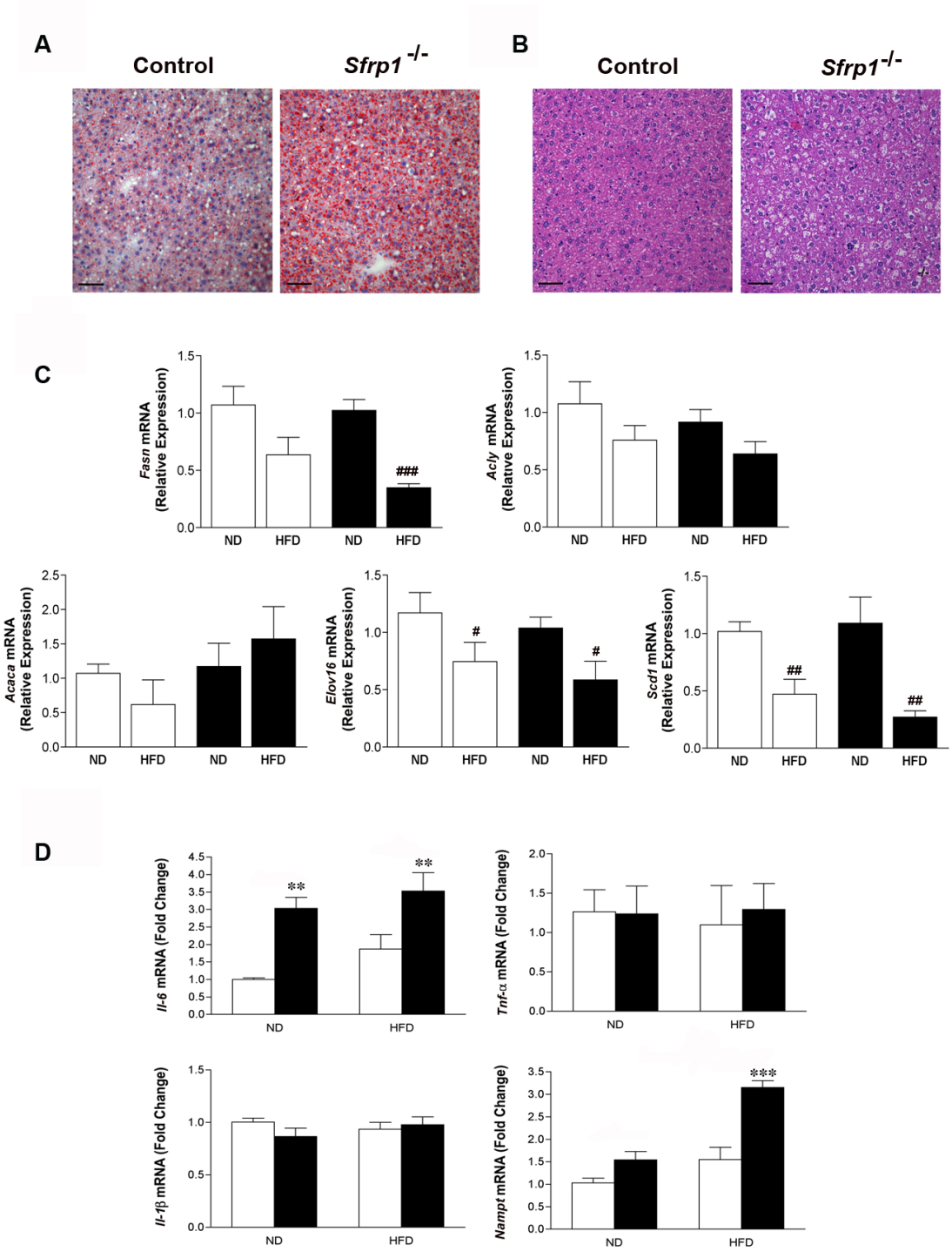

Figure 2.3. Hepatic steatosis and inflammation exhibited by *Sfrp1*$^{-/-}$ mice. (A) Steatosis is distinguished by Oil Red O staining of lipids. Images were captured at 400X and represent control mice and *Sfrp1*$^{-/-}$ mice on a HFD (scale bar 50 μm). (B) H&E staining of livers and captured as described above. (C) Total RNA from the livers in each group (n=6) was utilized for real-time PCR analysis of *Fasn*, *Acly*, and *Acaca, Elov*16, and *Scd*1 gene

expression. The results shown represent experiments performed in duplicate and normalized to the amplification of β-actin mRNA. Bars represent mean ± SEM of the relative expression with respect to ND fed mice. (D) Real-time PCR analysis of liver *Il-6, Tnf-α*, *Il-1β*, and *Nampt* gene expression was carried out as described above. Bars represent mean ± SEM of the difference in fold change compared with control ND fed mice. (*p<0.05, **p<0.01, ***p<0.001 significantly different from control mice fed a ND using Bonferroni's *t* test after a two-way ANOVA; $^{\#}$p<0.05, $^{\#\#}$p<0.01, $^{\#\#\#}$p<0.001 significantly different from respective ND fed mice using student's *t* test.)

2.3.6 Loss of Sfrp1 increases de novo lipogenesis in the gonadal fat pad

We demonstrate that mice deficient in Sfrp1 exhibit an increase in visceral fat pad weight, with the gonadal fat pad showing the highest significance (Fig. 2.1C). Therefore, to elucidate the contributing factors leading to the increased adiposity, we took a closer look at the gonadal fat pad de novo lipogenesis gene expression profile. Real-time PCR analysis revealed that the mRNA transcript levels of several de novo lipogenesis genes (Acaca, Acly, Fasn, Elov16, and Scd1) were affected by loss of Sfrp1. Specifically, a two-way ANOVA revealed that there was a significant effect on Acaca expression in response to Sfrp1 loss ($F_{1, 17}=27.30$; $P<0.0001$) and the HFD ($F_{1, 17}=20.46$; $P<0.001$), as well as a significant interaction between these two main effects ($F_{1, 17}=22.14$; $P<0.001$). Similarly, Acly expression was affected in response to Sfrp1 loss ($F_{1,15}=7.72$; $P<0.05$) as well as the HFD ($F_{1,15}=16.20$; $P<0.01$), and there was a significant interaction between these two main effects ($F_{1,15}=11.13$; $P<0.01$). Fasn expression was also altered in response to Sfrp1 loss ($F_{1, 16}=11.01$; $P<0.01$) as well as the HFD ($F_{1, 16}=19.04$; $P<0.001$), and there was a significant interaction between these two main effects ($F_{1, 16}=13.92$; $P<0.01$). Elov16 mRNA levels were affected by to Sfrp1 loss ($F_{1, 18}=5.53$; $P<0.05$) as well as the HFD ($F_{1, 18}=6.77$; $P<0.05$) and there was a significant interaction between these two main effects ($F_{1, 18}=4.41$; $P<0.05$). Lastly, Scd1 expression was affected by Sfrp1 loss ($F_{1, 18}=6.42$; $P<0.05$), though there was no effect in response to the HFD ($F_{1, 18}=0.90$; $P>0.05$) and there was no interaction between the main effects ($F_{1, 18}=1.31$; $P>0.05$) (Fig. 2.4A). As expected, when the

Sfrp1-/- mice were fed a HFD and insulin levels increased, the mRNA expression of these genes was reduced to basal levels, with the exception of Scd1 (Fig. 2.4A). We next sought to determine whether Sfrp1 loss affects the transcription factors involved in regulating the mRNA expression de novo lipogenesis genes. These transcription factors control the de novo lipogenesis process in response to either glucose levels (Chrebp-α, Chrebp-β) or insulin (Srebp1). The expression of each of these genes is significantly elevated in the gonadal fat pad of Sfrp1-/- mice on a ND (Fig. 2.4B). The Lxrα transcription factor (Nr1h3) is known to regulate cholesterol homeostasis and uptake, and our results demonstrate that there is a significant increase in expression of Nr1h3 mRNA in ND fed Sfrp1-/- mice (Fig. 2.4B). Interestingly, canonical Wnt signaling is enhanced in response Fasn [33] and analysis of Wnt ligands in the gonadal fat pad shows that Wnt3a is overexpressed in Sfrp1-/- mice (Fig. 2.S4).

2.3.7 Sfrp1-/- mice fed a HFD exhibit enhanced macrophage infiltration and cytokine production in the gonadal fat pad

Since visceral fat is prone to inflammation and Wnts have been shown to augment macrophage cytokine production [25], we investigated the inflammatory state of the gonadal fat pad. We first looked at the expression of F4/80 (macrophage marker) in control and Sfrp1-/- mice in response to a HFD and found that Sfrp1-/- mice exhibit a significant increase in F4/80 mRNA (Fig. 2.4C, right panel). The F4/80 protein is 160-kDa cell surface glycoprotein and under lipolytic conditions, F4/80 positive macrophages cluster around dying adipocytes and are referred to as Crown-like structures (CLS). These structures are frequently detected in fat tissue of obese patients and are associated with inflammation [34,35]. Our images reveal that more CLSs are present in Sfrp1-/- mice fed a HFD (Fig 2.4C, left panel) and quantification confirmed that these observations were significantly different from control animals on a HFD (Fig. 2.4C, right panel). We then looked at the gene expression of pro-inflammatory cytokines (Il-6, Tnf-α,

Il-1β and Nampt). A two-way ANOVA revealed that Il-6 mRNA expression is not affected by Sfrp1 loss ($F_{1, 13}=3.26$; $P>0.05$) but is significantly affected by the HFD ($F_{1, 13}=9.23$; $P<0.01$) and there is a significant interaction between these two main effects ($F_{1, 13}=4.72$; $P<0.05$). The expression of Nampt is affected by Sfrp1 loss ($F_{1, 17}=9.42$; $P<0.01$) but it is not significantly affected by the HFD ($F_{1, 17}=1.26$; $P>0.05$) and there is no significant interaction between these two main effects ($F_{1, 17}=0.65$; $P>0.05$). Although Tnf-α was not affected in response to Sfrp1 loss ($F_{1, 18}=0.82$; $P>0.05$) or in response to the HFD ($F_{1, 18}=1.04$; $P>0.05$), there is a significant interaction between these two main effects ($F_{1, 18}=4.48$; $P<0.05$). The expression of Il-1β was not affected by Sfrp1 loss ($F_{1, 20}=0.51$ $P>0.05$) or the HFD ($F_{1, 20}=0.12$; $P>0.05$) and there was no interaction between the main effects ($F_{1, 20}=1.83$; $P>0.05$).

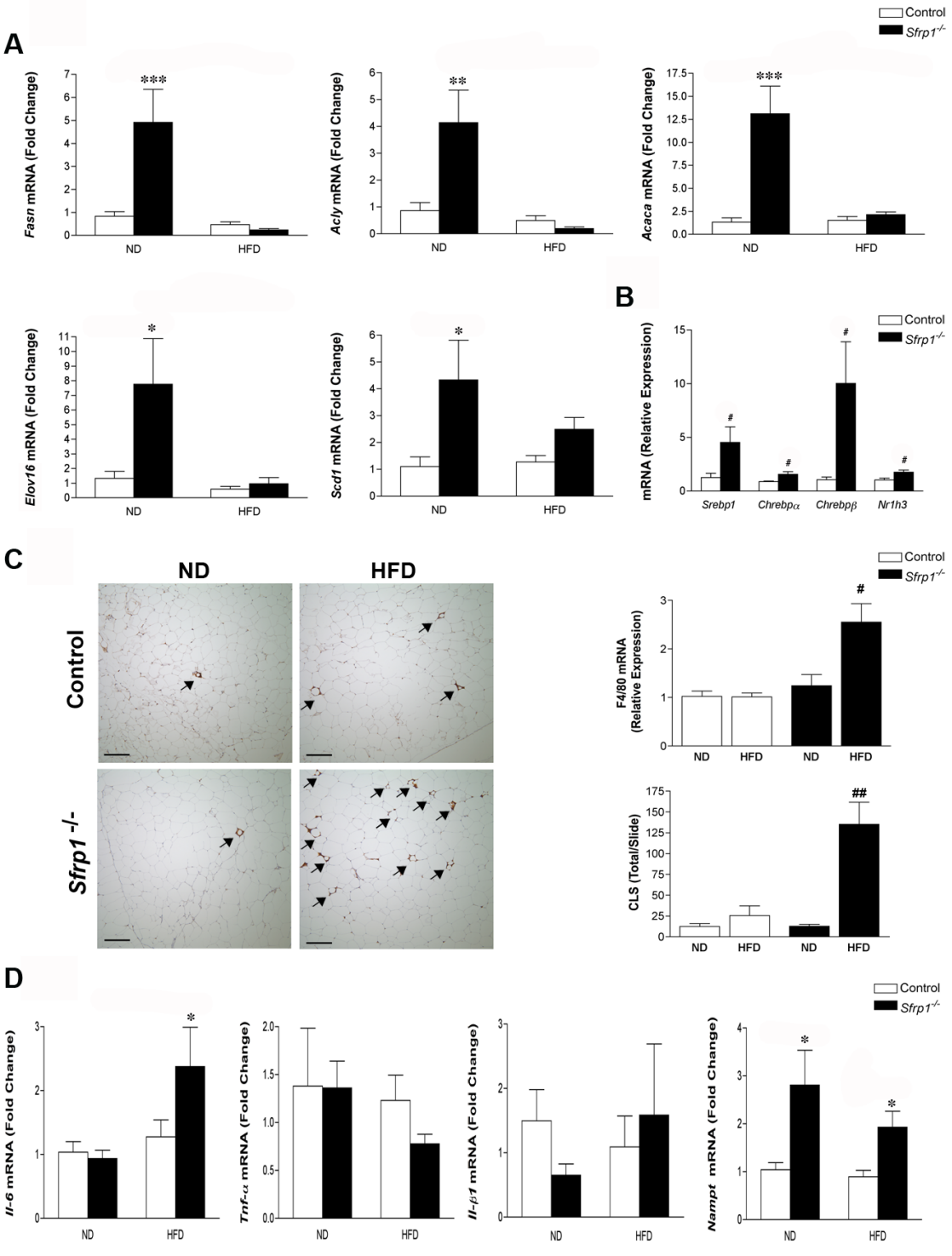

Figure 2.4. Analysis of de novo lipid synthesis and the inflammatory signature in the gonadal fat pad. (A) Total RNA from the gonadal fat pad in each group (n=6) was utilized for real-time PCR analysis of *Fasn*, *Acly*, and *Acaca, Elov*16, and *Scd*1 gene expression. The results shown represent experiments performed in duplicate and normalized to the amplification of β-actin mRNA. Bars represent mean ± SEM of the difference in fold

change compared with control ND fed mice. (B) Real-time PCR was carried out utilizing RNA from the gonadal fat pad of control mice and *Sfrp1*$^{-/-}$ mice on a ND to measure the relative mRNA expression of the following transcription factors: *Srebp1, Chrebp-*α, *Chrebp-*β, and *Nr1h3*. The experiments were carried out as described above and bars represent mean ± SEM of the difference in fold change compared with control ND fed mice. (C) *Left panel*, Gonadal fat pad sections were subjected to immunohistochemical analysis, stained for F4/80 (brown chromogen), and representative images were captured at 100X are displayed for mice in each treatment group (scale bar 200 μm). *Right upper panel*, gonadal fat pad RNA was used for real-time PCR analysis of F4/80 mRNA, experiments were carried out as described, and bars represent mean ± SEM of the relative expression with respect to ND fed mice. *Right lower panel,* The total number of CLSs (see arrow inset) was counted in F4/80 stained gonadal fat pad sections (n=4/genotype) (D) Real-time PCR analysis of liver *Il-*6*, Tnf-*α, *Il-*1β, and *Nampt* gene expression was carried out as described above. Bars represent mean ± SEM of the difference in fold change compared with control ND fed mice. (*p<0.05, **p<0.01, ***p<0.001 significantly different from control mice fed a ND using Bonferroni's *t* test after a two-way ANOVA; $^{\#}$p<0.05, $^{\#\#}$p<0.01, significantly different from respective ND fed mice using student's *t* test.)

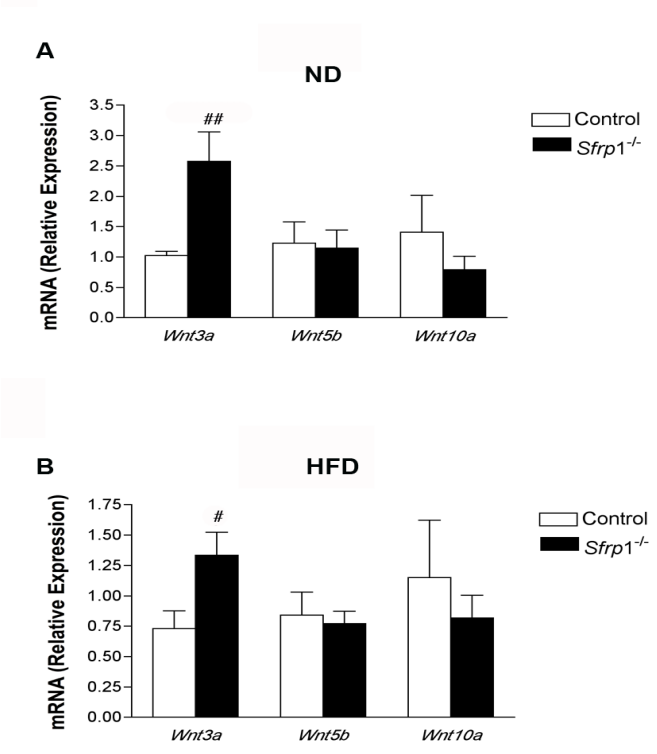

Figure 2.S4. Effect of Sfrp1 deficiency on Wnt ligand expression in the gonadal fat pad. Total RNA from the gonadal fat pad was used for real-time PCR analysis of Wnt3a, Wnt5b, and Wnt10a gene expression in mice from each treatment group (n=6). The results shown represent experiments performed in duplicate and normalized to the

amplification of β-actin mRNA. (A) Data depict relative mRNA expression in ND fed control and Sfrp1$_{-/-}$ mice. Bars represent mean ± SEM of the relative expression with respect to ND fed control mice. (B) Data depict relative mRNA expression in HFD fed control and Sfrp1$_{-/-}$ mice. Bars represent mean ± SEM of the relative expression with respect to ND fed control mice. ($^{\#}p<0.05$, $^{\#\#}p<0.01$, significantly different from respective ND fed mice using student's t test.)

2.4 Discussion

The present study demonstrates that loss of *Sfrp1* exacerbates adiposity, weight gain, glucose homeostasis and inflammation in mice on a HFD. It is well established that Wnt signaling is important for preadipocyte differentiation and adipogenesis [2]. Some ligands act as inhibitors, such as Wnt10a and Wnt10b [8,9], and other ligands promote adipogenesis such as Wnt5b and Wnt4 [11,12] in both a canonical and non-canonical fashion. We looked at the expression of Wnt ligands in the gonadal fat pad and found that there were no differences in the expression of *Wnt5b* or *Wnt10b* (Fig. 2.S4). However, *Sfrp1* loss did induce an increase in *Wnt3a* expression regardless of diet (Fig. 2.S4). Lagathu *et. al.* have previously shown that the *Sfrp1* profile expression in C57/Bl6 mice and humans exhibit a bell-shaped expression pattern in response to a HFD and a decrease in Wnt/β-catenin signaling [18]. Since we observed an increase in *Wnt3a* expression in the gonadal fat pad, we hypothesized that canonical Wnt/β-catenin signaling would be increased in *Sfrp1*$^{-/-}$ mice, but no differences were detected in the gonadal or liver tissue of hallmark canonical target transcripts including c-*Myc, Ccdn1* and *Axin2* (data not shown). However, given the body of literature linking Wnt signaling to breast cancer [38], we measured the expression of *Axin2* in mammary tissue of control and *Sfrp1*$^{-/-}$ mice fed a ND or HFD because it is a direct readout of Wnt signaling. We found that contrary to the gonadal fat pad, Sfrp1$^{-/-}$ mice fed a HFD exhibit an up-regulation of *Axin2* expression in the mammary fat pad (Fig. 2.S6). Collectively, some of the observed effects in response to *Sfrp1* loss

must be independent of Wnt signaling since SFRP1 affects a myriad of cell signaling pathways such as regulating thrombospondin, ADAM proteases and RANKL [37,39,40,41,42]

To determine the mechanism by which S*frp*1$^{-/-}$ mice exhibit enhanced growth of WAT fat depots, we analyzed genes involved in *de novo* lipogenesis. Lxr-α, Srebp1 and Chrebp are three transcription factors critical for regulating a majority of target genes that comprise this pathway [43]. The finding that the expression of these transcription factors and their targets are upregulated in S*frp*1$^{-/-}$ mice suggests a novel pathway in which loss of S*frp*1 enhances lipogenesis and may explain why heavier fat depots are observed in the S*frp*1$^{-/-}$ animals. Fatty acids are critical for embryonic development and also for the development of cancer. Interestingly, palmitate, an end product of the *de novo* lipid synthesis, is an important regulator of Wnt signaling [33]. Thus, *Sfrp*1 deficiency in some tissues may also regulate Wnt activity through indirect control of the *de novo* lipid synthesis transcriptional machinery. The regulation of *de novo* lipid synthesis by *Sfrp1* loss is a novel observation and future research will need to be carried out to determine whether palmitate production is higher in the tissues of S*frp*1$^{-/-}$ mice.

We clearly demonstrate that loss of *Sfrp1* results in a marked effect on fasting glucose levels and glucose clearance (Fig. 2.2A&B). Increased circulating glucose may be due to several factors including reduced insulin secretion, less β cells in pancreatic islets, insulin resistance, an impaired cellular ability to uptake glucose due to reduced glucose transporter levels, or overproduction of glucose in the liver by way of gluconeogenesis. Initially we hypothesized that S*frp*1$^{-/-}$ animals produced a reduced amount of active insulin because our insulin tolerance tests showed that S*frp*1$^{-/-}$ mice fed a HFD exhibited a very similar level of insulin resistance to control mice fed a HFD (Fig 2.S2E). However, our insulin ELISAs revealed that the S*frp*1$^{-/-}$ animals were in fact hyperinsulinemic on the HFD group as early as 2 weeks after starting the diet (Fig. 2.2C). Interestingly, islets harvested from S*frp*1$^{-/-}$ mice secrete significantly more insulin in response to

glucose (Fig. 2.S2A) and these data help explain the observed elevated serum insulin levels in response to S*frp*1 loss. This is in agreement with the literature, as both Wnt3a and Wnt5a enhance glucose stimulated insulin release from islet cells and addition of recombinant human SFRP1 and SFRP4 has been shown to inhibit insulin secretion [44]. We also took a closer look at the islets and the insulin being released from S*frp*1$^{-/-}$ mice and showed that insulin is cleaved properly and glucagon levels are not affected in response to Sfrp1 loss (Fig. 2.S2). However, although the number of pancreatic islets was increased in control mice fed a HFD as expected, this increase did not occur in response to S*frp*1 deficiency (Fig. 2.S2C) which could render S*frp*1$^{-/-}$ mice more susceptible to β cell burn out and further metabolic disregulation recapitulating a type-2 diabetes model. The reduction in glucose transporter expression (Fig. 2.2D, E & F) also partially explains the observed hyperglycemia. Additional research must be undertaken to investigate the relationship between S*frp*1 loss and metabolic syndromes.

Obesity can also be associated with hepatosteatosis, which results from lipid accumulation in the liver and associated inflammation. Loss of *Sfrp1* results is hepatosteatosis (Fig. 2.3A&B), which has been mechanistically demonstrated to be regulated by Il-6 as well as Ppar-α and Ppar-γ ligands leading to expression of *Fabp1*, *Chrebp* and other genes involved in *de novo* lipid synthesis [45,46]. However, S*frp*1 deficiency had very little effect on *de novo* lipid sythesis gene expression in the liver (Fig. 2.3D) suggesting that the accumulated lipid is likely due to increased transport and accumulation of lipid from other organs. For instance, lipid accumulation can also occur in response to changes in the levels of insulin that signal through the insulin receptor substrate (IRS) which upregulate fatty acid transport proteins (FATP) that uptake and store circulating lipids made elsewhere in the body [47]. Thus, the systemic hyperinsulinemia together with the increased *Il-6* expression (Fig. 2.3D) may also be driving the enhanced accumulation of lipid in the liver.

The increased macrophage infiltration and pro-inflammatory cytokine expression observed in S*frp*1$^{-/-}$ mice was expected based in the link between obesity and inflammation. Periera *et. al.* have also demonstrated that human SFRP1 plays a role in cytokine regulation by showing that addition of recombinant human SFRP1 to LPS-stimulated macrophages results in a reduction in the levels of *Il-6, Il-8* and IL-1β [24]. However, the selective upregulation *of Il*-6 over *Tnf*-α and *Il*-1β in our S*frp*1$^{-/-}$ mice (Fig. 2.3D; Fig. 2.4D; Fig. 2.5B) differs from other models for Wnt antagonist loss. Specifically, S*frp*5$^{-/-}$ mice exhibit an increase in the levels of all three inflammatory cytokines [21]. In addition, Mori *et. al.* showed that a compensatory increase in *Sfrp1* occurs in *Sfrp5* mutant mice and so we examined the levels of *Sfrp5, Sfrp4* and *Sfrp2* in gonadal adipose tissue and noted that expression of *Sfrp5* is increased in S*frp*1$^{-/-}$ mice fed a HFD, while the control animals demonstrated a decrease in *Sfrp5* (data not shown). We suspect that some of the heterotypic effects that we observe in the gonadal cytokine expression levels may be due to the replacement and slightly differential activity of *SFRP5.*

Nicotinamide Phosphoribosyltransferase (Nampt *aka* Visfatin and Pbef) is an adipokine that has recently generated excitement since its expression has strong correlation with obesity and type-2 diabetes [47,48,49,50]. Interestingly, Nampt has also been shown to promote glucose-induced insulin secretion, protect against islet death, and regulate *Il-6* as well as *Il-17* expression in immune cells [51,52]. We consistently observed increased tissue expression of *Nampt* in S*frp*1$^{-/-}$ mice (Fig. 2.3D; Fig. 2.4D; Fig. 2.5B) which suggests that *Sfrp1* may be responsible for controlling the expression of *Nampt* and that this upregulation may explain the increased insulin secretion (Fig. 2.2C) and *Il-6* expression (Fig. 2.3D; Fig. 2.4D; Fig. 2.5B).

The typical western diet is rich in fat and carbohydrates and is resulting in rapid overall weight gain in the US population that has been likened to an epidemic. Several recent studies have noted an association between increased BMI and modulation of expression of several SFRP

family members [70]. Furthermore, SNPs in the human *SFRP1* gene are associated with body composition suggesting that differences in *SFRP1* expression may play a role in regulating waist to hip ratios [71]. Thus, given the link between Wnt signaling, adipogenesis, diabetes and these epidemiological studies, it is important to ascertain whether SFRP family members are critical adipokines that can be used for the prevention of health issues related to weight gain and/or to identify higher risk individuals. This study focused on *Sfrp1* as it is expressed in and secreted from numerous cell types. This research is important because it supports the notion that Sfrp1 is a critical secreted protein that is capable of regulating weight gain, glucose homeostasis and insulin production through distinct targets on various cell types. The alteration of expression of other secreted factors such as *Il-6*, *Nampt*, *Tgf-β* and *Serpine1* are likely to partially explain the pleiotropic effects observed and will be the focus of future studies.

2.5 References

1. Faust IM, Johnson PR, Stern JS, Hirsch J (1978) Diet-induced adipocyte number increase in adult rats: a new model of obesity. Am J Physiol 235: E279-286.

2. Jo J, Gavrilova O, Pack S, Jou W, Mullen S, et al. (2009) Hypertrophy and/or Hyperplasia: Dynamics of Adipose Tissue Growth. PLoS Comput Biol 5: e1000324.

3. Yokota Y, Mori S, Narumi O, Kitajima K (2001) In vivo function of a differentiation inhibitor, Id2. IUBMB Life 51: 207-214.

4. Aarsland A, Chinkes D, Wolfe RR (1997) Hepatic and whole-body fat synthesis in humans during carbohydrate overfeeding. Am J Clin Nutr 65: 1774-1782.

5. Roberts R, Hodson L, Dennis AL, Neville MJ, Humphreys SM, et al. (2009) Markers of de novo lipogenesis in adipose tissue: associations with small adipocytes and insulin sensitivity in humans. Diabetologia 52: 882-890.

6. Postic C, Girard J (2008) Contribution of de novo fatty acid synthesis to hepatic steatosis and insulin resistance: lessons from genetically engineered mice. J Clin Invest 118: 829-838.

7. Ouchi N, Kihara S, Funahashi T, Matsuzawa Y, Walsh K (2003) Obesity, adiponectin and vascular inflammatory disease. Curr Opin Lipidol 14: 561-566.

8. Bennett CN, Ross SE, Longo KA, Bajnok L, Hemati N, et al. (2002) Regulation of Wnt signaling during adipogenesis. J Biol Chem 277: 30998-31004.

9. Ross SE, Hemati N, Longo KA, Bennett CN, Lucas PC, et al. (2000) Inhibition of adipogenesis by Wnt signaling. Science 289: 950-953.

10. Bennett CN, Hodge CL, MacDougald OA, Schwartz J (2003) Role of Wnt10b and C/EBPalpha in spontaneous adipogenesis of 243 cells. Biochem Biophys Res Commun 302: 12-16.

11. Kanazawa A, Tsukada S, Sekine A, Tsunoda T, Takahashi A, et al. (2004) Association of the gene encoding wingless-type mammary tumor virus integration-site family member 5B (WNT5B) with type 2 diabetes. Am J Hum Genet 75: 832-843.

12. Nishizuka M, Koyanagi A, Osada S, Imagawa M (2008) Wnt4 and Wnt5a promote adipocyte differentiation. FEBS Lett 582: 3201-3205.

13. Kawano Y, Kypta R (2003) Secreted antagonists of the Wnt signalling pathway. J Cell Sci 116: 2627-2634.

14. Krishnan V, Bryant HU, Macdougald OA (2006) Regulation of bone mass by Wnt signaling. J Clin Invest 116: 1202-1209.

15. Bovolenta P, Esteve P, Ruiz JM, Cisneros E, Lopez-Rios J (2008) Beyond Wnt inhibition: new functions of secreted Frizzled-related proteins in development and disease. J Cell Sci 121: 737-746.

16. Finch PW, He X, Kelley MJ, Uren A, Schaudies RP, et al. (1997) Purification and molecular cloning of a secreted, Frizzled-related antagonist of Wnt action. Proc Natl Acad Sci U S A 94: 6770-6775.

17. Bafico A, Gazit A, Pramila T, Finch PW, Yaniv A, et al. (1999) Interaction of frizzled related protein (FRP) with Wnt ligands and the frizzled receptor suggests alternative mechanisms for FRP inhibition of Wnt signaling. J Biol Chem 274: 16180-16187.

18. Lagathu C, Christodoulides C, Tan CY, Virtue S, Laudes M, et al. Secreted frizzled-related protein 1 regulates adipose tissue expansion and is dysregulated in severe obesity. Int J Obes (Lond) 34: 1695-1705.

19. Koza RA, Nikonova L, Hogan J, Rim JS, Mendoza T, et al. (2006) Changes in gene expression foreshadow diet-induced obesity in genetically identical mice. PLoS Genet 2: e81.

20. Mori H, Prestwich TC, Reid MA, Longo KA, Gerin I, et al. Secreted frizzled-related protein 5 suppresses adipocyte mitochondrial metabolism through WNT inhibition. J Clin Invest 122: 2405-2416.

21. Ouchi N, Higuchi A, Ohashi K, Oshima Y, Gokce N, et al. (2011) Sfrp5 is an anti-inflammatory adipokine that modulates metabolic dysfunction in obesity. Science 329: 454-457.

22. Sen M (2005) Wnt signalling in rheumatoid arthritis. Rheumatology (Oxford) 44: 708-713.

23. Blumenthal A, Ehlers S, Lauber J, Buer J, Lange C, et al. (2006) The Wingless homolog WNT5A and its receptor Frizzled-5 regulate inflammatory responses of human mononuclear cells induced by microbial stimulation. Blood 108: 965-973.

24. Pereira C, Schaer DJ, Bachli EB, Kurrer MO, Schoedon G (2008) Wnt5A/CaMKII signaling contributes to the inflammatory response of macrophages and is a target for the antiinflammatory action of activated protein C and interleukin-10. Arterioscler Thromb Vasc Biol 28: 504-510.

25. Pereira CP, Bachli EB, Schoedon G (2009) The wnt pathway: a macrophage effector molecule that triggers inflammation. Curr Atheroscler Rep 11: 236-242.

26. Barandon L, Casassus F, Leroux L, Moreau C, Allieres C, et al. (2011) Secreted frizzled-related protein-1 improves postinfarction scar formation through a modulation of inflammatory response. Arterioscler Thromb Vasc Biol 31: e80-87.

27. Barandon L, Couffinhal T, Ezan J, Dufourcq P, Costet P, et al. (2003) Reduction of infarct size and prevention of cardiac rupture in transgenic mice overexpressing FrzA. Circulation 108: 2282-2289.

28. Gauger KJ, Hugh JM, Troester MA, Schneider SS (2009) Down-regulation of sfrp1 in a mammary epithelial cell line promotes the development of a cd44high/cd24low population which is invasive and resistant to anoikis. Cancer Cell Int 9: 11.

29. Liu W, Singh R, Choi CS, Lee HY, Keramati AR, et al. Low density lipoprotein (LDL) receptor-related protein 6 (LRP6) regulates body fat and glucose homeostasis by modulating nutrient sensing pathways and mitochondrial energy expenditure. J Biol Chem 287: 7213-7223.

30. Liu H, Fergusson MM, Wu JJ, Rovira, II, Liu J, et al. Wnt signaling regulates hepatic metabolism. Sci Signal 4: ra6.

31. Cohen JC, Horton JD, Hobbs HH Human fatty liver disease: old questions and new insights. Science 332: 1519-1523.

32. Moschen AR, Kaser A, Enrich B, Mosheimer B, Theurl M, et al. (2007) Visfatin, an adipocytokine with proinflammatory and immunomodulating properties. J Immunol 178: 1748-1758.

33. Fiorentino M, Zadra G, Palescandolo E, Fedele G, Bailey D, et al. (2008) Overexpression of fatty acid synthase is associated with palmitoylation of Wnt1 and cytoplasmic stabilization of beta-catenin in prostate cancer. Lab Invest 88: 1340-1348.

34. Apovian CM, Bigornia S, Mott M, Meyers MR, Ulloor J, et al. (2008) Adipose macrophage infiltration is associated with insulin resistance and vascular endothelial dysfunction in obese subjects. Arterioscler Thromb Vasc Biol 28: 1654-1659.

35. Cinti S, Mitchell G, Barbatelli G, Murano I, Ceresi E, et al. (2005) Adipocyte death defines macrophage localization and function in adipose tissue of obese mice and humans. J Lipid Res 46: 2347-2355.

36. Gauger KJ, Shimono A, Crisi GM, Schneider SS Loss of SFRP1 promotes ductal branching in the murine mammary gland. BMC Dev Biol 12: 25.

37. Gauger KJ, Chenausky KL, Murray ME, Schneider SS (2011) SFRP1 reduction results in an increased sensitivity to TGF-beta signaling. BMC Cancer 11: 59.

38. Turashvili G, Bouchal J, Burkadze G, Kolar Z (2006) Wnt signaling pathway in mammary gland development and carcinogenesis. Pathobiology 73: 213-223.

39. Esteve P, Sandonis A, Cardozo M, Malapeira J, Ibanez C, et al. (2011) SFRPs act as negative modulators of ADAM10 to regulate retinal neurogenesis. Nat Neurosci 14: 562-569.

40. Hausler KD, Horwood NJ, Chuman Y, Fisher JL, Ellis J, et al. (2004) Secreted frizzled-related protein-1 inhibits RANKL-dependent osteoclast formation. J Bone Miner Res 19: 1873-1881.

41. Martin-Manso G, Calzada MJ, Chuman Y, Sipes JM, Xavier CP, et al. sFRP-1 binds via its netrin-related motif to the N-module of thrombospondin-1 and blocks thrombospondin-1 stimulation of MDA-MB-231 breast carcinoma cell adhesion and migration. Arch Biochem Biophys 509: 147-156.

42. Stuckenholz C, Lu L, Thakur PC, Choi TY, Shin D, et al. Sfrp5 modulates both Wnt and BMP signaling and regulates gastrointestinal organogensis in the zebrafish, Danio rerio. PLoS One 8: e62470.

43. Strable MS, Ntambi JM Genetic control of de novo lipogenesis: role in diet-induced obesity. Crit Rev Biochem Mol Biol 45: 199-214.

44. Mahdi T, Hanzelmann S, Salehi A, Muhammed SJ, Reinbothe TM, et al. Secreted frizzled-related protein 4 reduces insulin secretion and is overexpressed in type 2 diabetes. Cell Metab 16: 625-633.

45. Vida M, Serrano A, Romero-Cuevas M, Pavon FJ, Gonzalez-Rodriguez A, et al. IL-6 cooperates with peroxisome proliferator-activated receptor-alpha-ligands to induce liver fatty acid binding protein (LFABP) up-regulation. Liver Int.

46. Eissing L, Scherer T, Todter K, Knippschild U, Greve JW, et al. De novo lipogenesis in human fat and liver is linked to ChREBP-beta and metabolic health. Nat Commun 4: 1528.

47. Yoshino T, Kusunoki N, Tanaka N, Kaneko K, Kusunoki Y, et al. Elevated serum levels of resistin, leptin, and adiponectin are associated with C-reactive protein and also other clinical conditions in rheumatoid arthritis. Intern Med 50: 269-275.

48. Friebe D, Loffler D, Schonberg M, Bernhard F, Buttner P, et al. Impact of metabolic regulators on the expression of the obesity associated genes FTO and NAMPT in human preadipocytes and adipocytes. PLoS One 6: e19526.

49. Haider DG, Holzer G, Schaller G, Weghuber D, Widhalm K, et al. (2006) The adipokine visfatin is markedly elevated in obese children. J Pediatr Gastroenterol Nutr 43: 548-549.

50. Haider DG, Schindler K, Schaller G, Prager G, Wolzt M, et al. (2006) Increased plasma visfatin concentrations in morbidly obese subjects are reduced after gastric banding. J Clin Endocrinol Metab 91: 1578-1581.

51. Presumey J, Courties G, Louis-Plence P, Escriou V, Scherman D, et al. Nicotinamide phosphoribosyltransferase/visfatin expression by inflammatory monocytes mediates arthritis pathogenesis. Ann Rheum Dis.

52. Spinnler R, Gorski T, Stolz K, Schuster S, Garten A, et al. The adipocytokine Nampt and its product NMN have no effect on beta-cell survival but potentiate glucose stimulated insulin secretion. PLoS One 8: e54106.

53. Bi TQ, Che XM, Liao XH, Zhang DJ, Long HL, et al. Overexpression of Nampt in gastric cancer and chemopotentiating effects of the Nampt inhibitor FK866 in combination with fluorouracil. Oncol Rep 26: 1251-1257.

54. Bowlby SC, Thomas MJ, D'Agostino RB, Jr., Kridel SJ Nicotinamide phosphoribosyl transferase (Nampt) is required for de novo lipogenesis in tumor cells. PLoS One 7: e40195.

55. Reddy PS, Umesh S, Thota B, Tandon A, Pandey P, et al. (2008) PBEF1/NAmPRTase/Visfatin: a potential malignant astrocytoma/glioblastoma serum marker with prognostic value. Cancer Biol Ther 7: 663-668.

56. Wang B, Hasan MK, Alvarado E, Yuan H, Wu H, et al. NAMPT overexpression in prostate cancer and its contribution to tumor cell survival and stress response. Oncogene 30: 907-921.

57. Caton PW, Kieswich J, Yaqoob MM, Holness MJ, Sugden MC Nicotinamide mononucleotide protects against pro-inflammatory cytokine-mediated impairment of mouse islet function. Diabetologia 54: 3083-3092.

58. Dumont N, Crawford YG, Sigaroudinia M, Nagrani SS, Wilson MB, et al. (2009) Human mammary cancer progression model recapitulates methylation events associated with breast premalignancy. Breast Cancer Res 11: R87.

59. Fontana A, Constam DB, Frei K, Malipiero U, Pfister HW (1992) Modulation of the immune response by transforming growth factor beta. Int Arch Allergy Immunol 99: 1-7.

60. McDonald PP, Fadok VA, Bratton D, Henson PM (1999) Transcriptional and translational regulation of inflammatory mediator production by endogenous TGF-beta in macrophages that have ingested apoptotic cells. J Immunol 163: 6164-6172.

61. Fadok VA, Bratton DL, Konowal A, Freed PW, Westcott JY, et al. (1998) Macrophages that have ingested apoptotic cells in vitro inhibit proinflammatory cytokine production through autocrine/paracrine mechanisms involving TGF-beta, PGE2, and PAF. J Clin Invest 101: 890-898.

62. Bogdan C, Nathan C (1993) Modulation of macrophage function by transforming growth factor beta, interleukin-4, and interleukin-10. Ann N Y Acad Sci 685: 713-739.

63. Altintas MM, Azad A, Nayer B, Contreras G, Zaias J, et al. Mast cells, macrophages, and crown-like structures distinguish subcutaneous from visceral fat in mice. J Lipid Res 52: 480-488.

64. Dellas C, Loskutoff DJ (2005) Historical analysis of PAI-1 from its discovery to its potential role in cell motility and disease. Thromb Haemost 93: 631-640.

65. Fersching DM, Nagel D, Siegele B, Salat C, Heinemann V, et al. Apoptosis-related biomarkers sFAS, MIF, ICAM-1 and PAI-1 in serum of breast cancer patients undergoing neoadjuvant chemotherapy. Anticancer Res 32: 2047-2058.

66. Han B, Nakamura M, Mori I, Nakamura Y, Kakudo K (2005) Urokinase-type plasminogen activator system and breast cancer (Review). Oncol Rep 14: 105-112.

67. McMahon B, Kwaan HC (2008) The plasminogen activator system and cancer. Pathophysiol Haemost Thromb 36: 184-194.

68. Wang S, Cao Q, Wang X, Li B, Tang M, et al. PAI-1 4G/5G Polymorphism Contributes to Cancer Susceptibility: Evidence from Meta-Analysis. PLoS One 8: e56797.

69. Xu X, Xie Y, Lin Y, Xu X, Zhu Y, et al. PAI-1 promoter 4G/5G polymorphism (rs1799768) contributes to tumor susceptibility: Evidence from meta-analysis. Exp Ther Med 4: 1127-1133.

70. Bourlier V, Zakaroff-Girard A, Miranville A, De Barros S, Maumus M, et al. (2008) Remodeling phenotype of human subcutaneous adipose tissue macrophages. Circulation 117: 806-815.

71. Boudin E, Piters E, Fransen E, Nielsen TL, Andersen M, et al. Association study of common variants in the sFRP1 gene region and parameters of bone strength and body composition in two independent healthy Caucasian male cohorts. Mol Genet Metab 105: 508-515.

2.6 Appendix

2.6.1 Tables

Table 2.1: PCR primer sequences for real-time PCR analysis

G6pc	forward	5'- ACACCGACTACTACAGCAACAG -3'	Chrebp α	forward	5'- CGACACTCACCCACCTCTTC -3'
	reverse	5'- CCTCGAAAGATAGCAAGAGTA -3'		reverse	5'- TTGTTCAGCCGGATCTTGTC -3'
Pckl	forward	5'-CATATGCTGATCCTGGGCATAAC-3'	Chrebp- β	forward	5'- TCTGCAGATCGCGTGGAG -3'
	reverse	5'- CAAACTTCATCCAGGCAATGTC- 3'		reverse	5'- CTTGTCCCGGCATAGCAAC -3'
Slca4	forward	5'-GACGGACACTCCATCTGTTG -3'	Nrlh3	forward	5'- AGGAGTGTCGACTTCGCAAA -3'
	reverse	5'-GCCACGATGGAGACATAGC -3'		reverse	5'- CTCTTCTTGCCGCTTCAGTTT -3'
Slca2	forward	5'- CTGGAGCCCTCTTGATGGGA -3'	I-6	forward	5'-GCTACCAAACTGCATATAATCAGGA -3'
	reverse	5'-CTGGAGCCCTCTTGATGGGA -3'		reverse	5'-CCAGGTAGCTATGGTACTCCAGAA -3'
Fasn	forward	5'- GCTGCGGAAACTTCAGGAAAT -3'	Tnf- α	forward	5'-TGTCTCAGCCTCTTCTCATTCC -3'
	reverse	5'- AGAGACGTGTCACTCCTGGACTT -3'		reverse	5'-TGAGGGTCTGGGCCATAGAAC -3'
Acly	forward	5'-GCCCTGGAAGTGGAGAAGAT -3'	Il-I ß	forward	5'-TGTAATGAAAGACGGCACACC -3'
	reverse	5'CCGTCCACATTCAGGATAAGA- -3'		reverse	5'-TCTTCTTTGGGTATTGTTTGG -3'
Acaca	forward	5'-GCGTCGGGTAGATCCGGTT -3'	Nampt	forward	5'- GGCAGAAGCCGAGTTCAA -3'
	reverse	5'-CTCAGTGGGGCTTAGCTCTG -3'		reverse	5'- TGGGTGGGTATTGTTTATAGTGAG -3'
Elovl6	forward	5'- TCAGCAAAGCACCCGAAC -3'	F4/80	forward	5'-CTTTGGCTATGGGCTTCCAGTC -3'
	reverse	5'- AGCGACCATGTCTTTGTAGGAG -3'		reverse	5'-GCAAGGAGGACAGAGTTTATCCTG -3'
Sedl	forward	5'- CCCTGCGGATCTTCCTTATC -3'	Srebpfl	forward	5'- GGAGCCATGGATTGCACATT -3'
	reverse	5'- TGTGTTTCTGAGAACTTGTGGTG -3'		reverse	5'- GGCCCGGGAAGTCACTGT -3'

Table 2.2: Regression-adjusted mean change in insulin secretion from 0-15 minutes

Diet		
HFD	0.0789 ng/mL	0.022 ng/mL
ND	0.159 ng/mL ***	0.023 ng/mL
Genotype		
Sfrpl -1-	0.0809 ng/mL	0.023 ng/mL
Control	0.154 ng/mL **	0.022 ng/mL
Diet/Genotype		
HFD!Sfrpl -1-	0.007 ng/mL**	0.032 ng/mL
HFD/Control	0.147 ng/mL	0.031 ng/mL
ND /Sfrpl -1-	0.156 ng/mL	0.032 ng/mL
ND/Control	0.161 ng/mL	0.032 ng/mL

*p<0.0S,**p<0.0l:**p<0.00l

CHAPTER 3
RHODIOLA CRENULATA ATTENUATES DIET INDUCED OBESITY LIVER INFLAMMATION

3.1 Introduction

In the United States, more than 35% of the adult population is obese. More importantly, obesity associated inflammation predisposes one to several metabolic disorders including cardiovascular disease, non-alcoholic fatty liver (NAFLD) and type-2 diabetes [1].

A major organ affected by obesity-induced inflammation is the liver. It has been shown that increased lipid deposits in the liver leads to steotosis and an increase in inflammation [2], which in its turn decreases insulin sensitivity in the liver [3]. Both macrophages [4] and neutrophils [5] have been reported to contribute to liver insulin resistance.

Rhodiola sp. is a perennial herbaceous plant growing primarily at high altitudes in the arctic areas of Europe and Asia. It is an adaptogen [6] which has been traditionally used to increase physical endurance, reduce fatigue, prevent high altitude sickness, and relieve depression [7]. Several studies have reported that *Rhodiola rosea* as well as one of its major components, salidroside, attenuate pro-inflammatory responses in inflammation associated disease models for Alzheimers [8] and hepatitis [9] by attenuating IL-6, TNFα and IL-1β. In a diabetic rat model, *Rhodiola crenulata* was shown to decrease fasting insulin and serum triglyceride levels as well as improve insulin resistance [10]. Furthermore, in a clinical study with type 2 diabetic patients, *R.crenulata* treatment for 12–24 months significantly lowered blood glucose concentration, and improved liver and kidney function [11]. Despite these encouraging results, neither study assessed the mechanism by which *R.crenulata* treatment improved insulin resistance.

In this study, we aimed to investigate the effect of *R. crenulata* treatment on liver inflammation following placement of animals on a high fat/high carb diet for 12 weeks to induce

obesity. Our results suggest that an *R. crenulata* extract protects the liver from inflammation associated with diet-induced obesity (DIO) and this is associated with improved insulin sensitivity.

3.2 Materials and Methods

3.2.1 Animal care and treatment

This study was carried out in strict accordance with the recommendations in the Guide for the Care and Use of Laboratory Animals of the National Institutes of Health. This protocol was approved by the Baystate Medical Center Institutional Animal Care and Use Committee (IACUC). Female129/C57Blk6 mice (n=40) were individually housed in plastic cages with food and water provided continuously, and maintained on a 12:12 light cycle. Mice (n=10) were placed on either a normal diet [(ND) Harlan Teklad global 18% protein rodent diet (#2018) containing 2.8% fat, 18.6% protein] or placed on a high fat diet [(HFD) Bio-Serv (#F1850) containing 36.0 % fat, 36.2% carbohydrate, and 20.5% protein] starting at 10 weeks of age for 12 weeks. *R.crenulata* root extract powder (Barrington Chemical Corporation, Harrison, NY), containing a total of 132.0 mg/g dry weight (dw) of phenolic compounds (2.07±0.08 mg/g dw of Tyrosol, Coumaric 0.33±0.01 mg/g dw, and 6.17±0.31 of Gallic acid) as described in [12] , was dissolved in 10% ethanol hydroalcaholic solution and filter sterilized. *R.crenulata* and or equivalent volume of vehicle treatment (10% ethanol solution) was supplemented in the water at a concentration depending on average cage weight knowing that the average mouse imbibes 4.2 mL/day for an average consumption of 20-mg/kg/day concentration *R. crenulata*. Body weight was recorded and body composition was monitored with an Echo MRI-100 (Echo Model Systems, Houston TX) prior to initiating the study and at the end of the study. Upon completion of the study, mice were euthanized by CO_2 followed by cervical dislocation. The total body and

liver weights were recorded. The tissues were harvested and fixed in buffered formalin or flash frozen.

3.2.2 Immunohistochemistry (IHC)

IHC was performed on a DakoCytomation autostainer using the Envision HRP Detection system (Dako, Carpinteria, CA). Each tissue block was sectioned at 4 μm on a graded slide, deparaffinized in xylene, rehydrated in graded ethanols, and rinsed in Tris-phosphate-buffered saline (TBS). Heat induced antigen retrieval was performed in a microwave at 98ºC in 0.01 M citrate buffer. After cooling for 20 minutes, sections were rinsed in TBS and subjected to primary Ly6g antibody (NIMP-R14, Santa Cruz Biotechnology, Dallas, TX) for 45 minutes. Immunoreactivity was visualized by incubation with chromogen diaminobenzidine (DAB) for 5 minutes. Tissue sections were counterstained with hematoxylin, dehydrated through graded ethanol and xylene, and cover-slipped. Images were captured with an Olympus BX41 light microscope using SPOT Software 5.1 (SPOT™ Imaging Solutions, Detroit, MI). Positively stained epithelial cells from mammary glands were quantified and the percentage of positively labeled cells was calculated.

3.2.3 Analysis of hepatic steatosis

Frozen sections were used for the detection of lipid. Freshly dissected liver was cryoprotected in 30% sucrose overnight and then flash frozen in Tissue-Tek OCT compound (Sakura). Cryosections 10 μm thick were processed for Oil Red O staining in a 0.3% solution of Oil Red O (Sigma, St. Louis, MO) in 60% isopropanol for 15 min. After washes in 60% isopropanol, sections were counterstained with Mayer's hematoxylin. Images were captured with an Olympus BX41 light microscope using SPOTSOFTWARE.

3.2.4 RNA Isolation and Real-Time PCR

Total RNA was extracted from the gonadal fat pad and liver of mice in each treatment group (n=6) as described previously (26). Relative mRNA levels were quantified using quantitative real-time Polymerase Chain Reaction (qPCR) (Strategene Mx3005P, Agilent Technologies, La Jolla, CA). All values were normalized to the amplification of β–actin. The PCR primer sequences used are as follows: Il-6 forward; 5'-gctaccaaactgcatataatcagga-3'; Il-6 reverse; 5'-ccaggtagctatggtactccagaa-3' mKc forward; 5'-caatgagctgcgctgtcagtg-3'; mKc reverse; 5'-cttggggacacctttagcatc -3' Mip2 forward; 5'-ccaagggttgacttcaagaac-3'; Mip2 reverse; 5'-agcgaggcacatcaggtacg -3' F4/80 forward; 5'-ctttggctatgggcttccagtc-3'; F4/80 reverse; 5'-gcaaggaggacagagtttatcctg -3' Cd68 forward; 5'-cttctgctgtggaaatgcaa-3'; Cd68 reverse; 5'-agaggggctggtaggttgat -3' Tnfa forward; 5'-tgtctcagcctcttctcattcc-3'; Tnfa reverse; 5'-tgagggtctgggccatagaac -3' Elane forward; 5'-tgattatccagctcaatggc-3'; Elane reverse; 5'-acatggagttctgtcaccca -3' Ly6g forward; 5'-tgcgttgctctggagataga-3'; Ly6g reverse; 5'-cagagtggggcagatgg-3' Cd11b forward; 5'-ctgagaaatgacggtgagga-3'; Cd11b reverse; 5'-cagcaggctttacaaaccaa -3', βactin forward; 5'-ctaaggccaaccgtgaaaag-3'; βactin reverse; 5'-accagaggcatacagggaca -3'. Assays were performed using the 1-step 2X Brilliant SYBR Green qRT-PCR Master Mix Kit (Agilent Technologies) containing 200 nM forward primer, 200 nM reverse primer, and 100 ng total mRNA. The conditions for target mRNA amplification were performed as follows: 1 cycle of 50°C for 30 min; 1 cycle of 95°C for 10 min; 35 cycles each 95°C for 30s, 55°C for 1 min, and 72°C for 30s.

3.2.5 Insulin tolerance test

Mice were fasted for 4 hours, weighed, and their fasting blood glucose levels were measured from the tail vein using a glucometer (OneTouch Ultra; Lifescan, Milpitas, CA). Mice

were injected with human regular insulin (Eli Lilly, Indianapolis, IN) at a concentration of 0.8 unit of insulin per kg of body weight in the interpretational cavity and blood glucose levels were assessed 15, 30, 60, 90, and 120 minutes after injection.

3.2.6 Statistical Analysis

A two-way ANOVA with diet and *R. crenulata* treatment stimulation as the main effect was used for the analysis of the percent body fat experiment and post hoc tests were performed by Bonferroni's t test. (Graphpad Prism, San Diego, CA). Student's t-test was used to determine statistical significance between *R.crenulata* and vehicle treated groups. In all cases, p values < 0.05 were considered statistically significant. Graphpad Prism statistical analysis software (San Diego, CA) was used in this analysis and figure generation (http://www.graphpad.com/quickcalcs). Statistical outliers were identified in some data sets by applying Grubb's test (http://www.graphpad.com/quickcalcs), but the overall results were not altered by omission. A few samples were lost during processes; therefore, there are some unequal sample sizes.

3.3 Results

3.3.1 *R.crenulata* treatment does not alter body fat percentage or lipid deposits in livers in mice, but increases insulin sensitivity after 12-weeks of HFD feeding.

Since high fat diet (HFD) feeding for 12 weeks successfully results in diet induced obesity (DIO) [13], we subjected female 129/c57bl6 mice to a HFD and treated with a hydroalcoholic extract of *R. crenulata* or vehicle in their water for 12 weeks. HFD successfully induced obesity regardless of *R. crenulata* treatment, shown by body fat percentage content (fig. 3.1A). Next we examined whether there were differences in the level of lipid deposits in livers of HFD *R.crenulata* or vehicle treated mice. No differences in liver weight or fat deposits were observed

as shown by by Oil-red-O staining (fig. 3.1B and 3.1C). At 12 weeks following initiation of the, we performed an insulin tolerance test to determine if *R. crenulata* treatment rendered an improvement in insulin sensitivity in mice on a HFD. Indeed, *R.crenulata* treated mice demonstrated a significant improvement in the rate of glucose clearance following insulin stimulation (fig. 3.1D). These data confirmed previous results that show that *R. crenulata* improves insulin sensitivity under conditions of DIO.

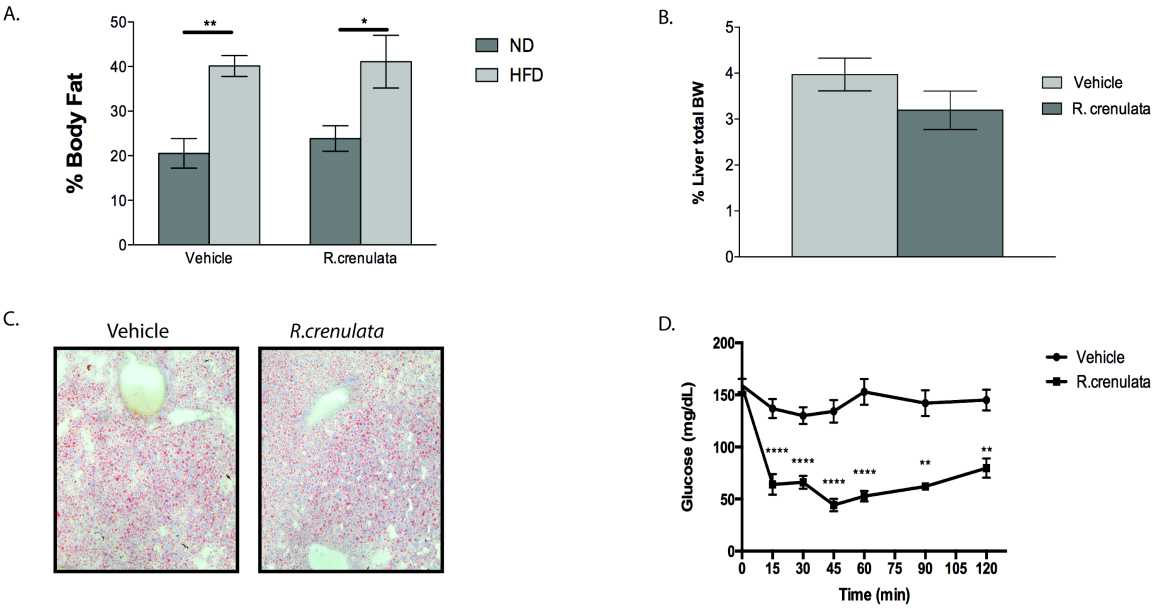

Figure 3.1. R. crenulata treatment enhances insulin sensitivity independently of liver lipid deposits. A. Bars represent mean ± SEM of percent body fat content of mice fed a normal diet (ND) or a high fat diet (HFD) and ± R. crenulata (n=10, **p<0.01, *p<0.05. Depicted significance is from adjusted p values from Bonferroni test post 2-way ANOVA analysis). B. Bars represent mean ± SEM of liver percent body weights (n=10, **p<0.01, Student's t test). C. Image representation of Oil-red-O staining analysis of paraffin embedded livers from HFD fed mice treated with R. crenulata or vehicle for 12 weeks. D. Insulin tolerance test (ITT) was performed at the end of the study. After a 4 h fast, mice were injected with 0.8U/kg BW insulin and blood glucose levels were monitored for 2 hours. (**p<0.01, ****p<0.0001, Student's t test.

3.3.2 *R. crenulata* treatment decreases liver inflammation and neutrophil infiltration in mice following 12-weeks on a HFD.

Considering that obesity is linked to liver inflammation (hepatitis), in addition to non-alcoholic fatty liver disease (NAFLD) (hepatosteatosis) [14] and *R. crenulata* treatment can attenuate liver inflammation in other disease models, we evaluated the gene transcript levels of pro-inflammatory cytokines Tnf-α and Il-6 and macrophage markers CD68 and F4/80 in our model. We observed a significant decrease in the mRNA transcript levels of Tnf-α, Il-6 and Cd68 in *R.crenulata* treated mice, suggesting an improvement in the fatty liver associated macrophage infiltration and polarization (fig. 3.2A). As neutrophil infiltration is also an established aspect of the inflammatory response to NAFLD and liver injury [5], we examined the gene transcript levels of neutrophil chemo-attractants Kc and Mip-2, as well as neutrophil markers Ly6G, Cd11b and the enzyme neutrophil elastase (Elane) in the liver. Real-time qPCR analysis revealed that there was a significant decrease in each of the genes, suggesting a decreased neutrophil infiltration response upon *R.crenulata* treatment (fig. 3.2B). We confirmed our PCR results with IHC analysis on paraffin embedded liver tissue using an anti-Ly6g antibody (NIMP-R14), which will predominantly stain neutrophils (fig. 3.2C). Our results show that there are significantly less positively stained cells in the livers of *R.crenulata* treated mice. Together, these results suggest that *R.crenulata* protects from obesity associated liver inflammation.

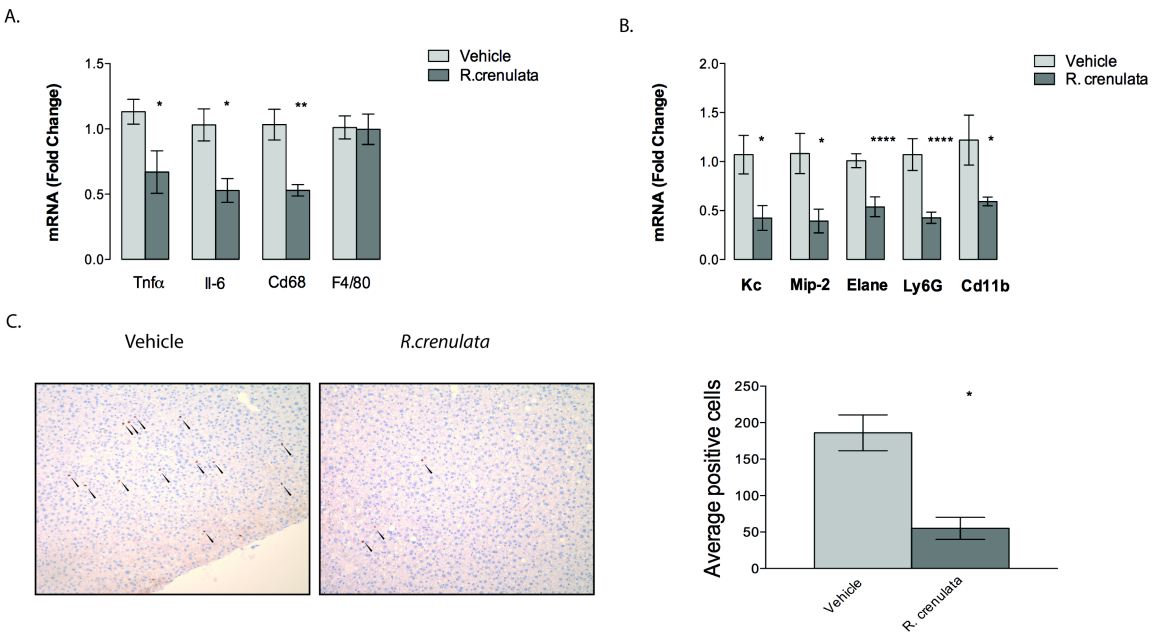

Figure 3.2. *R. crenulata* treatment decreases macrophage markers, associated pro-inflammatory cytokine transcripts and decreases neutrophil infiltration of livers from HFD fed mice. Total RNA from livers of HFD fed mice treated with *R.crenulata* or vehicle (n=6) was subjected to qPCR analysis for A. Tnfα, Il-6, F4/80 and CD68, B. Kc, Mip-2 Elane, Ly6G and Cd11b normalized to β–actin mRNA. Bars graphs represent the analysis result expressed as relative expression to vehicle treated mice. C. Image representation of IHC analysis with neutrophil marker NIMP-R14 antibody (anti-Ly6g) performed on paraffin embedded livers from HFD fed mice treated with *R. crenulata* or vehicle for 12 weeks. Bar graph represents quantified positive cells in each treatment group (n=4)

3.4 Discussion

R.crenulata has previously been shown to ameliorate blood glucose concentrations in a clinical study [11] in addition to improving the homeostasis model assessment of insulin resistance index (HOMA-IR) and excessive hepatic triglyceride accumulation in Zucker diabetic fatty rats [10]. Here we reveal that treatment with a hydroalcohlic extract of *R.crenulata* improves insulin sensitivity in a mouse model for diet-induced obesity (fig. 3.1D). This improvement happened independently of changes in fat content as *R. crenulata* did not change the diet induced increase in percent body fat. The effect of *R. crenulata* on insulin sensitivity also appeared independent of hepatosteatosis as no difference was noted in the amount of lipid

in the liver in response to treatment. These data suggest that *R. crenulata* changes how the livers responded to the fat accumulated by DIO. We hypothesized that *R. crenulata* would abrogate the inflammation associated with fat deposition in the liver. While numerous tissues respond to and depend upon insulin action to utilize blood glucose, we specifically focused on the liver since it is known to be one of the most important organs for blood glucose regulation and as an organ responsible for processing and metabolizing nutrients, it is likely to have higher exposure to the *R. crenulata* extract.

Macrophages play an important role in the process of NAFLD and insulin resistance [15], as in both cases, macrophages have been shown to increase the pro-inflammatory state and mediate insulin resistance. It has been shown that TNFα is the primary activator of macrophages in the liver post DIO and depletion of liver macrophages increases insulin sensitivity [16]. Furthermore, Park et al. showed that obesity can increase the risk of hepatic cancer development through persistent pro-inflammatory cytokine expression (TNFα and IL-6) [4].

Research has shown that it is not just macrophages which are involved in the liver inflammatory process, but neutrophils contribute as well. In fact, neutrophil liver infiltration is thought to be one of the primary responders to liver damage [5] . In a clinical study, neutrophil to lymphocyte ratio has been proposed as a marker for severity of liver steatosis and fibrosis [17]. Additionally, neutrophils have been shown to have a causal role in insulin resistance via expression of the enzyme neutrophil elastase (Elane) [18,19]. Hence identifying agents capable of attenuating macrophage and neutrophil infiltration and activation is of interest to ameliorate the inflammatory state associated with metabolic disease.

Several natural agents have been studied for possible anti-inflammatory behavior (reviewed in [20]) such as Berberine [21], Panax notoginseng saponins [22],curcumin [23] and

salidroside [9] They have been used successfully in pro-inflammatory disease models for Alzheimer's disease[8]and endotoxemia[24] to attenuate pro-inflammatory cytokine expressions and improve responses. In our study *R. crenulata* attenuated DIO induced liver inflammation and reduced liver neutrophil infiltration (fig. 3.2). This attenuation of liver inflammation by *R.crenulata* would be a possible mechanism for the observed increased insulin sensitivity.

3.5 Conclusion

Our results show that treatment with a hydroalcohlic extract of *R.crenulata* decreases DIO induced insulin resistance and attenuates liver inflammation despite not having an effect on weight gain or lipid deposition in the liver. These results support the use of *R.crenulata* as a supplement to attenuate some of the most deleterious metabolic effects of obesity.

3.6 References

[1] Eagon PK, Elm MS, Gerbarg PL, Houghton F Jr, Brown RP, Check JJ, et al. **Evaluation of the medicinal botanical Rhodiola rosea for estrogenicity**. Cancer Research 2004;64:663.

[2] DeSantis CE, Lin CC, Mariotto AB, Siegel RL, Stein KD, Kramer JL, et al. Cancer treatment and survivorship statistics, 2014. CA: a Cancer Journal for Clinicians 2014;64:252–71.

[3] EBCTCG ECTC. Effects of chemotherapy and hormonal therapy for early breast cancer on recurrence and 15-year survival: an overview of the randomised trials. The Lancet 2005.

[4] Hruska KS, Tilli MT, Ren S, Cotarla I, Kwong T, Li M, et al. Conditional over-expression of estrogen receptor alpha in a transgenic mouse model. Transgenic Res 2002;11:361–72.

[5] Madigan MP, Troisi R, Potischman N, Dorgan JF, Brinton LA, Hoover RN. Serum hormone levels in relation to reproductive and lifestyle factors in postmenopausal women (United States). Cancer Causes Control 1998;9:199–207.

[6] Verkasalo PK, Thomas HV, Appleby PN, Davey GK, Key TJ. Circulating levels of sex hormones and their relation to risk factors for breast cancer: a cross-sectional study in 1092 pre- and postmenopausal women (United Kingdom). Cancer Causes Control 2001;12:47–59.

[7] Eliassen AH, Missmer SA, Tworoger SS, Spiegelman D, Barbieri RL, Dowsett M, et al. Endogenous steroid hormone concentrations and risk of breast cancer among premenopausal women. J Natl Cancer Inst 2006;98:1406–15.

[8] Colditz GA, Hankinson SE, Hunter DJ, Willett WC, Manson JE, Stampfer MJ, et al. The use of estrogens and progestins and the risk of breast cancer in postmenopausal women. N Engl J Med 1995;332:1589–93.

[9] Panossian A, Wikman G, Sarris J. Rosenroot (Rhodiola rosea): Traditional use, chemical composition, pharmacology and clinical efficacy. Phytomedicine 2010.

[10] RA S, Aleksandrova IV, VK M, LN U, GG P. [Effect of Rhodiola rosea on the yield of mutation alterations and DNA repair in bone marrow cells]. Patologicheskaia Fiziologiia I Eksperimentalnaia Terapiia 1996.

[11] Majewska A, Grażyna H, Mirosława F, Natalia U, Agnieszka P, Alicja Z, et al. Antiproliferative and antimitotic effect, S phase accumulation and induction of apoptosis and necrosis after treatment of extract from Rhodiola rosea rhizomes on HL-60 cells. J Ethnopharmacol 2006;103:43–52.

[12] Liu Z, Li X, Simoneau AR, Jafari M, Zi X. Rhodiola rosea extracts and salidroside decrease the growth of bladder cancer cell lines via inhibition of the mTOR pathway and induction of autophagy. Mol Carcinog 2011;51:257–67.

[13] Tu Y, Roberts L, Shetty K, Schneider SS. Rhodiola crenulata induces death and inhibits growth of breast cancer cell lines. J Med Food 2008;11:413–23.

[14] Gauger KJ, Rodriguez-Cortes A. Rhodiola Crenulata inhibits the tumorigenic properties of invasive mammary epithelial cells with stem cell characteristics. Journal of Medicinal Food 2010.

[15] Kwon Y-I, Jang H-D, Shetty K. Evaluation of Rhodiola crenulata and Rhodiola rosea for management of type II diabetes and hypertension. Asia Pac J Clin Nutr 2006;15:425–32.

[16] Polakis P. Wnt signaling and cancer. Genes Dev 2000.

[17] Bisson I, Prowse DM. WNT signaling regulates self-renewal and differentiation of prostate cancer cells with stem cell characteristics. Cell Research 2009.

[18] Gupta N, Schmitt F, Grebhardt S, Mayer D. β-Catenin Is a Positive Regulator of Estrogen Receptor-α Function in Breast Cancer Cells. Cancers (Basel) 2011;3:2990–3001.

[19] Brown RP, Gerbarg PL, Ramazanov Z. Rhodiola rosea**: A Phytomedicinal Overview**. A Phytomedicinal … 2002:40–52.

3.7 Appendix

3.7.1 Unpublished data

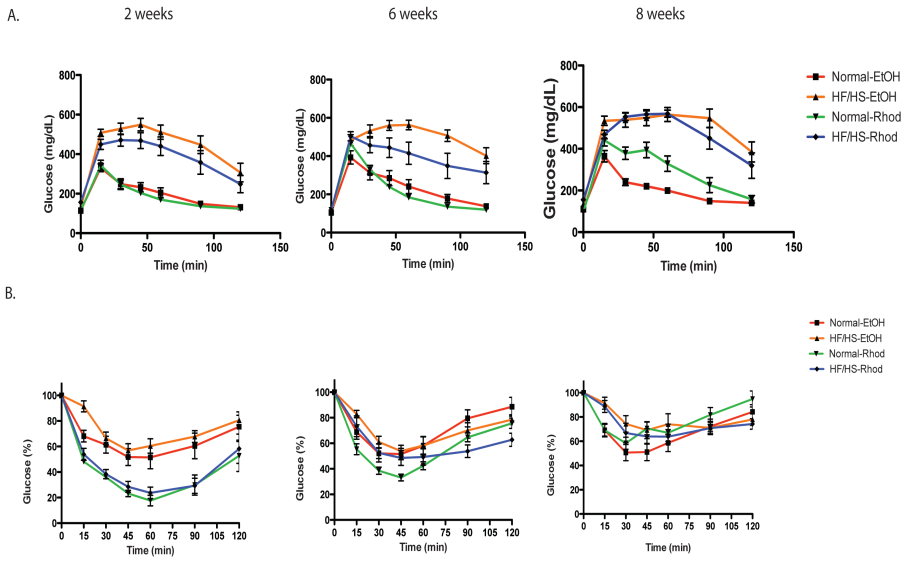

Figure 3.3 R.crenulata treatment had an early favorable affect on glucose clearance and insulin sensitivity, however it is lost over time in Sfrp1 -/- mice.

(A) Glucose tolerance test (GTT) was performed at three separate time points during the study (2 weeks, 6 weeks, and 12 weeks). After a 16-18 h fast, mice were injected with 2 g/kg BW glucose and blood glucose levels were monitored for 2 h. (B) Insulin tolerance test (ITT) was performed at the end of the study. After a 4 h fast, mice were injected with 0.8 U/kg BW insulin and blood glucose levels were monitored for 2 hours. Since the results were not of interest, no further analysis was performed on these mice.

CHAPTER 4
RHODIOLA CRENULATA INHIBITS CANONICAL WNT SIGNALING IN THE MDA-MB-231 TRIPLE NEGATIVE BREAST CANCER CELL LINE

The work presented in this chapter was done in collaboration with Carmen Mora, Elizabeth Amaro Gonzalez

4.1 Background:

Breast cancer is a collection of diseases characterized by an abnormal proliferation of the epithelium in the breast. Tumors are pathologically categorized by the expression of hormone receptors (Estrogen, Progesterone) or growth factor receptors (Her2/Neu). Among those subgroups of breast cancer, Triple Negative Breast Cancer (TNBC) is the most aggressive form of breast cancer since it lacks expression of these three receptors, making it challenging to target therapeutically [2].

Cancer cells maintain their characteristics and survival by activating embryonic and developmental signaling pathways. Current research is aimed at trying to inhibit these pathways to affect a cure. Interestingly, a number of phytochemicals have been shown to alter such pathways.

Rhodiola crenulata is a Tibetan plant that has been used in Eastern traditional medicine to relieve depression, anxiety, fatigue, and to aid in high altitude adjustment [3] . Studies have shown that *Rhodiola* species also have anti-neoplastic properties. *Rhodiola rosea*, the most studied specie of *Rhodiola*, and its active component, salidroside, have been shown to increase cell death in HL-60 leukemia cell lines [4] and induce autophagy in bladder cancer cell lines [5]. We have previously demonstrated *R. crenulata*'s ability to decrease tumor growth in mice harboring a syngeneic triple negative breast tumor derived from a p53 heterozygous animal [6]. Furthermore, in a human TNBC cell line, MDA-MB-231, we have shown that treatment with *R. crenulata* results in a decrease in tumorsphere formation and invasion *in vitro*, as well as an

increase in sensitivity to anoikis [1]. Taken together, these data suggest that *R. crenulata* may have effective anti-neoplastic activities towards aggressive breast cancer sub-types; however, the mechanism remains unclear.

A signaling pathway that is implicated in the regulation of cell fate, cell proliferation, morphology, and migration during normal development is the canonical WNT signaling pathway [7]. Dysregulation of this signaling pathway has been implicated in breast cancer, where it plays a role in cell invasion and cancer stem cell maintenance [8]. WNT ligands, secreted extracellular proteins, bind to their co-receptors Frizzled proteins and the LDL receptor-related proteins, LRP5 or LRP6, resulting in the activation of the canonical WNT/ β-catenin signaling pathway. Receptor activation leads to the inhibition of the β-catenin phosphorylation complex, composed of GSK3β, Axin, and APC, allowing increased stability and accumulation of β-catenin, followed by its nuclear localization. In the nucleus, β-catenin complexes with the transcription factors, TCF/LEF, and initiates the expression of specific target genes, such as Axin2, CyclinD1, and cMyc as well as others to drive stem cell maintenance, invasion, and proliferation. The observed effects of *R. crenulata* on the MDA-MB-231 aggressive cells were mimicked on TERT-siSFRP1 cells, an engineered cell line where WNT inhibitor secreted frizzeled related protein 1 (SFRP1), expression is knocked down and has been shown to have increased sensitivity to WNT/β-catenin signaling activation [9], hence suggestion the implication of this signaling pathway. Our previous studies indicated that *R. crenulata* inhibits stem-like behaviors and invasion; therefore, we hypothesized that *R. crenulata* treatment would inhibit the WNT/ β-catenin signaling pathway in MDA-MB-231 cells.

4.2 Materials and methods:

4.2.1 Treatments

R. crenulata root extract powder (Barrington Chemical Corporation, Harrison, NY), containing a total of 132.0 mg/g dry weight (dw) of phenolic compounds (2.07±0.08 mg/g dw of Tyrosol, Coumaric 0.33±0.01 mg/g dw, and 6.17±0.31 of Gallic acid) as described in [10], was dissolved in a hydroalcoholic solution (10% EtOH) and filter sterilized. All treatments were at 100 μg/ml concentration or equivalent volume of vehicle control (10% EtOH), with a final Etoh concentration of 0.01%, and cells were also stimulated with Wnt3a conditioned media (WNT3a expressing fibroblasts [ATCC CRL-2647]), media from control vector transfected cells (ATCC CRL-2648) or 1 μm of LiCl dissolved in diH_2O or equivalent volume of vehicle, for 24 hours. Treatment dose was chosen based on previous studies [6].

4.2.2 Cell Culture

MDA-MB-231 cells (ATCC, Manassas, VA, USA) were maintained at 37°C with 5% CO_2 in Dulbecco's modified Eagle's medium (DMEM, Life Technologies, Grand Island, NY) supplemented with 10% FBS and 20 μg/ml Gentamycin (Life Technologies, Grand Island, NY).

4.2.3 Cell Proliferation Assay

MDA-MB-231 cells ($1x10^5$ cells/well) in 6 well plates (N=3 per group), and treated as described above. Cells were collected by Trypsin (Life Technologies, Grand Island, NY), and counted using Vi-cell cell viability (Beckman Coulter Inc, Fullerton, CA).

4.2.4 RNA Isolation and Real-Time PCR

MDA-MB-231 cells were treated as described above and the total RNA was extracted as per manufacturer's protocol (Trizol, Life Technologies, Carlsbad, CA). Relative mRNA levels were quantified using quantitative real-time Polymerase Chain Reaction (qPCR) (Strategene Mx3005P, Agilent Technologies, La Jolla, CA). All values were normalized to the amplification of βactin. The PCR primer sequences used are as follows: Axin2 forward;5'-TGTGGGCAGTAAGAAACAGC-3';Axin2 reverse; 5'-GGTTCTCGGGAAATGAGGTA-3'; βactin forward; 5'-GAGGCGTACAGGGATAGC-3'; βactin reverse; 5'-ATGGATATCGCC-3'. Assays were performed using the 1-step 2X Brilliant SYBR Green qRT-PCR Master Mix Kit (Agilent Technologies) containing 200nM forward primer, 200nM reverse primer, and 100ng total mRNA. The conditions for target mRNA amplification were performed as follows: 1 cycle of 50°C for 30 min; 1 cycle of 95°C for 10 min; 35 cycles each 95°C for 30s, 55°C for 1 min, and 72°C for 30s.

4.2.5 Fluorescent Immunocytochemistry

MDA-MB-231 cells ($4.5x10^4$ cells/well) were plated on glass coverslips coated with Attachment Factor 1X (Life Technologies, Grand Island, NY), as described in manufacturer's protocol and treated as described above. The cells were fixed in 4% paraformaldehyde and permeabilized with 0.5% TritonX-100. Cells were washed three times with 1X PBS:Glycine (130mM NaCl, 7mM Na_2HPO_4, 3.5mM NaH_2PO_4, 100mM Glycine),and , blocked with 1X IF Buffer (130mM NaCl, 7mM Na_2HPO_4, 3.5mM NaH_2PO_4, 7mM NaN_3, 0.1% BSA, 0.2% TritonX-100, 0.05% Tween-20) plus 10% goat serum; followed by a 2° blocking step (1X IF buffer plus 10% goat serum plus 20μg/ml goat anti-mouse F(ab')$_2$] for 30-45min. Rabbit anti-active β-catenin (Cell Signaling Technology, Beverly MA) was diluted 1:100 into what? and incubated overnight at 4°C. Wells were washed three times in IF buffer , anti-rabbit 2° antibody coupled with Alexa Flour-

568 (Molecular Probes, Invitrogen) (1:500 in IF buffer) was incubated for 45-60 min. The coverslips were washed and mounted with Vecta-shield Mounting Medium for Fluorescence with DAPI (Vector Laboratories Inc., Burlingame, CA). Images were captured using Nikon Eclipse TE2000-U and MetaVue™ imaging software (Universal Imaging Corporation).

4.2.6 Western Blot Analysis

MDA-MB-231 cells were treated as described above and were lysed with RIPA buffer supplemented with phosphatase inhibitors and protease inhibitors (Sigma Aldrich®, St. Louis, MO). Lysate protein concentrations were measured by a BCA™ Protein Assay Kit (Pierce, Rockford, IL), 50µg/ml of protein was run on a 10% SDS-PAGE and transferred onto a PVDF membrane (Sigma Aldrich®, St. Louis, MO). Membrane was blocked for one hour with 5% milk in TBS-T and primary antibodies (Rabbit non-phospho (Active) β-catenin (Ser33/37/Thr41) (D13A1) 1:1000 5% BSA in TBS-T (Cell Signaling Technology, Danvers, MA); Rabbit β-actin 1:2000 (Abcam, Cambridge, MA) were incubated over overnight. Secondary antibody [goat anti-rabbit IgG-HRP 1:5000 (Santa Cruz Biotechnology, Dallas, TX) was incubated for 2 hours at room temperature. The blot was washed and developed using a Western Blot Luminol Reagent (Santa Cruz Biotechnology) and imaged with a Synopics 4.2 MP camera and G:Box Chemi-XT4 GENESys software (SYNGENE, Frederick, MD). Image J software was used for band density quantification.

4.2.7 Dual reporter luciferase Assay

MDA-MB-231 cells were transiently transfected with Super8xTOPFlash reporter construct (graciously provided by Randall Moon) and pRL-CMV using Lipofectamine 2000 (Sigma Aldrich®, St. Louis, MO), as per manufacturer instructions. Cells were then washed with 1X PBS and the Dual-Luciferase® Reporter Assay System (Promega) supplied protocol was followed for

lysis and measurements. Recorded Firefly and Renilla luciferase activity was measured using TD-20/20 Luminometer (Turner Designs, Sunnyvale, CA).

4.2.8 Statistical Analysis

All results were analyzed using a two-way ANOVA with *R. crenulata* treatment and Wnt3a or LiCl stimulation as the main effects. Post hoc tests were performed by Bonferroni's t test. (Graphpad Prism, San Diego, CA). Grubb's test was used on all data to identify statistical outliers (http://www.graphpad.com/quickcalcs).

4.3 Results

4.3.1 *R. crenulata* inhibits canonical WNT signaling in MDA-MB-231 cells

To evaluate *R. crenulata* treatment effects on β−catenin transcription, a dual luciferase reporter assay was performed on MDA-MB-231 cells expressing 8xTOPFlash reporter (β−catenin luciferase reporter) construct. The reporter construct transfected cells were treated with Wnt3a conditioned media to activate the WNT pathway in the presence or absence of *R. crenulata*. Wnt3a conditioned media treatment significantly increased luciferase activity, significant of β−catenin transcriptional activation. However the Wnt3a mediated increased luciferase levels were significantly repressed when *R. crenulata* was included in the treatment (Figure 1A). To confirm our findings with endogenous β−catenin transcriptional activity, we performed a qPCR analysis of WNT/β−catenin signaling canonical target gene, Axin2. Again, Wnt3a conditioned media treatment significantly increased Axin2 mRNA level; and this increase in expression was repressed when *R. crenulata* was included in the treatment (Figure 1B). Together, these results demonstrate that *R. crenulata* treatment inhibits Wnt3a-induced β−catenin transcriptional activity of exogenous and endogenous targets.

β−catenin stability is regulated by a phosphorylation at (Ser33/37/Thr41), and once that occurs, it is targeted for degradation. To investigate whether there was a change in the β−catenin activity, we probed protein extracts of the Wnt3a and *R. crenulata* treated cells via Western blot analysis with a non-phospho (active) β−catenin antibody (Figure 1C, upper panel). Densitometry analysis (Figure 1C, lower panel) confirmed that the active form of β−catenin was significantly increased by Wnt3a media at 24 hours and reversed with the addition of *R. crenulata*. Hence, *R. crenulata* treatment results in the abrogation of Wnt3a-induced β−catenin activity. It is Finally, we evaluated whether *R. crenulata* could inhibit WNT/β-catenin mediated cellular proliferation, induced by our Wnt3a conditioned media, as WNT signaling is well established mitogen [11]. Equal number of cells were incubated and treated Wnt3a conditioned media and in the presence or absence of *R. crenulata*, and cells were counted 24 hours later. Total cell counts were significantly increased in response to Wnt3a, and that *R. crenulata* treatment significantly decreased this Wnt3a mediated increase in total cell number (Figure 1D). Collectively, these data demonstrate that *R. crenulata* treatment inhibits canonical WNT signaling and function in MDA-MB-231 TNBC cells. To our knowledge, this is the first time that *R. crenulata* has been implicated in the inhibition of the WNT signaling pathway.

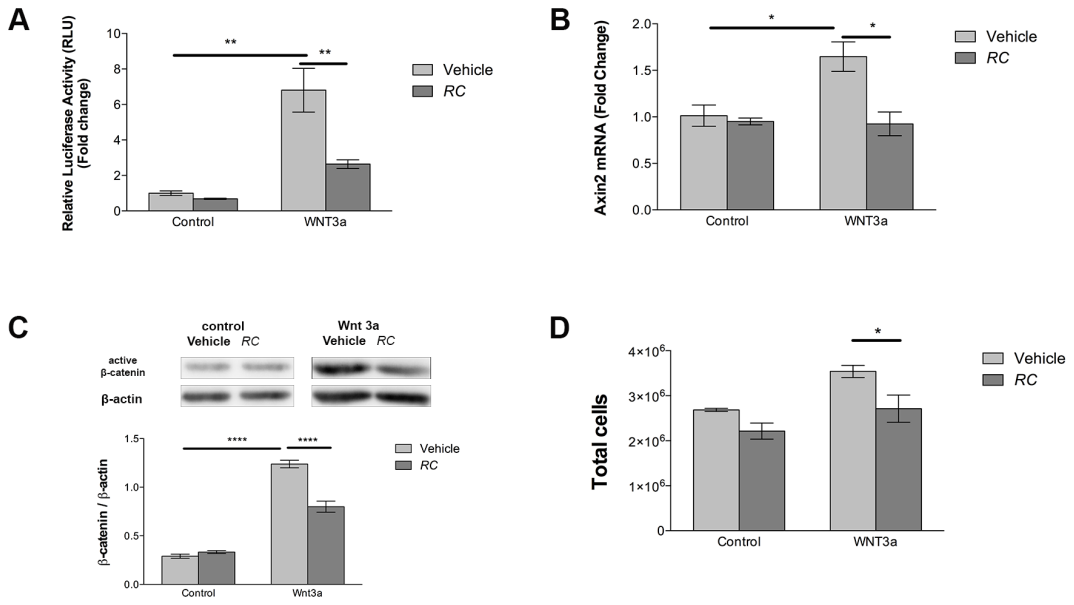

Figure 4.1: R. crenulata inhibits canonical WNT signaling in MDA-MB-231 cells in response to Wnt3a stimulus MDA-MB-231 cells were plated for 24 hours. Media was replaced with WNT3a conditioned media or media from control vector transfected cells and treated with 100ug/ml *R. crenulata* or vehicle (10% EtOH) for 24 hours. **A.** Bar representation of luciferase reporter assay mean ± SEM (N=4) of the difference in fold change compared with control vehicle treated cells (**p value< 0.01). **B.** Bar representation of Axin2 mRNA levels normalized to βactin mRNA in response to *R. crenulata* and Wnt3a stimulation. Bars represent mean ± SEM Axin2/ βactin and are expressed as relative expression of vehicle treated control cells (*p < 0.05). **C**. Upper panel: representative image of total protein lysates immuno-blotted with anti-(Active) β–catenin and normalizer βactin. Lower panel: Bar representation of band densities quantified and normalized to βactin. Bars represent mean and ± SEM of N=4 (****p value < 0.0001). **D.** Bar representation of total MDA-MB-231 cells after treatment Bars represent the mean and ± SEM of total cell counts (N=3, *p < 0.05. All depicted significance is from adjusted p values from Bonferroni test post 2-way ANOVA analysis). All experiments repeated at least 3 times.

4.3.2 *R. crenulata* inhibition is cytoplasmic in MDA.MB.231 cells.

R. crenulata inhibition of the canonical WNT pathway could be occurring at several levels. It could upregulate the secretion of known antagonists, it could stabilize the Axin/GSK3/APC degradation complex, it could inhibit nuclear translocation, or it could block interactions required for transcriptional activity in the nucleus. To narrow down the mechanism

of inhibition by which *R. crenulata* affects WNT/β−catenin signaling, we first aimed to eliminate extracellular signaling effectors by utilizing LiCl to activate β−catenin transcription in a β−catenin reporter assay. LiCl activates β−catenin transcription by inhibiting GSK3β, hence interrupting the complex that phosphorylates β−catenin. The outcome is β−catenin transcriptional activity that bypasses the upstream ligand activation of the extracellular receptors. As expected, LiCl treatment significantly increased luciferase activity the increased luciferase levels were significantly repressed when *R. crenulata* was included in the treatment (Figure 2A). The observed results suggest that the inhibition by *R. crenulata* must be happening in the cytoplasm. To rule out if *R. crenulata* inhibited β-catenin nuclear translocation we performed an immunocytochemistry (ICC) analysis using the active β−catenin antibody on MDA-MB-231 cells stimulated with Wnt3a media in the presence or absence of *R. crenulata*. Fluorescent immunocytochemistry images reveal the expected increase in nuclear β-catenin accumulation (Figure 2B, left lower panel), however this was not observed in the *R. crenulata* treated cells (Figure 2B, Right lower panel). There was a low level of detectable active β-catenin, but this appeared to be sequestered in discrete locations in the cytoplasm. Therefore, these results clearly demonstrate a marked decrease in β-catenin nuclear accumulation in response to *R. crenulata* treatment, confirming that the inhibition is occurring in the cytoplasm, more specifically between the β-catenin degradation complex and the nuclear localization steps.

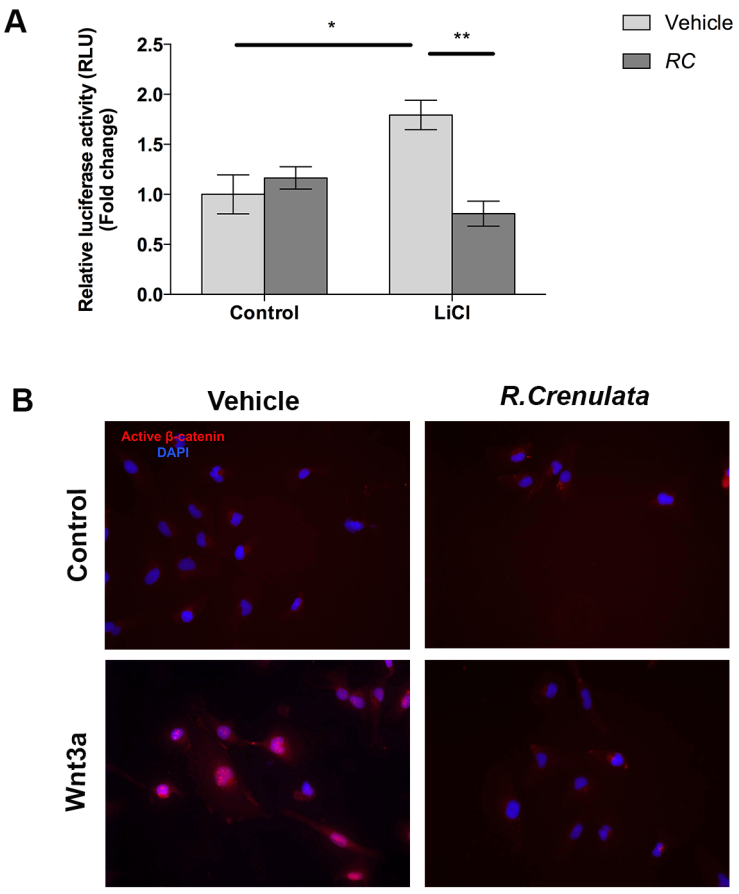

Figure 4 2: R. crenulata inhibition is cytoplasmic in MDA.MB.231 cells. A. R. crenulata inhibits β–catenin transcriptional activation upon 1μM LiCl treatment in MDA-MB-231 cells.Bar representation of luciferase reporter assay mean ± SEM of the difference

4.4 Discussion

The previously observed anti-neoplastic effects with the *R. crenulata* extract on breast cancer cells were encouraging [1]; however, no mechanism was implicated with the *R. crenulata* extract produced effects. In this study, our results demonstrate that *R.crenulata* inhibits β–catenin activity transcription activation. Since canonical WNT signaling is a well established mitogen and leads to increased in proliferation [11], we examined R.crenulata effects on this WNT mediate function and our results demonstrate a repression in the induced proliferation. Hence, it is plausible to hypothesize that R.crenulata inhibits other WNT related

functions such as invasion, and the maintenance of stem cell characteristics [8] In MDA-MB-231 cancer. We have previously shown that R. crenulata treatment inhibits β–catenin transcriptional activity in an aggressive glioblastoma cells (Mora et al,2015), hence *R.crenulata* induced β–catenin inhibition could occur in other cancer cells.

Rhodiola root extract is composed of multiple chemical compounds such as phenols, organic acids, flavonoids, and alkaloids [3]; [12]. Diverse cellular pathways and proteins have been reported to be affected by *Rhodiola* constituents such as ROS-AMPK-PKCξ [13,14], and these multifarious effects are most likely due to the complex nature of the *R. crenulata* root extract. It still remains unclear which component (or fraction) of *R. crenulata* mediates canonical WNT signaling inhibition, however, results from this study suggest that the inhibition is occurring in the cytoplasm (figure 2). This narrows down the span of possibilities of how bcatenin transcriptional inhibition immensely, however further research will lead to understanding the inhibitory mechanism and hopefully the fraction mediating this important event. Future studies will focus examining whether the anti cancer effects described *in vitro* and whether manipulation of the canonical WNT signaling would affect xenograph growth and development in MDA-MB-231 .

4.5 References

[1] Gauger KJ, Rodriguez-Cortes A. Rhodiola Crenulata inhibits the tumorigenic properties of invasive mammary epithelial cells with stem cell characteristics. Journal of Medicinal Food 2010.

[2] Andre F, Zielinski CC. Optimal strategies for the treatment of metastatic triple-negative breast cancer with currently approved agents. Annals of Oncology 2012;23:vi46–vi51.

[3] Khanum F, Bawa AS, Singh B. Rhodiola rosea: A Versatile Adaptogen. Comprehensive Reviews in Food Science and Food Safety 2005;4:55–62.

[4] Majewska A, Grażyna H, Mirosława F, Natalia U, Agnieszka P, Alicja Z, et al. Antiproliferative and antimitotic effect, S phase accumulation and induction of

apoptosis and necrosis after treatment of extract from Rhodiola rosea rhizomes on HL-60 cells. J Ethnopharmacol 2006;103:43–52.

[5] Liu Z, Li X, Simoneau AR, Jafari M, Zi X. Rhodiola rosea extracts and salidroside decrease the growth of bladder cancer cell lines via inhibition of the mTOR pathway and induction of autophagy. Mol Carcinog 2011;51:257–67.

[6] Tu Y, Roberts L, Shetty K, Schneider SS. Rhodiola crenulata induces death and inhibits growth of breast cancer cell lines. J Med Food 2008;11:413–23.

[7] Polakis P. Wnt signaling and cancer. Genes Dev 2000.

[8] Bisson I, Prowse DM. WNT signaling regulates self-renewal and differentiation of prostate cancer cells with stem cell characteristics. Cell Research 2009.

[9] Gauger KJ, Hugh JM, Troester MA, Schneider S. Down-regulation of sfrp1 in a mammary epithelial cell line promotes the development of a cd44high/cd24low population which is invasive and resistant to anoikis. Cancer Cell Int 2009;9:11.

[10] Kwon Y-I, Jang H-D, Shetty K. Evaluation of Rhodiola crenulata and Rhodiola rosea for management of type II diabetes and hypertension. Asia Pac J Clin Nutr 2006;15:425–32.

[11] Acebron SP, Niehrs C. Focus ReviewMitotic and mitogenic Wnt signalling. The EMBO Journal 2012;31:2705–13.

[12] Chen D, Fan J, Wang P, Zhu L, Jin Y, Peng Y, et al. Food Chemistry. Food Chemistry 2012;134:2126–33.

[13] Lee S-Y, Shi L-S, Chu H, Li M-H, Ho C-W, Lai F-Y, et al. Rhodiola crenulataand Its Bioactive Components, Salidroside and Tyrosol, Reverse the Hypoxia-Induced Reduction of Plasma-Membrane-Associated Na,K-ATPase Expression via Inhibition of ROS-AMPK-PKC ξPathway. Evidence-Based Complementary and Alternative Medicine 2013;2013:1–15.

[14] Chiang H-M, Chien Y-C, Wu C-H, Kuo Y-H, Wu W-C, Pan Y-Y, et al. Hydroalcoholic extract of Rhodiola rosea L. (Crassulaceae) and its hydrolysate inhibit melanogenesis in B16F0 cells by regulating the CREB/MITF/tyrosinase pathway. Food and Chemical Toxicology 2014;65:129–39.

CHAPTER 5
RHODIOLA CRENULATA INDUCES AN EARLY ESTROGENIC RESPONSE AND REDUCES PROLIFERATION AND TUMORSPHERE FORMATION OVER TIME IN MCF7 BREAST CANCER CELL LINES

The work presented in this chapter was done in collaboration with Cody Jacobs, Kelly Gauger (Gregory), Elizabeth M. Henchey and Jennifer Ser-Dolansky

5.1 Introduction

Breast cancer is the most common type of cancer among women. It has been estimated that each year more than 200,000 new cases are diagnosed in the United States [2]. Over 70% of all diagnosed breast cancer cases are positive for the estrogen receptor (ER) [3], where it is typically upregulated, allowing the cells to be more responsive to endogenous estrogen in the body.

Estrogen is a critical regulator of mammary growth and differentiation. The estrogen receptors found in the mouse mammary gland are primarily located on epithelial cells and adipocytes. In the developing mammary buds, pubertal estrogen drives the proliferation and extension of the ducts. Estrogen can also increase the progesterone receptor (PR) leading to enhanced progesterone responsiveness. Importantly, uncontrolled estrogenic activity can also drive breast cancer risk. For example, overexpression of ERα stimulates tumors in mice [4] and in women, the risk of breast cancer increases with higher circulating levels of E2 [5], [6], [7], [8]

The use of complementary and alternative medicine to treat ailments ranging from depression to glucose homeostasis [9] has gradually increased as an approach to benefit personal health and complement conventional medicine. Rhodiola sp. is a perennial herbaceous plant that grows primarily at high altitudes in the arctic areas of Europe and Asia. Rhodiola sp. roots have been traditionally used to increase physical endurance, reduce fatigue, prevent high altitude sickness, and to relieve mild to moderate depression [9]. Over the past decade, several

studies have documented that Rhodiola sp. possess anti-neoplastic effects. R. rosea, the most studied sp. of Rhodiola, decreases DNA damage in bone marrow cells from mice in response to the mutagen N-nitroso-N-methylurea [10] and increases cell death in several cancer cell lines [11]. Rhodiola Rosea and salidroside, an active compound in the plant, have also been shown to induce autophagy in bladder cancer cell lines [12]. Previously, we have demonstrated that R. crenulata can decrease tumor growth in mice harboring a syngeneic triple negative breast (TNBC) tumors [13] . Furthermore, we have shown that R. crenulata treatment decreases tumorsphere formation as well as invasion, and increases sensitivity to anoikis (cell death in response to loss of attachment) in human TNBC breast cancer lines [14]. However, the phytoestrogenic effects of Rhodiola sp. have not been carefully studied in ER+ normal or breast cancer cells. A unique study suggests that R. rosea is able to bind to the estrogen receptor [1], but ER transcriptional activity has not been described. It is imperative to elucidate ER transcriptional activity because Rhodiola rosea, commonly used to alleviate depression, might have deleterious mitogenic effects in the mammary gland of patients with ER+ breast cancer. In the work described here, we sought to determine whether an R. crenulata root extract exhibits estrogenic activity in ER+ breast cancer cells in vitro and whether it affects normal mammary epithelial proliferation and ER target gene expression in vivo. Our results suggest that R. crenulata extract contains estrogenic components, however, continuous treatment leads to decreases in MCF7 cell proliferation and tumorsphere formation.

5.2 Methods

5.2.1 Treatments

R. crenulata root extract powder (Barrington Chemical Corporation, Harrison, NY), containing a total of 132.0 mg/g dry weight (dw) of phenolic compounds (2.07±0.08 mg/g dw

of Tyrosol, Coumaric 0.33±0.01 mg/g dw, and 6.17±0.31 of Gallic acid) as described in [15], was dissolved in 10% ethanol and filter sterilized. All treatments were at 100 µg/ml concentration or equivalent volume of vehicle control (10% EtOH). Continuously treated MCF7 Cells were supplemented with R. crenulata or vehicle every 2 days for the length of the study. For estrogen transcription activity assessments, cells were plated and treated in charcoal stripped serum and phenol free medium (DMEM, Life Technologies, Grand Island, NY) to reduce background estrogenic activity. As a positive control, cells were stimulated with 10 nM of 17-βestradiol (Cat # E8875, Sigma Aldrich). Inhibitor ICI 182,780 (Tocris ,Ellisville, MO, USA) was used at a concentration of 20 nM. Lithium Cloride (LiCl) (Sigma Aldrich) was used at a concentration of 20 mM dissolved in sterile filtered distilled water.- Cell Culture

MCF7 cells (ATCC, Manassas, VA, USA) were maintained at 37°C with 5% CO2 in Dulbecco's Modified Eagle's medium (DMEM, Life Technologies, Grand Island, NY) supplemented with 10% FBS and 20 µg/ml Gentamycin (Life Technologies, Grand Island, NY) and 0.01 mg/ml of recombinant insulin.

5.2.2 Cell Proliferation Assay

MCF7 cells (3x105 cells/well) in 60 mm plates (N=3 per group), and treated as described above. Cells were collected by Trypsin (Life Technologies, Grand Island, NY), and counted using Vi-cell cell viability (Beckman Coulter Inc, Fullerton, CA). Cells were counted once a week for a period of 3 weeks. Doubling time for each read out period was calculated using the following equation Doubling time= Time ln2/ln(X(cell number at the end of the incubation time)/X(cell number at the beginning of the incubation time).

5.2.3 Dual reporter luciferase Assay

MCF7 cells were transiently transfected with the pGL3-Luc.3ERE Luciferase vector (kindly provided by Fern Murdoch, Northwestern University, Evanston, IL) or with Super8xTOPFlash reporter construct (graciously provided by Randall Moon) and pRL-CMV(Promega) using Lipofectamine 2000 (Sigma Aldrich®, St. Louis, MO), as per manufacturer instructions. Cells were then washed with 1X PBS and the Dual-Luciferase® Reporter Assay System (Promega) supplied protocol was followed for lysis and measurements. Recorded Firefly and Renilla luciferase activity was measured using TD-20/20 Luminometer (Turner Designs, Sunnyvale, CA).

5.2.4 RNA Isolation and Real-Time PCR

MCF7 cells were treated as described above and the total RNA was extracted as per manufacturer's protocol (Trizol, Life Technologies, Carlsbad, CA). Relative mRNA levels were quantified using quantitative real-time Polymerase Chain Reaction (qPCR) (Strategene Mx3005P, Agilent Technologies, La Jolla, CA). All values were normalized to the amplification of β−actin. The PCR primer sequences used are as follows: ERα forward; 5'-ATCCACCTGATGGCCAAG-3'; ERα reverse; 5'-GCTCCATGCCTTTGTTACTCA-3', PS2 forward; 5'-TCCCTCCAGAAGAGGAGTGT-3'; PS2 reverse; 5'-CAGAAGCGTGTCTGAGGTGT-3'. PR forward; 5'-TTACCATGTGGCAGATCCCACAG-3'; PR reverse; 5'-ACCATCCCTGCCAATATCTTGGG-3'; β−actin forward; 5'-GAGGCGTACAGGGATAGC-3'; β−actin reverse; 5'-ATGGATATCGCC-3'. Assays were performed using the 1-step 2X Brilliant SYBR Green qRT-PCR Master Mix Kit (Agilent Technologies) containing 200nM forward primer, 200nM reverse primer, and 100ng total mRNA. The conditions for target mRNA amplification were performed as follows: 1 cycle of 50°C for 30 min; 1 cycle of 95°C for 10 min; 35 cycles each 95°C for 30s, 55°C for 1 min, and 72°C for 30s.

5.2.5 Tumorsphere formation

3 weeks R. crenulata or Vehicle treated MCF7 cells were disassociated by Trypsin (Life Technologies, Grand Island, NY) and cell pellets were collected by centrifugation (5min, 1000g). Cells were then suspended in MammocultTM human medium kit (STEMCELL Technologies Inc., Vancouver, BC, Canada) and pipetted repeatedly to ensure single cell suspension. A total of 500 cells were plated on an AggreWellTM 800 plate (STEMCELL Technologies Inc.) and treated with *R. crenulata* or vehicle control retreated every 5 days for 3 weeks. Captured representative images were taken with a Nikon Eclipse TE2000-U using MetaVueTM software (Universal Imaging Corporation).

5.2.6 Western Blot Analysis

MCF7 cells were treated as described above and were lysed with RIPA buffer supplemented with phosphatase inhibitors and protease inhibitors (Sigma Aldrich®, St. Louis, MO). Lysate protein concentrations were measured by a BCATM Protein Assay Kit (Pierce, Rockford, IL), 50µg/ml of protein was run on a 10% SDS-PAGE and transferred onto a PVDF membrane (Sigma Aldrich®, St. Louis, MO). Membrane was blocked for one hour with 5% milk in TBS-T and primary antibodies (Rabbit non-phospho (Active) β-catenin (Ser33/37/Thr41) (D13A1) 1:1000 5% BSA in TBS-T (Cell Signaling Technology, Danvers, MA); Rabbit β-actin 1:2000 (Abcam, Cambridge, MA) were incubated over overnight. Secondary antibody [goat anti-rabbit IgG-HRP 1:5000 (Santa Cruz Biotechnology, Dallas, TX) was incubated for 2 hours at room temperature. The blot was washed and developed using a Western Blot Luminol Reagent (Santa Cruz Biotechnology) and imaged with a Synopics 4.2 MP camera and G:Box Chemi-XT4 GENESys software (SYNGENE, Frederick, MD). Image J software was used for band density quantification.

5.2.7 Animal care and treatment

This study was carried out in strict accordance with the recommendations in the Guide for the Care and Use of Laboratory Animals of the National Institutes of Health. The protocol was approved by the Baystate Medical Center Institutional Animal Care and Use Committee. Female129/C57Blk6 c (n=20) were split into two groups: 1. Vehicle treated group (N=10) and R. crenulata treated group. Each group was individually housed in plastic cages with food and water provided continuously, and maintained on a 12:12 light cycle. Mice were placed on a chow diet [Harlan Teklad global 18% protein rodent diet (#2018) containing 2.8% fat, 18.6% protein] for 12 weeks. Treatment was supplemented in the water at a 20 mg/kg/day concentration of R. crenulata or equivalent volume of vehicle control. Upon completion of the treatment, mice were euthanized by CO2 followed by cervical dislocation. Mammary glands (3rd, 4th, and 5th inguinal glands were harvested and fixed in 10% buffered formalin.

5.2.8 Immunohistochemistry (IHC)

IHC was performed on a DakoCytomation autostainer using the Envision HRP Detection system (Dako, Carpinteria, CA). Each tissue block was sectioned at 4 µm on a graded slide, deparaffinized in xylene, rehydrated in graded ethanols, and rinsed in Tris-phosphate-buffered saline (TBS). Heat induced antigen retrieval was performed in a microwave at 98ºC in 0.01 M citrate buffer. After cooling for 20 minutes, sections were rinsed in TBS and subjected to the following primary antibodies [ER (sc-542, Santa Cruz Biotechnology, Dallas, TX) ,PR (sc-538, Santa Cruz Biotechnology, Dallas,TX) and anti-BrdU (Rat monoclonal, Abcam, Cambridge MA) for 45 minutes. Immunoreactivity was visualized by incubation with chromogen diaminobenzidine (DAB) for 5 minutes. Tissue sections were counterstained with hematoxylin, dehydrated through graded ethanols and xylene, and cover-slipped. Images were captured with an Olympus BX41

light microscope using SPOT Software 5.1 (SPOT™Imaging Solutions, Detroit, MI). Total and positively stained epithelial cells from mammary glands were quantified and the percentage of positively labeled cells was calculated.

5.2.9 Statistical Analysis

For single treatments, results were analyzed using Student's t-test for R. crenulata treatment and combination treatments were analyzed by Two way ANOVA. Graphpad Prism statistical analysis software(San Diego, CA) was used in this analysis and figure generation. Grubb's test was used on all data to identify statistical outliers (http://www.graphpad.com/quickcalcs).

5.3 Results

5.3.1 *R. Crenulata* induces Estrogen transcription activity upon 24 hours of treatment.

To investigate whether the *R. crenulata* extract exhibits estrogenic activity, we treated ER+ MCF7 breast cancer cells expressing an ERE-Luc plasmid with 100 μg/ml of *R.crenulata* or vehicle control for 24 hours. A dual luciferase reporter assay showed that after 24 hours, *R. crenulata* significantly activates ER-mediated transcription in MCF7 cells (fig 5.1A). To determine whether these results corroborate with endogenous ER transcriptional activity, we performed a quantitative real-time PCR analysis of ERα target genes, PR and PS2. Our results demonstrate that the mRNA transcript levels of PR and PS2 are significantly increased in response to treatment with *R. crenulata* compared with vehicle treated cells (fig. 5.1B). Considering that estrogen is a potent mitogen in MCF7 cells, we examined proliferation in response to *R. crenulata* treatment in MCF7 cells using an automated cell counter. As expected, 24 hours following treatment with *R. crenulata,* we observed a significant increase in the number of

viable cells (fig 5.1C). Taken together, these results suggest that the *R. crenulata* extract contains estrogenic compounds capable of activating an ER-mediated response in MCF7 cells.

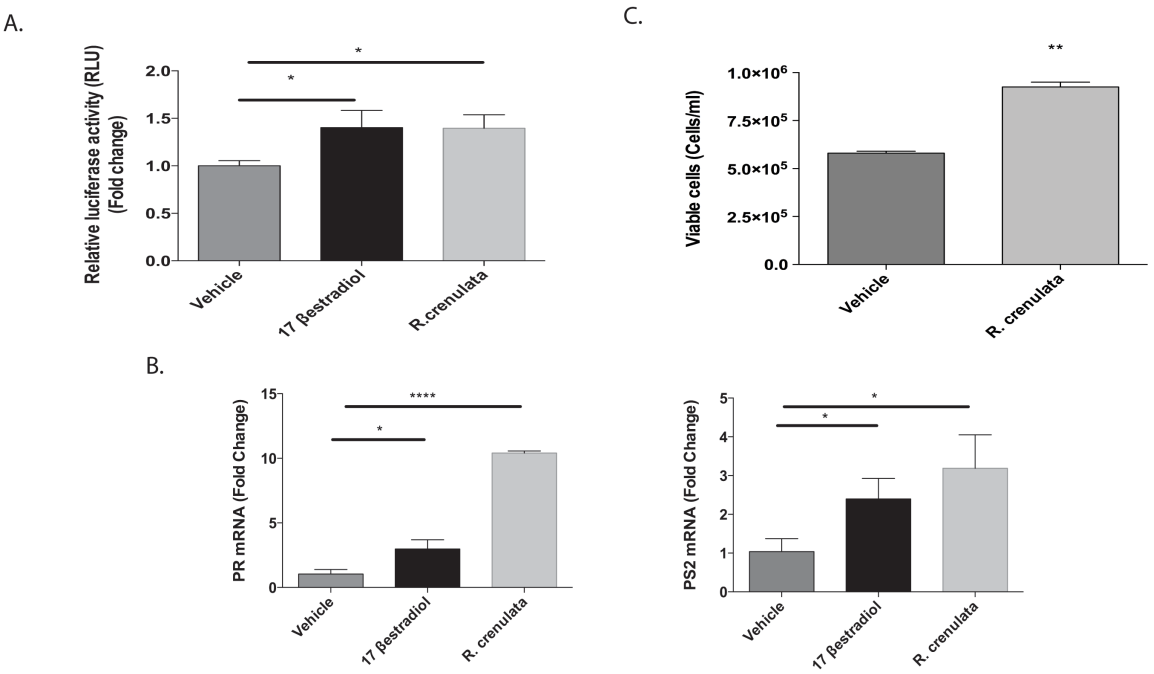

Figure 5.1. R. crenulata treatment induces ER transcriptional activation in MCF7 cells in vitro. MCF7cells were plated and after 24 hours, the media was replaced with charcoal stripped and phenol free media and cells were treated with 100 μg/ml R. crenulata or vehicle (10% EtOH) in the presence or absense of 10 nM 17 β–estradiol (positive control) for 24 hours. A. Bar graph representation of ERE-Luc plasmid luciferase reporter assay mean ± SEM (n=4) of the difference in fold change compared with control vehicle treated cells. B. Bar graph representation for qPCR analysis of ER target genes PR and PS2 mRNA levels normalized to βactin mRNA in response to R. crenulata and 17 β-estradiol treatment (n=3). Bars represent mean ± SEM of N=3. Results are expressed as relative expression of vehicle treated control cells. C. Bar graph representation of the mean ± SEM of MCF7 cell counts (n=3) cells after 24 hours treatment with R. crenulata or vehicle (*$p < 0.05$, **$p < 0.01$, ****$p<0.0001$).

5.3.2 Increased exposure time to *R. crenulata* diminishes the proliferative response observed in MCF7 cells and abolishes ER-mediated activity.

Since Rhodiola supplements are typically consumed over a period of time, we surmised that it would be more physiologically relevant to measure the growth pattern of MCF7 cells treated with *R. crenulata* over time. To that end, cells were plated at equal densities, treated

with *R. crenulata* or vehicle, counted over a period of 2 weeks, and the doubling time was calculated to assess changes in proliferation patterns. After 24 hours of treatment, results show that the doubling time of *R. crenulata* treated cells was 14.78 hours compared to 25.25 hours for the control vehicle treated cells (fig. 5.2A) in agreement with our previous study. Paradoxically, the later time points revealed a reverse in the proliferative pattern, a significant increase in doubling time in the *R. crenulata* treated cells was noted as early as 1 week.

Considering that *R. crenulata* reduced doubling times in MCF7 cells, we wanted to investigate whether ER transcriptional activity was also reduced following continuous treatment with *R .crenulata*. Therefore, we transfected an ERE-Luc plasmid into MCF7 cells which had been continuously treated with *R. crenulata* for 2 weeks. A dual luciferase reporter assay revealed that *R crenulata* treatment had reduced basal and 17-βestradiol -induced ER transcriptional activity (fig. 5.2B). Treatment with 10 nM 17-βestradiol significantly increased luciferase activity in both *R. crenulata* and vehicle treated cells suggesting that the receptor was still functional. Furthermore, the estrogen receptor antagonist, ICI 182,780, reduced luciferase activity in all treatments. This experiment suggests that ERα remains functional after a 2 week treatment with *R. crenulata* extract. Together these results indicate that longer treatment with *R. crenulata* reduces the overall proliferation and estrogenic response in ER+ MCF7 cancer cells, however the ERα remains fully functional.

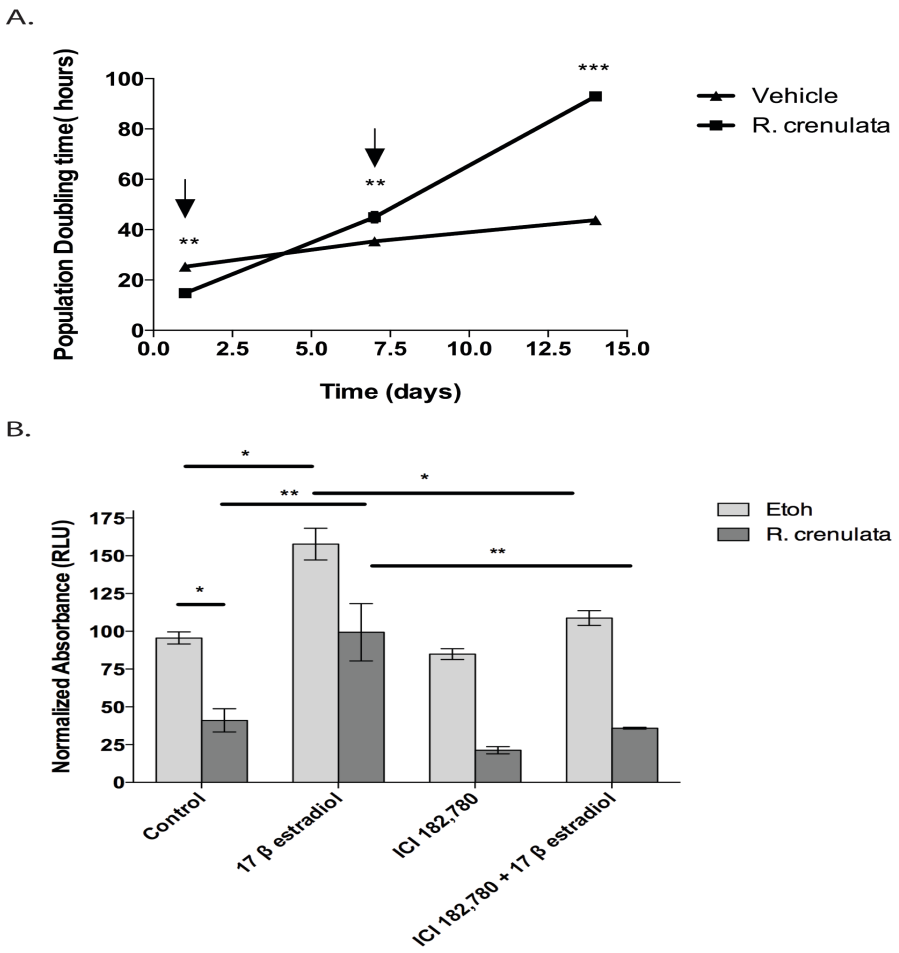

Figure 5.2. Continuous R. crenulata treatment alters MCF7 cell doubling time and abolishes ER-mediated activity. A. MCF7 cells were plated at 100,000 cells per well and treated with 100 μg/ml R .crenulata or vehicle (10% EtOH). Cells were counted at 1, 7, and 14 days and doubling time was calculated. Depicted results represent experiments performed in triplicate ± SEM. (*p < 0.05, **p < 0.01, *** < 0.001). B. MCF7 cells treated with R. crenulata and vehicle for 2 weeks were plated in 24 well plates and 24 hours later, the media was replace with charcoal stripped and phenol free media treated with 100 μg/ml R. crenulata or vehicle (10% EtOH) in the presense or absense of 10 nMof 17 β-estradiol (positive control) and or 20 nM ICI 182,780 (for 24 hours. Bar graph representation of ERE-Luc plasmid luciferase reporter assay mean ± SEM (N=3) (*p value< 0.05, **p value< 0.01, . All depicted significance is from adjusted p values from Bonferroni test post 2-way ANOVA analysis).

5.3.3 *R. crenulata* reduces the formation and maintenance of MCF7 tumorspheres.

The ability of cells to survive independent of attachment to surfaces and the ability to form tumorspheres are characteristics of resilient cancer cells. Our previous work with triple

negative breast cancer cells lines has suggested that *R. crenulata* reduces the tumorsphere generating abilities in these aggressive cell lines [14]. To assess this capability in less aggressive ER+ MCF7 cells, we plated a single cell suspension of MCF7 cells which had been previously treated with *R. crenulata* or vehicle for 2 weeks in low attachment plates and tumorsphere formation was monitored over 21 days. Within the first week, both *R. crenulata* and vehicle treated cells were able to form small tumorspheres under the described conditions (Week 1, fig. 5.3). However, over time, there were fewer *R. crenulata* treated tumorspheres compared to vehicle treated MCF7 cells. Additionally, vehicle treated tumorspheres increased in size compared to *R. crenulata* treated cells, an observation that persisted for the duration of the study (Week 2 ,3 fig. 5.3). These data suggest that treatment with a hydroalcoholic *R. crenulata* root extract reduces tumorsphere formation in ER+ MCF7 cells.

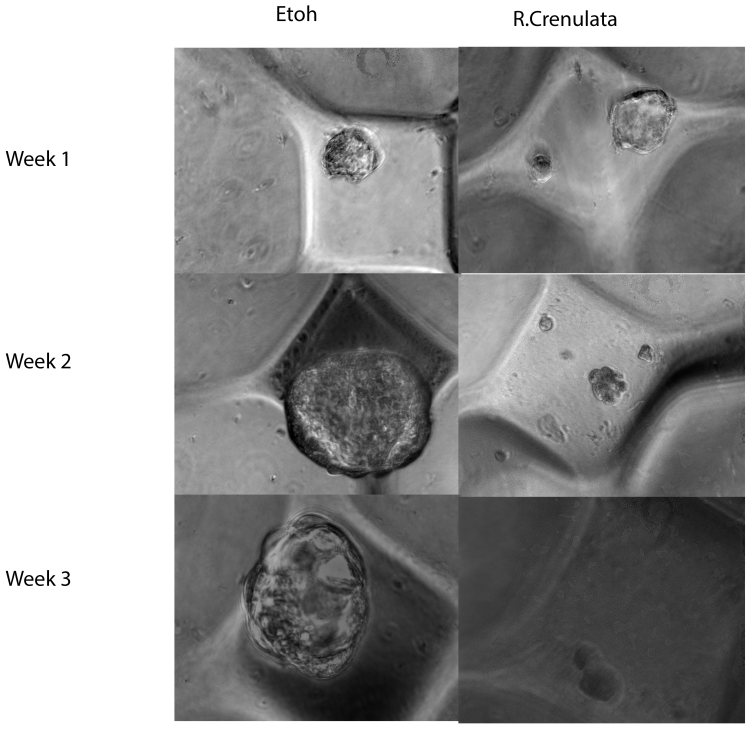

Figure 5.3. MCF7 tumorsphere formation is reduced in response to *R.crenulata* treatment. A total of 500 MCF7 cells were plated in an AggreWell^{TM} 800 plate, treated

with vehicle or *R. crenulata* and retreated every 5 days for 3 weeks. Phase contrast images were captured at weeks 1, 2 and 3. Images were captured at 20X magnification.

5.3.4 *R. crenulata* alters ERα expression and reduces β−catenin activity over time.

A 24 hour treatment with *R. crenulata* increased proliferation and ER activity while continuous treatment resulted in a decrease in proliferation and dampened the estrogenic response as well. Since ERα regulates the mitogenic effect of estrogen, we wanted to test whether *R. crenulata* treatment could alter ERα gene expression levels. Quantitative real-time PCR analysis revealed that ERα mRNA transcript levels were significantly increased in *R. crenulata* treated cells when compared with vehicle treated cells after 24 hours of treatment (fig. 5.4A). However, ERα mRNA levels were decreased after 2 weeks of continous treatment (fig. 5.4B). These results suggest that longer treatments with *R. crenulata* reduces estrogenic responses in ER+ MCF7 cancer cells by reducing the expression of ERα.

Since ER transciptional activity is known to be regulated by β-catenin and we have previously demonstrated that *R. crenulata* treatment inhibts β-catenin and decreases stem-like behaviors in more aggressive cancer cells [14] (Mora et al 2015, in press) we wanted to determine whether *R. crenulata* regulates β−catenin activity in these cells as well. To investigate whether there was a change in the β−catenin activity as defined by level of phosphorylation at (Ser33/37/Thr41), we probed protein extracts of 24 hour *R. crenulata* or vehicle treated cells via Western Blot analysis with a non-phospho (active) β−catenin antibody. To enhance active β−catenin levels, cells were treated with the GSK3 inhibitor, LiCl. As expected, LiCl treatment resulted in an increase in the amount of active β−catenin in MCF7 cells whereas *R. crenulata* treatment marginaly reduced it (fig. 5.4C, upper panel). To further confirm this observation, we transfected MCF7 cells with a β−catenin luciferase reporter construct (Super 8xTOPFlash Reporter) and treated the cells with *R. crenulata* or vehicle and stimulated β−catenin activity

with LiCl for 24 hrs. As expected, LiCl treatment resulted in increased β−catenin transcriptional activity and *R. crenulata* treatment significantly reduced this activity (fig 4.4C, lower panel). Thus, *R. crenulata* treatment inhibits β−catenin transcriptional activation in MCF7 cells. Finally we wanted to determine whether *R. crenulata* treatment reduced the amount of active β−catenin after 2 weeks of treatment. Western blot analysis probed with active β−catenin demonstrates a decrease in the level of active β−catenin in the MCF7 cells treated with *R. crenulata* for 2 weeks (fig. 4.4D,upper panel). Densitometry analysis normalizing the proteins to β-actin confirms a signifcant reduction in active β−catenin levels as well (fig. 4.4D, lower panel). Hence, these results suggest a possible mechanism by which *R. crenulata* negatively affects MCF7 neaoplastic behaviors.

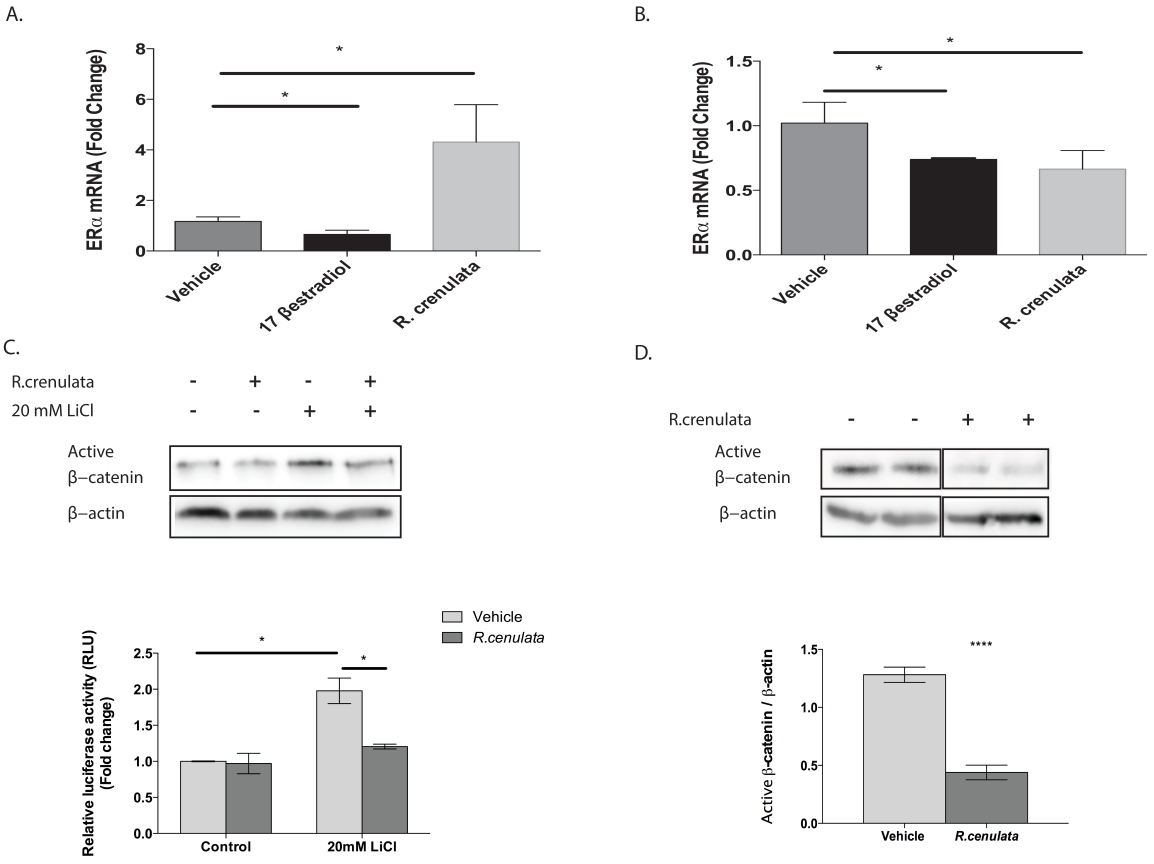

Figure 5.4. R.crenulata alters ERα expression and reduces β−catenin activity over time. A. & B. Bar graph representation for qPCR analysis of ERα mRNA levels normalized to β−actin mRNA in response to R. crenulata and 17 β-estradiol treatment (n=3) at A. 24

hours or B. 2 weeks. Bars represent mean ± SEM of n=3. Results are expressed as relative expression of vehicle treated control cells. C. R.crenulata reduces LiCl induced β–catenin activity Upper panel: representative image of total protein lysates immuno-blotted with anti-(active) β–catenin and normalizer βactin. Lower panel: Bar graph representation of β–catenin luciferase reporter assay mean ± SEM of the difference in fold change compared with control vehicle treated cells (N=4 *p value< 0.05). D. Upper panel: representative image of total protein lysaetes from MCF7 cells treated with R.crenulata or vehicle for 2 weeks immuno-blotted with anti-(active) β–catenin and normalizer βactin(N of 2 per treatment group). Lower panel: Bar representation of band densities quantified and normalized to actin. Bars represent mean ± SEM of N=4 (****p value < 0.0001).

5.3.5 R. crenulata does not change ER expression or activity in murine mammary glands.

R. crenulata is often taken as an anti-depressant and to date no known toxicities have not been noted. Given the short term estrogenic effect of *R. crenulata* on MCF7 cells, we wished to examine whether the expression of estrogen associated targets could be noted in the mammary glands of mice fed *R. crenulata* for 12 weeks. Ten week old 129/C57BLK6 female mice were provided *R. crenulata* in their water for 12 weeks. The amount of water imbibed was measured and calculated to be 20 mg/kg/day of *R. crenulata*. At the end of the study, we examined the expression of ER and PR by IHC. The number of positively stained cells was counted and our results reveal that there was no significant change with the inclusion of *R. crenulata* (fig 5.5,A, B).

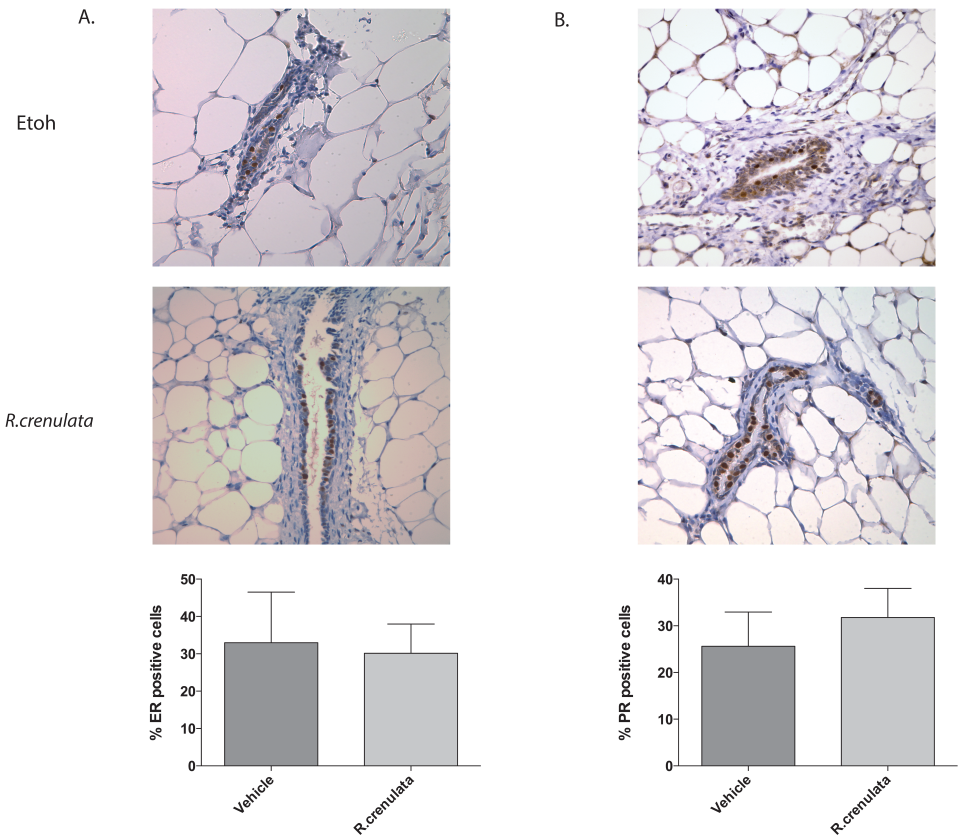

Figure 5.5. Estrogen receptor and progesterone receptor expression in mammary fat pads from 129/C57BLK6 female mice treated with *R. crenulata*. Image representation of IHC analysis performed on paraffin embedded mammary fat pads from mice treated with *R. crenulata* or vehicle for 12 weeks. A. ERα B. PR. Associated bar graphs represent the quantification of percentage of positively stained epithelial cells normalized to total of epithelial cells.

5.4 Discussion

The present study demonstrates that the *R.crenulata* extract contains components with estrogenic activity (fig. 5.1). However, these effects changed with prolonged treatment with *R. crenulata*. Cell doubling times were longer than the vehicle treated cells. After 2 weeks of *R. crenulata* treatment, MCF7 cells exhibited a decreased response to *R. crenulata* estrogenic response, but still remained responsive to activators and inhibitors (17 βestradiol and ICI 182,780), suggesting that the ERα receptor remains functional. In association with the changes

in doubling time, we found that prolonged exposure to *R. crenulata* reduced ERα mRNA (fig. 4A,B) levels and reduced β-catenin activation(fig. 5.4C,D).

β−catenin transcriptional activity ,via canonical WNT signaling, is implicated in the regulation of cell fate, proliferation, morphology, and migration during normal development [16]. Dysregulation of this signaling pathway has been implicated in breast cancer [17]; more specifically as a critical factor in cancer stem like behavior and tumorsphere initiating activity. Therefore,the *R.crenulata* effects on β−catenin support a mechanism to explain the inhibition of tumorsphere formation with extended *R.crenulata* treatment .

Additionally, ERα transcriptional activity has been shown to be affected by the levels of β−catenin levels. Specifically, Gupta et. al has demonstrated that β−catenin knockdown results in reduced ERα responsiveness to 17 βestradiol [18]. In our laboratory, we previously showed that in cells deficient in WNT signaling antagonist Secreted frizzeled related protein 1(SFRP1), where β−catenin transcriptional activity is increased, the cells' estrogenic transcriptional response to 17 βestradiol is enhanced (Gregory et al.,in press). Hence, a second explanation for the reduced estrogenic effects could be a result of delayed influence of *R. crenulata* on β-catenin levels and activity.

The safety and toxicity of *Rhodiola sp.* have been examined in several studies. For mild to moderate depression up to 400-700 mg *R. rosea* containing 3% rosavins and 1% salidroside has been given without noted side effects [19] . Since *Rhodiola sp.* supplements have gained popularity, we felt it was important to show that *Rhodiola sp.* contain estrogenic phytochemicals that can act on ER + cancer cells. However, our assessment in normal mammary glands of mice treated for 12 weeks with *R.crenulata* resulted in no changes in ER levels or activity. Future studies will have to be performed to determine whether this lack of effect *in*

vivo is due to low level of accumulation in the breast, a lack of effect on normal cells, or because of the extended treatment time.

5.5 References

[1] Eagon PK, Elm MS, Gerbarg PL, Houghton F Jr, Brown RP, Check JJ, et al. **Evaluation of the medicinal botanical Rhodiola rosea for estrogenicity**. Cancer Research 2004;64:663.

[2] DeSantis CE, Lin CC, Mariotto AB, Siegel RL, Stein KD, Kramer JL, et al. Cancer treatment and survivorship statistics, 2014. CA: a Cancer Journal for Clinicians 2014;64:252–71.

[3] EBCTCG ECTC. Effects of chemotherapy and hormonal therapy for early breast cancer on recurrence and 15-year survival: an overview of the randomised trials. The Lancet 2005.

[4] Hruska KS, Tilli MT, Ren S, Cotarla I, Kwong T, Li M, et al. Conditional over-expression of estrogen receptor alpha in a transgenic mouse model. Transgenic Res 2002;11:361–72.

[5] Madigan MP, Troisi R, Potischman N, Dorgan JF, Brinton LA, Hoover RN. Serum hormone levels in relation to reproductive and lifestyle factors in postmenopausal women (United States). Cancer Causes Control 1998;9:199–207.

[6] Verkasalo PK, Thomas HV, Appleby PN, Davey GK, Key TJ. Circulating levels of sex hormones and their relation to risk factors for breast cancer: a cross-sectional study in 1092 pre- and postmenopausal women (United Kingdom). Cancer Causes Control 2001;12:47–59.

[7] Eliassen AH, Missmer SA, Tworoger SS, Spiegelman D, Barbieri RL, Dowsett M, et al. Endogenous steroid hormone concentrations and risk of breast cancer among premenopausal women. J Natl Cancer Inst 2006;98:1406–15.

[8] Colditz GA, Hankinson SE, Hunter DJ, Willett WC, Manson JE, Stampfer MJ, et al. The use of estrogens and progestins and the risk of breast cancer in postmenopausal women. N Engl J Med 1995;332:1589–93.

[9] Panossian A, Wikman G, Sarris J. Rosenroot (Rhodiola rosea): Traditional use, chemical composition, pharmacology and clinical efficacy. Phytomedicine 2010.

[10] RA S, Aleksandrova IV, VK M, LN U, GG P. [Effect of Rhodiola rosea on the yield of mutation alterations and DNA repair in bone marrow cells]. Patologicheskaia Fiziologiia I Eksperimentalnaia Terapiia 1996.

[11] Majewska A, Grażyna H, Mirosława F, Natalia U, Agnieszka P, Alicja Z, et al. Antiproliferative and antimitotic effect, S phase accumulation and induction of apoptosis and necrosis after treatment of extract from Rhodiola rosea rhizomes on HL-60 cells. J Ethnopharmacol 2006;103:43–52.

[12] Liu Z, Li X, Simoneau AR, Jafari M, Zi X. Rhodiola rosea extracts and salidroside decrease the growth of bladder cancer cell lines via inhibition of the mTOR pathway and induction of autophagy. Mol Carcinog 2011;51:257–67.

[13] Tu Y, Roberts L, Shetty K, Schneider SS. Rhodiola crenulata induces death and inhibits growth of breast cancer cell lines. J Med Food 2008;11:413–23.

[14] Gauger KJ, Rodriguez-Cortes A. Rhodiola Crenulata inhibits the tumorigenic properties of invasive mammary epithelial cells with stem cell characteristics. Journal of Medicinal Food 2010.

[15] Kwon Y-I, Jang H-D, Shetty K. Evaluation of Rhodiola crenulata and Rhodiola rosea for management of type II diabetes and hypertension. Asia Pac J Clin Nutr 2006;15:425–32.

[16] Polakis P. Wnt signaling and cancer. Genes Dev 2000.

[17] Bisson I, Prowse DM. WNT signaling regulates self-renewal and differentiation of prostate cancer cells with stem cell characteristics. Cell Research 2009.

[18] Gupta N, Schmitt F, Grebhardt S, Mayer D. β-Catenin Is a Positive Regulator of Estrogen Receptor-α Function in Breast Cancer Cells. Cancers (Basel) 2011;3:2990–3001.

[19] Brown RP, Gerbarg PL, Ramazanov Z. Rhodiola rosea**: A Phytomedicinal Overview**. A Phytomedicinal … 2002:40–52.

CHAPTER 6
DISCUSSION

6.1 Sfrp1 obesity model: Further direction to understand the effects of *R. crenulata*

In chapter 2, we investigated the effects of HFD feeding on adiposity, glucose metabolism and inflammation in mice lacking expression of SFRP1. Our results demonstrate that SFRP1 is an important protein required for maintaining appropriate cellular signaling in response to the onset of obesity. As shown by the results, Sfrp1 deficiency affected several factors as it exacerbated weight gain, dysregulated glucose homeostasis in several tissues (decreased expression of glucose transporters [Slc2a2 and Slc2a4], aberrantly upregulated hepatic gluconeogenesis regulators [G6pc and Pck1], aberrant insulin secretion), and increased inflammation marked by an increase in macrophage infiltration and an expression of pro-inflammatory genes, in mice in response to diet induced obesity (DIO) [1]. Collectively these results mimic an extreme obesity model, however further characterization of the role of SFRP1 *in vitro* would be of advantage, to delineate the different factors.

Our results showed that glucose clearance was dysregulated as early as 2 weeks of HFD feeding, and that occurred independent of weight gain at that time point (fig. 2.1, 2.2). This suggested that glucose metabolism occurred first and was further exacerbated by increased adiposity. Inflammation is an important contributor to insulin resistance and glucose homeostasis. A sustained pro-inflammatory state was noted in our animals, however, the time frame for induction of inflammation remains unknown. It is possible that HFD feeding lead to an early inflammation which contributed to the dysregulation of glucose metabolism. This could be tested by examining animal tissues as early as two weeks, and by including a third group treated with a commercially available anti-inflammatory drug.

Another organ system that should be examined is the gastrointestinal tract. It has been long shown that insulin stimulation is increased through Incretins, a hormone released by enteroendocrine cells present in intestinal epithelium [2]. A study has shown that incretin production is regulated by the WNT/β–catenin signaling pathway [3]. We did not determine whether canonical WNT signaling is increased in the intestinal tissue in response to Sfrp1 deficiency, subsequently affecting incretin levels. We noted that insulin levels were consistently higher in the Sfrp1 $^{-/-}$ mice, and an increase in incretin levels could be a possible factor contributing to this observation, in addition to the increase Sfrp1 $^{-/-}$ islets sensitivity to high glucose stimulation (fig. 2.S2.A).

Understanding the discussed factors would be beneficial in understanding how *R.crenulata* treatment ameliorated glucose clearance and increased insulin sensitivity in Sfrp1 $^{-/-}$ at the early time point in the study (2 weeks)(fig. 3.3) The study described in chapter 3 of this dissertation, shows that *R. crenulata* attenuated DIO induced liver inflammation, hence if the inflammation induction is an event that occurs early in the HFD Sfrp1 $^{-/-}$ fed mice, *R. crenulata* could attenuate inflammation in the livers of these mice, which were shown to have an increase in pro-inflammatory cytokines and steotosis. Hence, further understanding of the Sfrp1 $^{-/-}$ on DIO would be beneficial.

6.2 *R. crenulata* and obesity complications: Future directions

It was previously shown that *R. crenulata* can inhibit adipogenesis *in vitro* [4], however our results demonstrate that there was no change in body fat percentage in mice on HFD treated with *R.crenulata* or vehicle. Additionally, studies have shown that salidroside improved glucose uptake in skeletal muscle and adipocytes[5,6] and lowered fasting insulin levels in ZDF diabetic rats[7]. The referenced studies [5-7] used concentrations of *Rhodiola sp.* or salidroside

of 80 μg/ml for *in vitro* salidroside study, and 500 mg/kg for the *in vivo* RC study. Our observations in both Sfrp1-/- mice and 129/C57Bl6 mouse models occurred using a dose of 20 mg/kg. We used this dose since Sfrp1-/- became very sensitive to insulin during the ITT analysis, and this dose was kept for the 129/C57Bl6 mice in order to compare between both studies. Therefore, dose analysis would be beneficial since the beneficial effects vary depending on the dosage. Since our dose is considerably lower than the published studies, and we only noted improvement in liver inflammation, we rationalize that the liver has higher exposure to the *R. crenulata* since it is known to be an organ responsible for processing and metabolizing nutrients. Hence further analysis with higher dosage could affect other organs and result in an earlier improvement in glucose metabolism.

6.3 *R.crenulata* and WNT signaling: How does it occur?

In chapter 4, we demonstrated for the first time that *R.crenulata* treatment inhibits β–catenin transcriptional activity (fig. 4.1). We further attempted to define the mechanism of inhibition in MDA-MB-231 cells, and we were able to narrow the possible targets and demonstrate that it occurs in the cytoplasm. We first hypothesized that this inhibition is occurring due to increased GSK3β. When WNT/β–catenin signaling is on, GSK3β is phosphorylated on Ser9, which renders it unable to phosphorylate. As a result, β–catenin accumulates in the cytoplasm and translocate to the nucleus where it transcribes WNT target genes. This phosphorylation event is decreased when WNT/β–catenin signaling is off. However, using monoclonal antibodies against GSK3βpSER9, we were unable to detect a change in phosphorylation levels (data not shown).

Current data from our laboratory suggests that *R. crenulata* affects cellular respiration of MDA-MB-231 breast cancer cells. Respiration at the cellular level is based on the

consumption of glucose. A recent study in MDA-MB-231 cells demonstrated that β–catenin nuclear translocation is dependent on its acetylation, which is regulated by glucose availability [8]. Our results simply indicate that inhibition by *R. crenulata* occurs upstream of the nuclear translocation, hence acetylation could conceivably be part of this mechnaism.

6.4 References

[1] Gauger KJ, Bassa LM, Henchey EM, Wyman J, Bentley B, Brown M, et al. Mice Deficient in Sfrp1 Exhibit Increased Adiposity, Dysregulated Glucose Metabolism, and Enhanced Macrophage Infiltration. PLoS ONE 2013;8:e78320. doi:10.1371/journal.pone.0078320.

[2] García-Jiménez C. Wnt and incretin connections. Vitam Horm 2010;84:355–87. doi:10.1016/B978-0-12-381517-0.00014-X.

[3] García-Martínez JM, Chocarro-Calvo A, Moya CM, García-Jiménez C. WNT/β-catenin increases the production of incretins by entero-endocrine cells. Diabetologia 2009;52:1913–24. doi:10.1007/s00125-009-1429-1.

[4] Lee OH, Kwon YI, Apostolidis E, Shetty K. Rhodiola-induced inhibition of adipogenesis involves antioxidant enzyme response associated with pentose phosphate pathway. Phytotherapy … 2011. doi:10.1002/ptr.3236.

[5] Li H-B, Ge Y-K, Zheng X-X, Zhang L. Salidroside stimulated glucose uptake in skeletal muscle cells by activating AMP-activated protein kinase. European Journal of Pharmacology 2008;588:165–9. doi:10.1016/j.ejphar.2008.04.036.

[6] Shu-Hai W. [Effects of salidroside on carbohydrate metabolism and differentiation of 3T3-L1 adipocytes]. Zhong Xi Yi Jie He Xue Bao 2004;2:193–5.

[7] Wang J, Rong X, Li W, Yang Y, Yamahara J, Li Y. Rhodiola crenulata root ameliorates derangements of glucose and lipid metabolism in a rat model of the metabolic syndrome and type 2 diabetes. J Ethnopharmacol 2012;142:782–8. doi:10.1016/j.jep.2012.05.063.

[8] Chocarro-Calvo A, García-Martínez JM, Ardila-González S, la Vieja De A, García-Jiménez C. Glucose-Induced β-Catenin Acetylation Enhances Wnt Signaling in Cancer. Molcel 2013;49:474–86. doi:10.1016/j.molcel.2012.11.022.

BIBLIOGRAPHY

An R. Prevalence and Trends of Adult Obesity in the US, 1999-2012. ISRN Obes 2014;2014:185132.

Ogden CL, Carroll MD, Kit BK, Flegal KM. Prevalence of obesity among adults: United States, 2011-2012. NCHS Data Brief 2013:1–8.

Flegal KM, Carroll MD, Ogden CL, Curtin LR. Prevalence and Trends in Obesity Among US Adults, 1999-2008. Jama 2010;303:235–41.

Polednak AP. Estimating the number of U.S. incident cancers attributable to obesity and the impact on temporal trends in incidence rates for obesity-related cancers. Cancer Detect Prev 2008;32:190–9.

Hotamisligil GS. Inflammation and metabolic disorders. Nature 2006.

Sun K, Kusminski CM, Scherer PE. Adipose tissue remodeling and obesity. J Clin Invest 2011;121:2094–101.

Moon B, Kwan J, Duddy N. Resistin inhibits glucose uptake in L6 cells independently of changes in insulin signaling and GLUT4 translocation. American Journal of … 2003.

Stephens JM, Pekala PH. Transcriptional repression of the C/EBP-alpha and GLUT4 genes in 3T3-L1 adipocytes by tumor necrosis factor-alpha. Regulations is coordinate and independent of protein synthesis. J Biol Chem 1992;267:13580–4.

Stephens JM, Lee J, Pilch PF. Tumor necrosis factor-alpha-induced insulin resistance in 3T3-L1 adipocytes is accompanied by a loss of insulin receptor substrate-1 and GLUT4 expression without a loss of insulin receptor-mediated signal transduction. J Biol Chem 1997;272:971–6.

Rui L, Aguirre V, Kim JK, Shulman GI, Lee A, Corbould A, et al. Insulin/IGF-1 and TNF-alpha stimulate phosphorylation of IRS-1 at inhibitory Ser307 via distinct pathways. J Clin Invest 2001;107:181–9.

Hotamisligil GS, Shargill NS, Spiegelman BM. Adipose expression of tumor necrosis factor-alpha: direct role in obesity-linked insulin resistance. Science 1993;259:87–91.

Cheung AT. An in Vivo Model for Elucidation of the Mechanism of Tumor Necrosis Factor- (TNF-)-Induced Insulin Resistance: Evidence for Differential Regulation of Insulin Signaling by TNF. Endocrinology 1998;139:4928–35.

De Taeye BM, Novitskaya T, McGuinness OP, Gleaves L, Medda M, Covington JW, et al. Macrophage TNF- contributes to insulin resistance and hepatic steatosis in diet-induced obesity. AJP: Endocrinology and Metabolism 2007;293:E713–25.

Uysal KT, Wiesbrock SM, Marino MW, Hotamisligil GS. Protection from obesity-induced insulin resistance in mice lacking TNF-α function. Nature 1997;389:610–4.

Pradhan AD, Manson JE, Rifai N, Buring JE, Ridker PM. C-reactive protein, interleukin 6, and risk of developing type 2 diabetes mellitus. Jama 2001;286:327–34.

Hong E-G, Ko HJ, Cho Y-R, Kim H-J, Ma Z, Yu TY, et al. Interleukin-10 prevents diet-induced insulin resistance by attenuating macrophage and cytokine response in skeletal muscle. Diabetes 2009;58:2525–35.

Cai D, Yuan M, Frantz DF, Melendez PA, Hansen L, Lee J, et al. Local and systemic insulin resistance resulting from hepatic activation of IKK-β and NF-κB. Nature Medicine 2005;11:183–90.

Park EJ, Lee JH, Yu G-Y, He G, Ali SR, Holzer RG, et al. Dietary and Genetic Obesity Promote Liver Inflammation and Tumorigenesis by Enhancing IL-6 and TNF Expression. Cell 2010;140:197–208.

Akdis CA, Blaser K. Mechanisms of interleukin-10-mediated immune suppression. Immunology 2001;103:131–6.

Gordon S, Taylor PR. Monocyte and macrophage heterogeneity. Nat Rev Immunol 2005;5:953–64.

Gordon S. Alternative activation of macrophages. Nat Rev Immunol 2003;3:23–35.

Cinti S. Adipocyte death defines macrophage localization and function in adipose tissue of obese mice and humans. The Journal of Lipid Research 2005;46:2347–55.

Suganami T, Ogawa Y. Adipose tissue macrophages: their role in adipose tissue remodeling. Journal of Leukocyte Biology 2010;88:33–9.

Xu H, Barnes GT, Yang Q, Tan G, Yang D, Chou CJ, et al. Chronic inflammation in fat plays a crucial role in the development of obesity-related insulin resistance. J Clin Invest 2003;112:1821–30.

Weisberg SP, McCann D, Desai M, Rosenbaum M, Leibel RL, Ferrante AW Jr. Obesity is associated with macrophage accumulation in adipose tissue. J Clin Invest 2003;112:1796–808.

Osborn O, Olefsky JM. The cellular and signaling networks linking the immune system and metabolism in disease. Nature Medicine 2012;18:363–74.

Lee J. Adipose tissue macrophages in the development of obesity-induced inflammation, insulin resistance and type 2 Diabetes. Arch Pharm Res 2013;36:208–22.

Pham CTN. Neutrophil serine proteases: specific regulators of inflammation. Nat Rev Immunol 2006;6:541–50.

Talukdar S, Oh DY, Bandyopadhyay G, Li D, Xu J, McNelis J, et al. Neutrophils mediate insulin resistance in mice fed a high-fat diet through secreted elastase. Nature Medicine 2012;18:1407–12.

Nijhuis J, Rensen SS, Slaats Y, van Dielen FMH, Buurman WA, Greve JWM. Neutrophil Activation in Morbid Obesity, Chronic Activation of Acute Inflammation. Obesity 2009;17:2014–8.

Waki H, Yamauchi T, Kamon J, Kita S, Ito Y, Hada Y, et al. Generation of Globular Fragment of Adiponectin by Leukocyte Elastase Secreted by Monocytic Cell Line THP-1. Endocrinology 2005;146:790–6.

Elgazar-Carmon V, Rudich A, Hadad N, Levy R. Neutrophils transiently infiltrate intra-abdominal fat early in the course of high-fat feeding. The Journal of Lipid Research 2008;49:1894–903.

Mansuy-Aubert V, Zhou QL, Xie X, Gong Z, Huang J-Y, Khan AR, et al. Imbalance between Neutrophil Elastase and its Inhibitor α1-Antitrypsin in Obesity Alters Insulin Sensitivity, Inflammation, and Energy Expenditure. Cell Metabolism 2013;17:534–48.

DeSantis CE, Lin CC, Mariotto AB, Siegel RL, Stein KD, Kramer JL, et al. Cancer treatment and survivorship statistics, 2014. CA: a Cancer Journal for Clinicians 2014;64:252–71.

Siegel R, Naishadham D, Jemal A. Cancer statistics, 2013. CA: a Cancer Journal for Clinicians 2013;63:11–30.

Breen N, Gentleman JF, Schiller JS. Update on mammography trends. Cancer 2010;117:2209–18.

Ellison RC, Zhang Y, McLennan CE, Rothman KJ. Exploring the relation of alcohol consumption to risk of breast cancer. Am J Epidemiol 2001;154:740–7.

Pharoah PD, Day NE, Duffy S, Easton DF, Ponder BA. Family history and the risk of breast cancer: a systematic review and meta-analysis. Int J Cancer 1997;71:800–9.

Brinton LA, Schairer C, Hoover RN, Fraumeni JF. Menstrual factors and risk of breast cancer. Cancer Invest 1988;6:245–54.

Nelson HD, Humphrey LL, Nygren P, Teutsch SM, Allan JD. Postmenopausal Hormone Replacement Therapy. Jama 2002;288:872–10.

Grivennikov SI, Greten FR, Karin M. Immunity, inflammation, and cancer. Cell 2010.

Singletary SE. Rating the risk factors for breast cancer. Ann Surg 2003;237:474–82.

Tretli S. Height and weight in relation to breast cancer morbidity and mortality. A prospective study of 570,000 women in Norway. International Journal of Cancer 1989;44:23–30.

FRCPath PJSR-F, MD PLP. Breast Cancer 2Gene expression profiling in breast cancer: classification, prognostication, and prediction. The Lancet 2011;378:1812–23.

Alizart M, Saunus J, Cummings M, Lakhani SR. Molecular classification of breast carcinoma. Diagnostic Histopathology 2012;18:97–103.

Goldhirsch A, Wood WC, Coates AS, Gelber RD, Thurlimann B, Senn HJ, et al. Strategies for subtypes--dealing with the diversity of breast cancer: highlights of the St. Gallen International Expert Consensus on the Primary Therapy of Early Breast Cancer 2011. Ann. Oncol., vol. 22, 2011, pp. 1736–47.

EBCTCG EBCTCG. Effect of radiotherapy after breast-conserving surgery on 10-year recurrence and 15-year breast cancer death: meta-analysis of individual patient data for 10â€ˆ801 women in 17 randomised trials. The Lancet 2011;378:1707–16.

Buchholz TA. Radiotherapy and survival in breast cancer. The Lancet 2011;378:1680–2.

Bennett CN. Regulation of Wnt Signaling during Adipogenesis. Journal of Biological Chemistry 2002;277:30998–1004.

Ross SE, Hemati N, Longo KA, Bennett CN, Lucas PC, Erickson RL, et al. Inhibition of Adipogenesis by Wnt Signaling. Science 2000;289:950–3.

Bennett CN, Hodge CL, MacDougald OA, Schwartz J. Role of Wnt10b and C/EBPα in spontaneous adipogenesis of 243 cells. Biochemical and Biophysical Research Communications 2003;302:12–6.

Lagathu C, Christodoulides C, Tan CY, Virtue S, Laudes M, Campbell M, et al. Secreted frizzled-related protein 1 regulates adipose tissue expansion and is dysregulated in severe obesity. International Journal of Obesity 2010;34:1695–705.

Mori H, Prestwich TC, Reid MA, Longo KA, Gerin I, Cawthorn WP, et al. Secreted frizzled-related protein 5 suppresses adipocyte mitochondrial metabolism through WNT inhibition. J Clin Invest 2012;122:2405–16.

Pereira C, Schaer DJ, Bachli EB, Kurrer MO, Schoedon G. Wnt5A/CaMKII Signaling Contributes to the Inflammatory Response of Macrophages and Is a Target for the Antiinflammatory Action of Activated Protein C and Interleukin-10. Arteriosclerosis, Thrombosis, and Vascular Biology 2008;28:504–10.

Pereira CP, Bachli EB, Schoedon G. The Wnt pathway: A macrophage effector molecule that triggers inflammation. Current Atherosclerosis Reports 2009;11:236–42.

Barandon L, Casassus F, Leroux L, Moreau C, Allieres C, Lamaziere JMD, et al. Secreted Frizzled-Related Protein-1 Improves Postinfarction Scar Formation Through a Modulation of Inflammatory Response. Arteriosclerosis, Thrombosis, and Vascular Biology 2011;31:e80–7.

Kim SH, Hyun SH, Choung SY. Antioxidative effects of Cinnamomi cassiaeand Rhodiola roseaextracts in liver of diabetic mice. BioFactors 2006;26:209–19.

Senthilkumar R, Parimelazhagan T, Chaurasia OP, Srivastava RB. Free radical scavenging property and antiproliferative activity of Rhodiola imbricata Edgew extracts in HT-29 human colon cancer cells. Asian Pacific Journal of Tropical Medicine 2012;6:11–9.

Battistelli M, De Sanctis R, De Bellis R, Cucchiarini L, Dachà M, Gobbi P. Rhodiola rosea as antioxidant in red blood cells: ultrastructural and hemolytic behaviour. Eur J Histochem 2005;49:243–54.

Li HX, Sze SCW, Tong Y, Ng TB. Production of Th1- and Th2-dependent cytokines induced by the Chinese medicine herb, Rhodiola algida, on human peripheral blood monocytes. J Ethnopharmacol 2009;123:257–66.

Brown RP, Gerbarg PL, Ramazanov Z. Rhodiola rosea**: A Phytomedicinal Overview**. A Phytomedicinal … 2002:40–52.

Zheng K, Guo A, Bi C, Zhu K, Chan G, Fu Q, et al. The Extract of Rhodiolae Crenulatae Radix et Rhizoma Induces the Accumulation of HIF-1 αvia Blocking the Degradation Pathway in Cultured Kidney Fibroblasts. Planta Med 2010;77:894–9.

Liu Z, Li X, Simoneau AR, Jafari M, Zi X. Rhodiola rosea extracts and salidroside decrease the growth of bladder cancer cell lines via inhibition of the mTOR pathway and induction of autophagy. Mol Carcinog 2011;51:257–67.

progress of research study on pharmacological action of rhodiola rosea. Acute Chinese Medicine and Pharmacology 2003;31:57–9.

Kwon Y-I, Jang H-D, Shetty K. Evaluation of Rhodiola crenulata and Rhodiola rosea for management of type II diabetes and hypertension. Asia Pac J Clin Nutr 2006;15:425–32.

Abidov M, Crendal F, Grachev S, Seifulla R, Ziegenfuss T. Effect of Extracts from Rhodiola Rosea and Rhodiola Crenulata (Crassulaceae) Roots on ATP Content in Mitochondria of Skeletal Muscles. Bulletin of Experimental Biology and Medicine 2003;136:585–7.

Li H-B, Ge Y-K, Zheng X-X, Zhang L. Salidroside stimulated glucose uptake in skeletal muscle cells by activating AMP-activated protein kinase. European Journal of Pharmacology 2008;588:165–9.

Shu-Hai W. [Effects of salidroside on carbohydrate metabolism and differentiation of 3T3-L1 adipocytes]. Zhong Xi Yi Jie He Xue Bao 2004;2:193–5.

Lee OH, Kwon YI, Apostolidis E, Shetty K. Rhodiola-induced inhibition of adipogenesis involves antioxidant enzyme response associated with pentose phosphate pathway. Phytotherapy … 2011.

Wang J, Rong X, Li W, Yang Y, Yamahara J, Li Y. Rhodiola crenulata root ameliorates derangements of glucose and lipid metabolism in a rat model of the metabolic syndrome and type 2 diabetes. J Ethnopharmacol 2012;142:782–8.

RA S, Aleksandrova IV, VK M, LN U, GG P. [Effect of Rhodiola rosea on the yield of mutation alterations and DNA repair in bone marrow cells]. Patologicheskaia Fiziologiia I Eksperimentalnaia Terapiia 1996.

Majewska A, Grażyna H, Mirosława F, Natalia U, Agnieszka P, Alicja Z, et al. Antiproliferative and antimitotic effect, S phase accumulation and induction of apoptosis and necrosis after treatment of extract from Rhodiola rosea rhizomes on HL-60 cells. J Ethnopharmacol 2006;103:43–52.

OA B, Matveev BP. The effect of a Rhodiola rosea extract on the incidence of recurrences of asuperficial bladder cancer (experimental clinical research). Urol Nefrol Mosk 1995:46–7.

Tu Y, Roberts L, Shetty K, Schneider SS. Rhodiola crenulata induces death and inhibits growth of breast cancer cell lines. J Med Food 2008;11:413–23.

Gauger KJ, Rodriguez-Cortes A. Rhodiola Crenulata inhibits the tumorigenic properties of invasive mammary epithelial cells with stem cell characteristics. Journal of Medicinal Food 2010.

Eagon PK, Elm MS, Gerbarg PL, Houghton F Jr, Brown RP, Check JJ, et al. Evaluation of the medicinal botanical Rhodiola rosea for estrogenicity. Cancer Research 2004;64:663.

Faust IM, Johnson PR, Stern JS, Hirsch J (1978) Diet-induced adipocyte number increase in adult rats: a new model of obesity. Am J Physiol 235: E279-286.

Jo J, Gavrilova O, Pack S, Jou W, Mullen S, et al. (2009) Hypertrophy and/or Hyperplasia: Dynamics of Adipose Tissue Growth. PLoS Comput Biol 5: e1000324.

Yokota Y, Mori S, Narumi O, Kitajima K (2001) In vivo function of a differentiation inhibitor, Id2. IUBMB Life 51: 207-214.

Aarsland A, Chinkes D, Wolfe RR (1997) Hepatic and whole-body fat synthesis in humans during carbohydrate overfeeding. Am J Clin Nutr 65: 1774-1782.

Roberts R, Hodson L, Dennis AL, Neville MJ, Humphreys SM, et al. (2009) Markers of de novo lipogenesis in adipose tissue: associations with small adipocytes and insulin sensitivity in humans. Diabetologia 52: 882-890.

Postic C, Girard J (2008) Contribution of de novo fatty acid synthesis to hepatic steatosis and insulin resistance: lessons from genetically engineered mice. J Clin Invest 118: 829-838.

Ouchi N, Kihara S, Funahashi T, Matsuzawa Y, Walsh K (2003) Obesity, adiponectin and vascular inflammatory disease. Curr Opin Lipidol 14: 561-566.

Bennett CN, Ross SE, Longo KA, Bajnok L, Hemati N, et al. (2002) Regulation of Wnt signaling during adipogenesis. J Biol Chem 277: 30998-31004.

Ross SE, Hemati N, Longo KA, Bennett CN, Lucas PC, et al. (2000) Inhibition of adipogenesis by Wnt signaling. Science 289: 950-953.

Bennett CN, Hodge CL, MacDougald OA, Schwartz J (2003) Role of Wnt10b and C/EBPalpha in spontaneous adipogenesis of 243 cells. Biochem Biophys Res Commun 302: 12-16.

Kanazawa A, Tsukada S, Sekine A, Tsunoda T, Takahashi A, et al. (2004) Association of the gene encoding wingless-type mammary tumor virus integration-site family member 5B (WNT5B) with type 2 diabetes. Am J Hum Genet 75: 832-843.

Nishizuka M, Koyanagi A, Osada S, Imagawa M (2008) Wnt4 and Wnt5a promote adipocyte differentiation. FEBS Lett 582: 3201-3205.

Kawano Y, Kypta R (2003) Secreted antagonists of the Wnt signalling pathway. J Cell Sci 116: 2627-2634.

Krishnan V, Bryant HU, Macdougald OA (2006) Regulation of bone mass by Wnt signaling. J Clin Invest 116: 1202-1209.

Bovolenta P, Esteve P, Ruiz JM, Cisneros E, Lopez-Rios J (2008) Beyond Wnt inhibition: new functions of secreted Frizzled-related proteins in development and disease. J Cell Sci 121: 737-746.

Finch PW, He X, Kelley MJ, Uren A, Schaudies RP, et al. (1997) Purification and molecular cloning of a secreted, Frizzled-related antagonist of Wnt action. Proc Natl Acad Sci U S A 94: 6770-6775.

Bafico A, Gazit A, Pramila T, Finch PW, Yaniv A, et al. (1999) Interaction of frizzled related protein (FRP) with Wnt ligands and the frizzled receptor suggests alternative mechanisms for FRP inhibition of Wnt signaling. J Biol Chem 274: 16180-16187.

Lagathu C, Christodoulides C, Tan CY, Virtue S, Laudes M, et al. Secreted frizzled-related protein 1 regulates adipose tissue expansion and is dysregulated in severe obesity. Int J Obes (Lond) 34: 1695-1705.

Koza RA, Nikonova L, Hogan J, Rim JS, Mendoza T, et al. (2006) Changes in gene expression foreshadow diet-induced obesity in genetically identical mice. PLoS Genet 2: e81.

Mori H, Prestwich TC, Reid MA, Longo KA, Gerin I, et al. Secreted frizzled-related protein 5 suppresses adipocyte mitochondrial metabolism through WNT inhibition. J Clin Invest 122: 2405-2416.

Ouchi N, Higuchi A, Ohashi K, Oshima Y, Gokce N, et al. (2011) Sfrp5 is an anti-inflammatory adipokine that modulates metabolic dysfunction in obesity. Science 329: 454-457.

Sen M (2005) Wnt signalling in rheumatoid arthritis. Rheumatology (Oxford) 44: 708-713.

Blumenthal A, Ehlers S, Lauber J, Buer J, Lange C, et al. (2006) The Wingless homolog WNT5A and its receptor Frizzled-5 regulate inflammatory responses of human mononuclear cells induced by microbial stimulation. Blood 108: 965-973.

Pereira C, Schaer DJ, Bachli EB, Kurrer MO, Schoedon G (2008) Wnt5A/CaMKII signaling contributes to the inflammatory response of macrophages and is a target for the antiinflammatory action of activated protein C and interleukin-10. Arterioscler Thromb Vasc Biol 28: 504-510.

Pereira CP, Bachli EB, Schoedon G (2009) The wnt pathway: a macrophage effector molecule that triggers inflammation. Curr Atheroscler Rep 11: 236-242.

Barandon L, Casassus F, Leroux L, Moreau C, Allieres C, et al. (2011) Secreted frizzled-related protein-1 improves postinfarction scar formation through a modulation of inflammatory response. Arterioscler Thromb Vasc Biol 31: e80-87.

Barandon L, Couffinhal T, Ezan J, Dufourcq P, Costet P, et al. (2003) Reduction of infarct size and prevention of cardiac rupture in transgenic mice overexpressing FrzA. Circulation 108: 2282-2289.

Gauger KJ, Hugh JM, Troester MA, Schneider SS (2009) Down-regulation of sfrp1 in a mammary epithelial cell line promotes the development of a cd44high/cd24low population which is invasive and resistant to anoikis. Cancer Cell Int 9: 11.

Liu W, Singh R, Choi CS, Lee HY, Keramati AR, et al. Low density lipoprotein (LDL) receptor-related protein 6 (LRP6) regulates body fat and glucose homeostasis by modulating nutrient sensing pathways and mitochondrial energy expenditure. J Biol Chem 287: 7213-7223.

Liu H, Fergusson MM, Wu JJ, Rovira, II, Liu J, et al. Wnt signaling regulates hepatic metabolism. Sci Signal 4: ra6.

Cohen JC, Horton JD, Hobbs HH Human fatty liver disease: old questions and new insights. Science 332: 1519-1523.

Moschen AR, Kaser A, Enrich B, Mosheimer B, Theurl M, et al. (2007) Visfatin, an adipocytokine with proinflammatory and immunomodulating properties. J Immunol 178: 1748-1758.

Fiorentino M, Zadra G, Palescandolo E, Fedele G, Bailey D, et al. (2008) Overexpression of fatty acid synthase is associated with palmitoylation of Wnt1 and cytoplasmic stabilization of beta-catenin in prostate cancer. Lab Invest 88: 1340-1348.

Apovian CM, Bigornia S, Mott M, Meyers MR, Ulloor J, et al. (2008) Adipose macrophage infiltration is associated with insulin resistance and vascular endothelial dysfunction in obese subjects. Arterioscler Thromb Vasc Biol 28: 1654-1659.

Cinti S, Mitchell G, Barbatelli G, Murano I, Ceresi E, et al. (2005) Adipocyte death defines macrophage localization and function in adipose tissue of obese mice and humans. J Lipid Res 46: 2347-2355.

Gauger KJ, Shimono A, Crisi GM, Schneider SS Loss of SFRP1 promotes ductal branching in the murine mammary gland. BMC Dev Biol 12: 25.

Gauger KJ, Chenausky KL, Murray ME, Schneider SS (2011) SFRP1 reduction results in an increased sensitivity to TGF-beta signaling. BMC Cancer 11: 59.

Turashvili G, Bouchal J, Burkadze G, Kolar Z (2006) Wnt signaling pathway in mammary gland development and carcinogenesis. Pathobiology 73: 213-223.

Esteve P, Sandonis A, Cardozo M, Malapeira J, Ibanez C, et al. (2011) SFRPs act as negative modulators of ADAM10 to regulate retinal neurogenesis. Nat Neurosci 14: 562-569.

Hausler KD, Horwood NJ, Chuman Y, Fisher JL, Ellis J, et al. (2004) Secreted frizzled-related protein-1 inhibits RANKL-dependent osteoclast formation. J Bone Miner Res 19: 1873-1881.

Martin-Manso G, Calzada MJ, Chuman Y, Sipes JM, Xavier CP, et al. sFRP-1 binds via its netrin-related motif to the N-module of thrombospondin-1 and blocks thrombospondin-1 stimulation of MDA-MB-231 breast carcinoma cell adhesion and migration. Arch Biochem Biophys 509: 147-156.

Stuckenholz C, Lu L, Thakur PC, Choi TY, Shin D, et al. Sfrp5 modulates both Wnt and BMP signaling and regulates gastrointestinal organogensis in the zebrafish, Danio rerio. PLoS One 8: e62470.

Strable MS, Ntambi JM Genetic control of de novo lipogenesis: role in diet-induced obesity. Crit Rev Biochem Mol Biol 45: 199-214.

Mahdi T, Hanzelmann S, Salehi A, Muhammed SJ, Reinbothe TM, et al. Secreted frizzled-related protein 4 reduces insulin secretion and is overexpressed in type 2 diabetes. Cell Metab 16: 625-633.

Vida M, Serrano A, Romero-Cuevas M, Pavon FJ, Gonzalez-Rodriguez A, et al. IL-6 cooperates with peroxisome proliferator-activated receptor-alpha-ligands to induce liver fatty acid binding protein (LFABP) up-regulation. Liver Int.

Eissing L, Scherer T, Todter K, Knippschild U, Greve JW, et al. De novo lipogenesis in human fat and liver is linked to ChREBP-beta and metabolic health. Nat Commun 4: 1528.

Yoshino T, Kusunoki N, Tanaka N, Kaneko K, Kusunoki Y, et al. Elevated serum levels of resistin, leptin, and adiponectin are associated with C-reactive protein and also other clinical conditions in rheumatoid arthritis. Intern Med 50: 269-275.

Friebe D, Loffler D, Schonberg M, Bernhard F, Buttner P, et al. Impact of metabolic regulators on the expression of the obesity associated genes FTO and NAMPT in human preadipocytes and adipocytes. PLoS One 6: e19526.

Haider DG, Holzer G, Schaller G, Weghuber D, Widhalm K, et al. (2006) The adipokine visfatin is markedly elevated in obese children. J Pediatr Gastroenterol Nutr 43: 548-549.

Haider DG, Schindler K, Schaller G, Prager G, Wolzt M, et al. (2006) Increased plasma visfatin concentrations in morbidly obese subjects are reduced after gastric banding. J Clin Endocrinol Metab 91: 1578-1581.

Presumey J, Courties G, Louis-Plence P, Escriou V, Scherman D, et al. Nicotinamide phosphoribosyltransferase/visfatin expression by inflammatory monocytes mediates arthritis pathogenesis. Ann Rheum Dis.

Spinnler R, Gorski T, Stolz K, Schuster S, Garten A, et al. The adipocytokine Nampt and its product NMN have no effect on beta-cell survival but potentiate glucose stimulated insulin secretion. PLoS One 8: e54106.

Bi TQ, Che XM, Liao XH, Zhang DJ, Long HL, et al. Overexpression of Nampt in gastric cancer and chemopotentiating effects of the Nampt inhibitor FK866 in combination with fluorouracil. Oncol Rep 26: 1251-1257.

Bowlby SC, Thomas MJ, D'Agostino RB, Jr., Kridel SJ Nicotinamide phosphoribosyl transferase (Nampt) is required for de novo lipogenesis in tumor cells. PLoS One 7: e40195.

Reddy PS, Umesh S, Thota B, Tandon A, Pandey P, et al. (2008) PBEF1/NAmPRTase/Visfatin: a potential malignant astrocytoma/glioblastoma serum marker with prognostic value. Cancer Biol Ther 7: 663-668.

Wang B, Hasan MK, Alvarado E, Yuan H, Wu H, et al. NAMPT overexpression in prostate cancer and its contribution to tumor cell survival and stress response. Oncogene 30: 907-921.

Caton PW, Kieswich J, Yaqoob MM, Holness MJ, Sugden MC Nicotinamide mononucleotide protects against pro-inflammatory cytokine-mediated impairment of mouse islet function. Diabetologia 54: 3083-3092.

Dumont N, Crawford YG, Sigaroudinia M, Nagrani SS, Wilson MB, et al. (2009) Human mammary cancer progression model recapitulates methylation events associated with breast premalignancy. Breast Cancer Res 11: R87.

Fontana A, Constam DB, Frei K, Malipiero U, Pfister HW (1992) Modulation of the immune response by transforming growth factor beta. Int Arch Allergy Immunol 99: 1-7.

McDonald PP, Fadok VA, Bratton D, Henson PM (1999) Transcriptional and translational regulation of inflammatory mediator production by endogenous TGF-beta in macrophages that have ingested apoptotic cells. J Immunol 163: 6164-6172.

Fadok VA, Bratton DL, Konowal A, Freed PW, Westcott JY, et al. (1998) Macrophages that have ingested apoptotic cells in vitro inhibit proinflammatory cytokine production through autocrine/paracrine mechanisms involving TGF-beta, PGE2, and PAF. J Clin Invest 101: 890-898.

Bogdan C, Nathan C (1993) Modulation of macrophage function by transforming growth factor beta, interleukin-4, and interleukin-10. Ann N Y Acad Sci 685: 713-739.

Altintas MM, Azad A, Nayer B, Contreras G, Zaias J, et al. Mast cells, macrophages, and crown-like structures distinguish subcutaneous from visceral fat in mice. J Lipid Res 52: 480-488.

Dellas C, Loskutoff DJ (2005) Historical analysis of PAI-1 from its discovery to its potential role in cell motility and disease. Thromb Haemost 93: 631-640.

Fersching DM, Nagel D, Siegele B, Salat C, Heinemann V, et al. Apoptosis-related biomarkers sFAS, MIF, ICAM-1 and PAI-1 in serum of breast cancer patients undergoing neoadjuvant chemotherapy. Anticancer Res 32: 2047-2058.

Han B, Nakamura M, Mori I, Nakamura Y, Kakudo K (2005) Urokinase-type plasminogen activator system and breast cancer (Review). Oncol Rep 14: 105-112.

McMahon B, Kwaan HC (2008) The plasminogen activator system and cancer. Pathophysiol Haemost Thromb 36: 184-194.

Wang S, Cao Q, Wang X, Li B, Tang M, et al. PAI-1 4G/5G Polymorphism Contributes to Cancer Susceptibility: Evidence from Meta-Analysis. PLoS One 8: e56797.

Xu X, Xie Y, Lin Y, Xu X, Zhu Y, et al. PAI-1 promoter 4G/5G polymorphism (rs1799768) contributes to tumor susceptibility: Evidence from meta-analysis. Exp Ther Med 4: 1127-1133.

Bourlier V, Zakaroff-Girard A, Miranville A, De Barros S, Maumus M, et al. (2008) Remodeling phenotype of human subcutaneous adipose tissue macrophages. Circulation 117: 806-815.

Boudin E, Piters E, Fransen E, Nielsen TL, Andersen M, et al. Association study of common variants in the sFRP1 gene region and parameters of bone strength and body composition in two independent healthy Caucasian male cohorts. Mol Genet Metab 105: 508-515.

Hruska KS, Tilli MT, Ren S, Cotarla I, Kwong T, Li M, et al. Conditional over-expression of estrogen receptor alpha in a transgenic mouse model. Transgenic Res 2002;11:361–72.

Madigan MP, Troisi R, Potischman N, Dorgan JF, Brinton LA, Hoover RN. Serum hormone levels in relation to reproductive and lifestyle factors in postmenopausal women (United States). Cancer Causes Control 1998;9:199–207.

Verkasalo PK, Thomas HV, Appleby PN, Davey GK, Key TJ. Circulating levels of sex hormones and their relation to risk factors for breast cancer: a cross-sectional study in 1092 pre- and postmenopausal women (United Kingdom). Cancer Causes Control 2001;12:47–59.

Eliassen AH, Missmer SA, Tworoger SS, Spiegelman D, Barbieri RL, Dowsett M, et al. Endogenous steroid hormone concentrations and risk of breast cancer among premenopausal women. J Natl Cancer Inst 2006;98:1406–15.

Colditz GA, Hankinson SE, Hunter DJ, Willett WC, Manson JE, Stampfer MJ, et al. The use of estrogens and progestins and the risk of breast cancer in postmenopausal women. N Engl J Med 1995;332:1589–93.

Panossian A, Wikman G, Sarris J. Rosenroot (Rhodiola rosea): Traditional use, chemical composition, pharmacology and clinical efficacy. Phytomedicine 2010.

Polakis P. Wnt signaling and cancer. Genes Dev 2000.

Bisson I, Prowse DM. WNT signaling regulates self-renewal and differentiation of prostate cancer cells with stem cell characteristics. Cell Research 2009.

Gupta N, Schmitt F, Grebhardt S, Mayer D. β-Catenin Is a Positive Regulator of Estrogen Receptor-α Function in Breast Cancer Cells. Cancers (Basel) 2011;3:2990–3001.

Andre F, Zielinski CC. Optimal strategies for the treatment of metastatic triple-negative breast cancer with currently approved agents. Annals of Oncology 2012;23:vi46–vi51.

Khanum F, Bawa AS, Singh B. Rhodiola rosea: A Versatile Adaptogen. Comprehensive Reviews in Food Science and Food Safety 2005;4:55–62.

Liu Z, Li X, Simoneau AR, Jafari M, Zi X. Rhodiola rosea extracts and salidroside decrease the growth of bladder cancer cell lines via inhibition of the mTOR pathway and induction of autophagy. Mol Carcinog 2011;51:257–67.

Gauger KJ, Hugh JM, Troester MA, Schneider S. Down-regulation of sfrp1 in a mammary epithelial cell line promotes the development of a cd44high/cd24low population which is invasive and resistant to anoikis. Cancer Cell Int 2009;9:11.

Acebron SP, Niehrs C. Focus ReviewMitotic and mitogenic Wnt signalling. The EMBO Journal 2012;31:2705–13.

Chen D, Fan J, Wang P, Zhu L, Jin Y, Peng Y, et al. Food Chemistry. Food Chemistry 2012;134:2126–33.

Lee S-Y, Shi L-S, Chu H, Li M-H, Ho C-W, Lai F-Y, et al. Rhodiola crenulataand Its Bioactive Components, Salidroside and Tyrosol, Reverse the Hypoxia-Induced Reduction of Plasma-Membrane-Associated Na,K-ATPase Expression via Inhibition of ROS-AMPK-PKC ξPathway. Evidence-Based Complementary and Alternative Medicine 2013;2013:1–15.

Chiang H-M, Chien Y-C, Wu C-H, Kuo Y-H, Wu W-C, Pan Y-Y, et al. Hydroalcoholic extract of Rhodiola rosea L. (Crassulaceae) and its hydrolysate inhibit melanogenesis in B16F0 cells by regulating the CREB/MITF/tyrosinase pathway. Food and Chemical Toxicology 2014;65:129–39.

Gauger KJ, Bassa LM, Henchey EM, Wyman J, Bentley B, Brown M, et al. Mice Deficient in Sfrp1 Exhibit Increased Adiposity, Dysregulated Glucose Metabolism, and Enhanced Macrophage Infiltration. PLoS ONE 2013;8:e78320. doi:10.1371/journal.pone.0078320.

García-Jiménez C. Wnt and incretin connections. Vitam Horm 2010;84:355–87. doi:10.1016/B978-0-12-381517-0.00014-X.

García-Martínez JM, Chocarro-Calvo A, Moya CM, García-Jiménez C. WNT/β-catenin increases the production of incretins by entero-endocrine cells. Diabetologia 2009;52:1913–24. doi:10.1007/s00125-009-1429-1.

Chocarro-Calvo A, García-Martínez JM, Ardila-González S, la Vieja De A, García-Jiménez C. Glucose-Induced β-Catenin Acetylation Enhances Wnt Signaling in Cancer. Molcel 2013;49:474–86. doi:10.1016/j.molcel.2012.11.022.